MEASUREMENT AND COMPUTATIONAL MODELLING OF INTERMOLECULAR INTERACTIONS IN FLUIDS

by

RICHARD V NHLEBELA
B Sc Hons (Natal)

A thesis submitted in partial fulfilment
of the requirements for the degree of
Master of Science
in the Discipline of Physics
School of Chemical and Physical Sciences
University of Natal

PIETERMARITZBURG
JANUARY 2000

Acknowledgements

I wish to express my sincere thanks and appreciation to all the people who contributed to this project in various ways. I would especially like to extend my gratitude to the following persons:

Dr. V. W. Couling, my supervisor, for his constant interest, guidance and encouragement during his supervision of this thesis;

Prof. R. E. Raab and Prof. C. Graham for their efforts to make my dream of obtaining a university higher degree come true by ensuring that financial matters were taken care of;

Dr. Diane Grayson and all the other staff members of the Science Foundation Program for discovering my academic potential at university: surely without them I wouldn't be where I am today; and

Zanele Nhlebela, my wife, for her unconditional support, interest and encouragement.

Finally I wish to make known my deep appreciation and gratitude to De Beers Diamond Research Laboratories for their generous financial assistance, and for the career which has been set aside for me at DRL as the new millennium begins.

DECLARATION

This thesis describes research undertaken at the University of Natal, Pietermaritzburg, under the supervision of Dr V. W. Couling.

I hereby certify that this thesis is the result of my own original work, unless specifically indicated to the contrary in the text, and that this work has not already been accepted for any other degree and is not being submitted in candidature for any other degree.

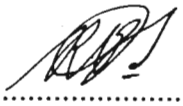

.....

R. V. Nhlebela

I hereby certify that this statement is correct.

Vincent Couling.

.....

V. W. Couling

(SUPERVISOR)

School of Chemical and Physical Sciences

Discipline of Physics

University of Natal

Pietermaritzburg

January 2000

Abstract

The molecular theory of the second light-scattering virial coefficient B_ρ describing the effects of interacting pairs of molecules on the depolarization ratio ρ of Rayleigh-scattered light is reviewed, both for interacting linear and nonlinear molecules. The molecular tensor theory of B_ρ for nonlinear molecules is extended for the first time to include in the scattered intensity those contributions arising from field gradient effects and induced quadrupole moments in the molecular interactions. The expressions for contributions to B_ρ are evaluated numerically for the nonlinear polar molecule dimethyl ether.

We have used an existing light-scattering apparatus to investigate the pressure-dependence of the depolarization ratio ρ for dimethyl ether, allowing B_ρ to be extracted. The measured value is compared with the calculated value, theory and experiment being found to agree to within 9%.

This success in modelling B_ρ for dimethyl ether spurred us on to extend our investigation to the second Kerr-effect virial coefficient B_K. The molecular-tensor theory of B_K for nonlinear molecules is reviewed, and is applied in this work to dimethyl ether. The calculated B_K values generally lie within the uncertainty limits of the available measured data over their full range of temperatures. We have used a recently-commissioned Kerr cell to undertake our own measurement of B_K for dimethyl ether at room temperature. This value is in good agreement with the findings of our molecular model, and is in reasonable agreement with the other measured data.

This thesis serves to reaffirm recent claims that comprehensive dipole-induced-dipole theories of molecular interaction effects explain the observed phenomena adequately provided one works to higher orders in the molecular tensors so that the series of contributing terms has converged to a meaningful numerical result, and provided the full symmetry of the molecules is allowed for.

Contents

Chapter 1

Introduction and Aims

1.1 Introduction and The Aim of This Work

Theoretical studies of the effects of molecular interactions on the optical properties of gases have, until recently, been limited to the very restricted classes of spherical and linear molecules. There are two principal reasons for this. Firstly, to derive complete molecular-tensor theories to describe the contributions even of pair interactions to the various molecular-optic phenomena such as electric-field-induced birefringence, molar refraction and depolarized light-scattering requires an almost prohibitively large volume of algebraic manipulation. Secondly, the dipole-induced-dipole (DID) model of Silberstein [1], where the dipoles induced in molecules by an incident light wave $\mathcal{E}_0(t)$ interact with one another leading to DID coupling, appears to break down in calculations of the various second virial coefficients of large quasi-spherical molecules [2,3]. This has led to a degree of scepticism in the application of DID theory to molecules of lower symmetry.

Recent theoretical studies of molecular interactions have been extended to molecules with symmetry lower than linear [4-7], the advent of modern symbolic manipulation packages such as Macsyma having brought the extensive algebraic and tensor manipulation into the realm of the feasible. It has now been established that, provided full account is taken of molecular symmetry, the DID model accounts reliably for the contribution made by interacting pairs of molecules to both the depolarization ratio of Rayleigh-scattered light

[4,5,7], and to the molecular Kerr constant in electro-optic birefringence [4,6].

A useful investigation is to establish whether a unique set of molecular parameters, used in the molecular-tensor theories of the various optical phenomena, will yield agreement between experiment and theory for the full range of virial coefficients of the different effects. It is in this vein that we present in this thesis a theoretical investigation of the second pressure, second light-scattering and second Kerr-effect virial coefficients of the low-symmetry dimethyl ether molecule, and an extensive comparison with the available measured data. Where possible, new measurements have been undertaken in this work itself, allowing for a critical comparison of theory and experiment.

1.2 References

[1] Silberstein, L., 1917, *Phil. Mag.*, **33,** 92, 521.

[2] Watson, R. C., and Rowell, R. L., 1974, *J. chem. Phys.*, **52,** 132.

[3] Dunmur, D. A., Hunt, D. C., and Jessup, N. E., 1979, *Molec. Phys.*, **37,** 713.

[4] Couling, V. W., 1995, Ph D thesis, University of Natal (Pietermaritzburg).

[5] Couling, V. W., and Graham, C., 1996, *Molec. Phys.*, **87,** 779.

[6] Couling, V. W., and Graham, C., 1998, *Molec. Phys.*, **93,** 31.

[7] Couling, V. W., Graham, C., and McKenzie, J. M., 1999, *Molec. Phys.*, **96,** 921.

Chapter 2

Calculation of the Second Light-scattering Virial Coefficient of Dimethyl Ether

2.1 A General Theory of Light Scattering

The scattering of light by a single molecule can be considered to arise when the incident light wave induces oscillating multipole moments in the molecule, which then give rise to retarded scalar and vector potentials and therefore to electric and magnetic fields at all points. Landau and Lifshitz [1] and Buckingham and Raab [2] have related these fields to the electric and magnetic multipole moments of the system. At a point a distance R from an origin O fixed within molecule's system of oscillating charges, where R is very much larger than both the dimensions of the system of charges and the wavelength of the retarded light, the scattered electric field $E_\alpha^{(s)}$ can be considered to be a plane wave, and is then given by [2]

$$E_\alpha^{(s)} = -\frac{1}{(4\pi\varepsilon_0)Rc^2}\left[\left(\ddot{\mu}_\alpha - n_\alpha n_\beta \ddot{\mu}_\beta\right) - \frac{1}{c}\varepsilon_{\alpha\beta\gamma} n_\beta \ddot{m}_\gamma + \frac{1}{3c}\left(n_\beta \dddot{\theta}_{\alpha\beta} - n_\alpha n_\beta n_\gamma \dddot{\theta}_{\beta\gamma}\right) + \cdots\right] \qquad (2.1)$$

where n_α is a unit vector in the direction in which the light wave is scattered, μ_α and m_α are the induced electric and magnetic dipole moments respectively and $\theta_{\alpha\beta}$ is the induced *traceless* electric quadrupole moment. Explicit forms of these moments are presented in Appendix A.

The experiments of R. J. Strutt, the fourth Baron Rayleigh, [13] revealed that if a linearly polarized light beam is allowed to traverse a gas sample, the light scattered at right angles to the incident beam by the gas molecules is, in general, not completely linearly polarized. Scattering occurs since the oscillating electric and magnetic fields of the incident light waves set the bound electric charges of the molecules into motion, leading to the emission of secondary light waves in all directions. The extent of scattering and depolarization depends on the nature of the scattering medium: the light scattered by different gas molecules was found by Rayleigh to be depolarized to different extents.

Consider the arrangement in figure 2.1 where the origin of a space-fixed system of axes O(x,y,z) is placed within a macroscopic gas sample containing a large number N of identical gas molecules. Let this system be under the influence of a uniform, parallel beam of incident light which is linearly polarized in the vertical xz plane and travelling in the z direction. The wavelength of the incident light is assumed to be very large relative to the dimensions of the gas molecules, and its frequency is supposed to be well below that of any electronic absorption transition. The Rayleigh-scattered light is observed at a point on the y-axis, with the depolarization ratio being defined as

$$\rho = \frac{I_z}{I_x}, \tag{2.2}$$

where I_z and I_x are the scattered light intensities with the electric vector parallel to the z and x axes respectively.

For observations of the light beam scattered along the y-axis of the space-fixes axes (x,y,z) where the z is the direction of propagation of the light wave, the unit vector n_α appearing in equation (2.1) becomes $(n_x,n_y,n_z) = (0,1,0)$. The terms in the quadrupole and magnetic

moments in equation (2.1) can safely be dropped [9] since their contributions are much smaller than that of the electric dipole moment. Equation (2.1) becomes

$$E_{\alpha}^{(s)} = \frac{1}{(4\pi\varepsilon_0)Rc^2}\sum_{p=1}^{N} \ddot{\mu}_{\alpha}^{(p)}(t') \tag{2.3}$$

where $\ddot{\mu}_{\alpha}^{(p)}$ is the dipole acceleration of the p^{th} molecule in the assembly of N molecules which are contributing to the electric dipole radiation. Since the electric dipole μ_α is a function of the electric field E_β, the first order partial time derivative of the electric dipole moment is

$$\dot{\mu}_{\alpha} = \frac{\partial \mu_{\alpha}}{\partial t} = \frac{\partial \mu_{\alpha}}{\partial E_{\beta}}\frac{\partial E_{\beta}}{\partial t}, \tag{2.4}$$

so that the second order partial derivative is

$$\ddot{\mu}_{\alpha} = \frac{\partial^2 \mu_{\alpha}}{\partial t^2} = \frac{\partial E_{\beta}}{\partial t}\frac{\partial E_{\gamma}}{\partial t}\frac{\partial^2 \mu_{\alpha}}{\partial E_{\beta}\partial E_{\gamma}} + \frac{\partial \mu_{\alpha}}{\partial E_{\beta}}\frac{\partial^2 E_{\beta}}{\partial t^2}. \tag{2.5}$$

The first term of equation (2.5) is non-linear in the field, and even with the use of a very intense laser beam this term can be safely neglected. Hence equation (2.5) becomes

$$\ddot{\mu}_{\alpha} = \frac{\partial \mu_{\alpha}}{\partial E_{\beta}}\frac{\partial^2 E_{\beta}}{\partial t^2}. \tag{2.6}$$

Since $E_\alpha = E_\alpha^{(0)}\exp(-i\omega(t-\frac{R}{c}))$, we have

$$\frac{\partial^2 E_{\beta}}{\partial t^2} = -\omega^2 E_{\beta}. \tag{2.7}$$

If λ is the wavelength of the incident beam, then use of the well known result

$c = \lambda f = \dfrac{\lambda\omega}{2\pi}$ yields

$$\left(\frac{2\pi}{\lambda}\right)^2 c^2 = \omega^2, \tag{2.8}$$

so that equation (2.7) becomes

$$\frac{\partial^2}{\partial t^2} E_\beta = -\left(\frac{2\pi}{\lambda}\right)^2 c^2 E_\beta. \tag{2.9}$$

Now equations (2.9), (2.6) and (2.3) give

$$E_\alpha^{(s)} = \frac{1}{(4\pi\varepsilon_0)Rc^2} \sum_{p=1}^{N} \frac{\partial \mu_\alpha^{(p)}}{\partial E_\delta^{(p)}} E_\delta^{(p)} \tag{2.10}$$

where $E_\delta^{(p)}$ signifies the value of the electric field at the p^{th} molecule. In light of equation (2.10), it is useful to introduce the *differential polarizability* $\pi_{\alpha\beta}^{(p)}$ which is defined as

$$\pi_{\alpha\beta}^{(p)} = \frac{\partial \mu_\alpha^{(p)}}{\partial E_\beta^{(p)}}. \tag{2.11}$$

In general, the intensity of a light wave with electric field vector $\underset{\sim}{E}$ is given by

$$I = \frac{1}{2\mu_0 c} \underset{\sim}{E}.\underset{\sim}{E}^* \tag{2.12}$$

where the asterisk denotes the complex conjugate. Equation (2.2) then yields

$$\rho = \frac{I_z}{I_x} = \frac{\langle E_z E_z^* \rangle}{\langle E_x E_x^* \rangle} = \frac{\left\langle \sum_{p=1}^{N} \sum_{q=1}^{N} \pi_{zx}^{(p)} \pi_{zx}^{(q)} e^{i\chi_{pq}} \right\rangle}{\left\langle \sum_{p=1}^{N} \sum_{q=1}^{N} \pi_{xx}^{(p)} \pi_{xx}^{(q)} e^{i\chi_{pq}} \right\rangle} \tag{2.13}$$

where χ_{pq} is the phase difference in the light scattered by molecules p and q as seen at the observation point, and where the angular brackets indicate an average over all configurations of the specimen. This equation, first obtained by Buckingham and Stephen, has been used as a basis for the calculation of the depolarization ratio of linear, quasi-linear, and non-linear molecules [14, 21,6].

2.2 Non-interacting Molecules

For non-interacting molecules, the intermolecular fields arising at any molecule due to the permanent and induced multipole moments of the other molecules in the assembly are negligible. It is the applied light wave's electric field $\mathcal{E}_0$ which is sole cause of the induced electric dipole moment $\mu_\alpha^{(p)}$ of the p^{th} molecule, and so the differential polarizability $\pi_{\alpha\beta}$ becomes simply the molecular polarizability $\alpha_{\alpha\beta}$. Moreover, the average phase relationship between the fields from any one pair of the interacting molecules vanishes to zero, self-correlations alone contributing to the summation in equation (2.13). Furthermore, since the molecules are assumed to be identical, the summations in equation (2.13) can be replaced by N times the contribution of a single representative molecule 1. We have

$$\rho = \frac{N\left\langle \alpha_{zx}^{(1)} \alpha_{zx}^{(1)} \right\rangle}{N\left\langle \alpha_{xx}^{(1)} \alpha_{xx}^{(1)} \right\rangle} \tag{2.14}$$

where the angular brackets represent an average over all unbiased orientations of a molecule. The molecular tensors appearing in equation (2.14) are referred to the space-fixed axes

(x,y,z), and they must be projected into the molecule-fixed axes (1,2,3). The projection of the tensors from one set of axes into another is a standard procedure, which yields

$$\left\langle \alpha^{(1)}_{zx}\alpha^{(1)}_{zx}\right\rangle = \alpha^{(1)}_{ij}\alpha^{(1)}_{kl}\left\langle a_i^z a_k^z a_j^x a_l^x\right\rangle \tag{2.15}$$

and

$$\left\langle \alpha^{(1)}_{xx}\alpha^{(1)}_{xx}\right\rangle = \alpha^{(1)}_{ij}\alpha^{(1)}_{kl}\left\langle a_i^x a_k^x a_j^x a_l^x\right\rangle. \tag{2.16}$$

Here, a_i^α is the direction cosine between the α space-fixed and i molecule-fixed axes, and the average is over isotropic orientations of molecule 1 in the space-fixed axes.

The results of standard isotropic averages are [4,32]:

$$\left\langle a_i^z a_k^z a_j^x a_l^x\right\rangle = \tfrac{1}{30}(4\delta_{ik}\delta_{jl} - \delta_{ij}\delta_{kl} - \delta_{il}\delta_{kj}) \tag{2.17}$$

and

$$\left\langle a_i^x a_k^x a_j^x a_l^x\right\rangle = \tfrac{1}{15}(\delta_{ik}\delta_{jl} + \delta_{ij}\delta_{kl} + \delta_{il}\delta_{kj}). \tag{2.18}$$

Using these results in equations (2.15) and (2.16) yields

$$\begin{aligned}\left\langle \alpha^{(1)}_{zx}\alpha^{(1)}_{zx}\right\rangle &= \tfrac{1}{30}\left(4\delta^{(1)}_{ij}\delta^{(1)}_{ij} - \delta^{(1)}_{ii}\delta^{(1)}_{ij}\right)\alpha_{ij}\alpha_{kl} \\ &= \tfrac{2}{30}(\alpha_{11}^2 + \alpha_{22}^2 + \alpha_{33}^2 - \alpha_{11}\alpha_{22} - \alpha_{11}\alpha_{33} - \alpha_{22}\alpha_{33}),\end{aligned} \tag{2.19}$$

which is applicable to both linear and non-linear molecules, and

$$\begin{aligned}\left\langle \alpha^{(1)}_{xx}\alpha^{(1)}_{xx}\right\rangle &= \tfrac{1}{15}(2\alpha^{(1)}_{ij}\alpha^{(1)}_{ij} + \alpha^{(1)}_{ii}\alpha^{(1)}_{kk}) \\ &= \tfrac{1}{15}\left(3\alpha_{11}^2 + 3\alpha_{22}^2 + 3\alpha_{33}^2 + 2\alpha_{11}\alpha_{22} + 2\alpha_{11}\alpha_{33} + 2\alpha_{22}\alpha_{33}\right).\end{aligned} \tag{2.20}$$

For linear molecules $\alpha^{(1)}_{ij}$ is diagonal with

$$\alpha_{11} = \alpha_{22} = \alpha_{\perp} \text{ and } \alpha_{33} = \alpha_{\parallel}. \tag{2.21}$$

The mean polarizability α is

$$\alpha = \tfrac{1}{3}\alpha_{ii} = \tfrac{1}{3}\left(2\alpha_{\perp} + \alpha_{\parallel}\right), \tag{2.22}$$

while the anisotropy in the polarizability is defined as

$$\Delta\alpha = \alpha_{\parallel} - \alpha_{\perp}. \tag{2.23}$$

For non-linear molecules with D_{2h} and C_{2v} symmetry, $\alpha_{\alpha\beta}$ is diagonal with three independent components, which are α_{11}, α_{22} and α_{33}. The mean polarizability α is

$$\alpha = \tfrac{1}{3}\alpha_{ii} = \tfrac{1}{3}\left(\alpha_{11} + \alpha_{22} + \alpha_{33}\right) \tag{2.24}$$

while the anisotropy in the polarizability tensor is often defined as [5,33]

$$\Delta\alpha = \frac{1}{\sqrt{2}}\left[\left(\alpha_{11} - \alpha_{22}\right)^2 + \left(\alpha_{22} - \alpha_{33}\right)^2 + \left(\alpha_{33} - \alpha_{11}\right)^2\right]^{\frac{1}{2}}. \tag{2.25}$$

Using equations (2.24) and (2.25) in equation (2.20) we obtain

$$\left\langle \alpha_{xx}^{(1)}\alpha_{xx}^{(1)} \right\rangle = \alpha^2 + \tfrac{4}{45}(\Delta\alpha)^2. \tag{2.26}$$

The use of equations (2.23) and (2.21) in equation (2.19) gives

$$\begin{aligned}\left\langle \alpha_{zx}^{(1)}\alpha_{zx}^{(1)} \right\rangle &= \tfrac{1}{30}\left(4\delta_{ij}^{(1)}\delta_{ij}^{(1)} - \delta_{ii}^{(1)}\delta_{ij}^{(1)}\right)\alpha_{ij}\alpha_{kl} \\ &= \tfrac{2}{30}(\alpha_{11}^2 + \alpha_{22}^2 + \alpha_{33}^2 - \alpha_{11}\alpha_{22} - \alpha_{11}\alpha_{33} - \alpha_{22}\alpha_{33}) \\ &= \tfrac{1}{15}(\Delta\alpha)^2,\end{aligned}$$

and this result, together with equation (2.26), when substituted in equation (2.14), gives

$$\rho_0 = \frac{\tfrac{1}{15}(\Delta\alpha)^2}{\alpha^2 + \tfrac{4}{45}(\Delta\alpha)^2}. \tag{2.27}$$

The anisotropy in the molecular polarizability tensor was originally defined as the dimensionless quantity κ [6] where

$$\kappa^2 = \frac{\left(3\alpha_{ij}\alpha_{ij} - \alpha_{ii}\alpha_{jj}\right)}{2\alpha_{ii}\alpha_{jj}} = \frac{(\Delta\alpha)^2}{9\alpha^2}. \tag{2.28}$$

This applies to both linear and non-linear molecules, and a relationship between κ and ρ_0 can now be deduced using equations (2.27) and (2.28):

$$\rho_0 = \frac{3\kappa^2}{5+4\kappa^2}. \tag{2.29}$$

This expression was first derived by Bridge and Buckingham [6], and can be used to obtain values for κ from measured values of ρ_0 for various different gaseous species.

2.3 Interacting Molecules

Studies of the molecular-optic phenomena of gases have confirmed that certain bulk properties, such as molar refraction and total polarization, are in fact density dependent even for gases of atomic species [6]. These findings are an indication of the presence of molecular interactions. The effects of these interactions can be accounted for by the virial expansion of the relevant macroscopic variables. Suppose that Q is a measurable bulk property of a real gas. Then the observed value of Q can be expanded into terms in inverse powers of the molar volume V_m [7] to give

$$Q = A_Q + \frac{B_Q(T)}{V_m} + \frac{C_Q(T)}{V_m^2} + \cdots \tag{2.30}$$

where $B_Q(T)$, $C_Q(T)$,$\cdots$ are functions of temperature alone, and are called the second,

third, ... , Q- virial coefficients respectively. The physical interpretation of B_Q, C_Q, *etc.* is that they represent the contributions to Q arising from the interactions between pairs, triplets, ... , of molecules respectively. From equation (2.30) it is seen that in the limit of an infinite dilution $\left(\text{i.e. } V_m \to \infty\right)$ Q tends to A_Q, which is the value of Q corresponding to a perfect gas of independent molecules.

2.3.1 The virial expansion of the depolarization ratio

The insight that has been gained from the preceding discussion can now be used in the specific case of the depolarization ratio ρ of Raleigh-scattered light. The virial expansion becomes [17]

$$\rho(T) = \rho_0 + \frac{B_\rho(T)}{V_m} + \frac{C_\rho(T)}{V_m^2} + \cdots \tag{2.30}$$

where B_ρ and C_ρ are the second and third light-scattering virial coefficients respectively.

The virial coefficients depend on the temperature of the gas as well as on the frequency of the incident light. B_ρ and C_ρ describe the contributions to ρ arising from interactions between pairs and triplets of molecules respectively. The series can be extended to account for the contributions due to even higher order interactions, although these become successively smaller as the series is rapidly converging. In this work, we have limited our investigation to pair interactions. Experimentally, B_ρ may be deduced from measured data by plotting a graph of ρ versus V_m^{-1}. The plot will have a linear relationship between ρ and V_m^{-1} where pair interactions are predominant, the graph deviating from linearity only when triplet and higher order interactions become significant. For our purposes we truncate equation (2.30) to

$$\rho(T) = \rho_0 + \frac{B_\rho(T)}{V_m} \tag{2.31}$$

where ρ_0 is the limit of ρ at zero density.

A complete molecular tensor theory of B_ρ for interacting non-linear molecules is now presented. In a gas, these molecules are moving randomly relative to one another and so the scattered light waves emitted by each of these molecules arrive at the distant observation point with different and randomly fluctuating phases. This allows the summation in equation (2.8) to be considerably simplified. Apart from the self-correlation, there is a significant correlation of phase only when pairs of molecules are in the process of a closer encounter. Since the interaction mechanism for all terms (*with one exception*) is significant only at short ranges of about 0.5 nm to 2 nm, which are a small fraction of typical wavelengths of about 500nm, the phase differences χ_{12} between beams from interacting molecules p and q are effectively zero. The exception is the term $\left\langle \pi_{xx}^{(1)} \pi_{xx}^{(2)} \cos\chi_{12} \right\rangle$, as established by Benoît and Stockmayer [26]. This means that there is no need for the general retention of χ_{pq}, $\exp(i\,\chi_{pq})$ being set to unity in all but the abovementioned term. Thus, allowing only for self-correlation and pairwise contributions to the coherent fields, the summations in equation (2.13) are replaced by N times the contribution of a representative molecule 1, averaged over all pair encounters, giving

$$\rho = \frac{N\left\langle \pi_{zx}^{(1)} \pi_{zx}^{(1)} \right\rangle + N\left\langle \pi_{zx}^{(1)} \pi_{zx}^{(2)} \right\rangle}{N\left\langle \pi_{xx}^{(1)} \pi_{xx}^{(1)} \right\rangle + N\left\langle \pi_{xx}^{(1)} \pi_{xx}^{(2)} \cos\chi_{12} \right\rangle}, \tag{2.32}$$

where the angular brackets now indicate an average over pair interactions, and $\pi_{\alpha\beta}^{(p)}$ is the differential polarizability of molecule p in the space-fixed axes (x,y,z) located within a gas sample. The probability that molecule 1 has neighbour in the range $d\tau$ at τ is related to the intermolecular potential energy $U_{12}(\tau)$ by [10]

$$P(\tau) = \frac{N_A}{\Omega V_m} \exp\left(-U_{12}(\tau)/kT\right) \tag{2.33}$$

where $\Omega = \frac{1}{V_m}\int d\tau$ is the integral over the orientational co-ordinates of the neighbouring molecule 2, N_A is Avogadro's number and T is the absolute temperature.

To obtain expressions for the differential polarizabilities in equation (2.32), as defined in equation (2.12), the treatment of Graham [11] is followed. The dipole moment μ_α and quadrupole moment $\theta_{\alpha\beta}$ induced in a molecule by an electric field E_α and electric field gradient $E_{\alpha\beta}$ are (Buckingham [12])

$$\mu_\alpha = \alpha_{\alpha\beta} E_\beta + \tfrac{1}{3} A_{\alpha\beta\gamma} E_{\beta\gamma} + \cdots \tag{2.34}$$

and

$$\theta_{\alpha\beta} = A_{\gamma\alpha\beta} E_\gamma + C_{\alpha\beta\gamma\delta} E_{\gamma\delta} + \cdots . \tag{2.35}$$

It has been argued [12] that the total oscillating dipole moment of molecule 1, $\mu_\alpha^{(1)}$, arises in part from the direct polarizing action of the incident light wave $\mathcal{E}_0$, and in part from the field F_α and field gradient $F_{\alpha\beta}$ at molecule 1 due to the oscillating moments of a neighbouring molecule 2, equation (2.34) becoming

$$\mu_\alpha^{(1)}(\mathcal{E}_0) = \alpha_{\alpha\beta}^{(1)}\left(\mathcal{E}_{0\beta} + F_\beta^{(1)}\right) + \tfrac{1}{3} A_{\alpha\beta\gamma}^{(1)}\left(\mathcal{E}_{0\beta\gamma} + F_{\beta\gamma}^{(1)}\right) + \cdots . \tag{2.36}$$

Here, $\mathcal{E}_{0\beta}$ and $\mathcal{E}_{0\beta\gamma}$ are the field and field gradient of the incident light wave at molecule 1, while $F_{\beta}^{(1)}$ and $F_{\beta\gamma}^{(1)}$ are the oscillating field and field gradient arising at molecule 1 due to the oscillating multipole moments of molecule 2. The field gradient $\mathcal{E}_{0\beta\gamma}$ of the incident light wave makes no significant contribution to the electric dipole moment $\mu_{\alpha}^{(1)}$ of molecule 1 since the dimensions of each molecule in the gas sample are usually very much smaller than the wavelength of the incident light wave, and therefore this contribution is neglected . Thus equation (2.36) becomes

$$\mu_{\alpha}^{(1)}\left(\mathcal{E}_0\right) = \alpha_{\alpha\beta}^{(1)}\left(\mathcal{E}_{0\beta} + F_{\beta}^{(1)}\right) + \tfrac{1}{3} A_{\alpha\beta\gamma}^{(1)} F_{\beta\gamma}^{(1)} + \cdots \tag{2.37}$$

If the oscillating octopoles and higher order multipoles on molecule 2 are neglected then the field $F_{\beta}^{(1)}$ and field gradient $F_{\gamma\delta}^{(1)}$ at molecule 1 due to the oscillating dipole and quadrupole moments of molecule 2 are given by [12]

$$F_{\beta}^{(1)} = T_{\beta\gamma}^{(1)}\mu_{\gamma}^{(2)} - \tfrac{1}{3} T_{\beta\gamma\delta}^{(1)}\theta_{\gamma\delta}^{(2)} \tag{2.38}$$

and

$$F_{\beta\gamma}^{(1)} = T_{\beta\gamma\delta}^{(1)}\mu_{\delta}^{(2)} - \tfrac{1}{3} T_{\beta\gamma\delta\varepsilon}^{(1)}\theta_{\delta\varepsilon}^{(2)} \tag{2.39}$$

where the T-tensors are defined as [12]

$$T_{\alpha\beta}^{(1)} = \frac{1}{4\pi\varepsilon_0}\nabla_{\alpha}\nabla_{\beta}\frac{1}{R} = \frac{1}{4\pi\varepsilon_0}\frac{1}{R^5}\left(3R_{\alpha}R_{\beta} - R^2\delta_{\alpha\beta}\right), \tag{2.40}$$

$$\begin{aligned} T_{\alpha\beta\gamma}^{(1)} &= -\frac{1}{4\pi\varepsilon_0}\nabla_{\alpha}\nabla_{\beta}\nabla_{\gamma}\frac{1}{R} \\ &= \frac{3}{4\pi\varepsilon_0}\frac{1}{R^7}\left(5R_{\alpha}R_{\beta}R_{\gamma} - R^2\left(R_{\alpha}\delta_{\beta\gamma} + R_{\beta}\delta_{\alpha\gamma} + R_{\gamma}\delta_{\alpha\beta}\right)\right), \end{aligned} \tag{2.41}$$

and

$$T^{(1)}_{\alpha\beta\gamma\delta} = -\tfrac{1}{4\pi\varepsilon_0}\nabla_\alpha\nabla_\beta\nabla_\gamma\nabla_\delta = \frac{3}{4\pi\varepsilon_0}\frac{1}{R^9}[5R_\alpha R_\beta R_\gamma R_\delta$$
$$-5R^2(R_\alpha R_\beta\delta_{\gamma\delta} + R_\alpha R_\gamma\delta_{\beta\delta} + R_\gamma\delta_{\alpha\beta} \qquad (2.42)$$
$$+R_\alpha R_\delta\delta_{\beta\gamma} + R_\beta R_\gamma\delta_{\alpha\delta} + R_\beta R_\delta\delta_{\alpha\gamma}$$
$$+R_\gamma R_\delta\delta_{\alpha\beta}) + R^4(\delta_{\alpha\beta}\delta_{\gamma\delta} + \delta_{\alpha\gamma}\delta_{\beta\delta} + \delta_{\alpha\delta}\delta_{\beta\gamma})],$$

where

$$\nabla_\alpha = \left(\frac{\partial}{\partial R_\alpha}\right), \qquad (2.43)$$

$$T^{(2)}_{\alpha\cdots} = (-1)^n T^{(1)}_{\alpha\cdots} \qquad (2.44)$$

for the nth rank T-tensor, and R_α is the vector from the origin of molecule 1 to the origin of molecule 2.

In equations (2.40) and (2.41), $\mu^{(2)}_\alpha$ and $\theta^{(2)}_{\gamma\delta}$ are the oscillating dipole and quadrupole moments induced on molecule 2 by the field and the field gradient arising due to the presence of both the incident light wave and the oscillating electric dipole and quadrupole moments of molecule 1. With the use of equations analogous to (2.34) and (2.35), we can obtain the explicit forms of expressions of $\mu^{(2)}_\alpha$ and $\theta^{(2)}_{\gamma\delta}$.

Now substituting the expressions of $\mu^{(1)}_\alpha$, $\mu^{(2)}_\alpha$, $\theta^{(1)}_{\gamma\delta}$ and $\theta^{(2)}_{\gamma\delta}$ into equations (2.37) and (2.39) yields

$$F^{(1)}_\beta = T^{(1)}_{\beta\gamma}\left[\alpha^{(2)}_{\gamma\delta}\left(\mathcal{E}_{0\delta} + F^{(2)}_\delta\right) + \tfrac{1}{3}A^{(2)}_{\gamma\delta\varepsilon}F^{(2)}_{\delta\varepsilon}\right] - \tfrac{1}{3}T^{(1)}_{\beta\gamma\delta}\left[A^{(2)}_{\varepsilon\gamma\delta}\left(\mathcal{E}_{0\varepsilon} + F^{(2)}_\varepsilon\right) + C^{(2)}_{\gamma\delta\varepsilon\phi}F^{(2)}_{\varepsilon\phi}\right]. \qquad (2.45)$$

Here $F_{\delta}^{(2)}$ and $F_{\delta\varepsilon}^{(2)}$ refer to the field and the field gradient at molecule 2 due to the oscillating dipole and quadrupole moments of molecule1, and their expressions are analogous to those of $F_{\delta}^{(1)}$ and $F_{\delta\varepsilon}^{(1)}$.

Substituting the expressions of $F_{\delta}^{(2)}$ and $F_{\delta\varepsilon}^{(2)}$ into (2.45) yields

$$\begin{aligned} F_{\beta}^{(1)} = {} & T_{\beta\gamma}^{(1)}\alpha_{\gamma\delta}^{(2)}\mathscr{E}_{0\delta} + T_{\beta\gamma}^{(1)}\alpha_{\gamma\delta}^{(2)}(T_{\delta\varepsilon}^{(2)}\mu_{\varepsilon}^{(1)} - \tfrac{1}{3}T_{\delta\varepsilon\phi}^{(2)}\theta_{\varepsilon\phi}^{(1)}) \\ & + \tfrac{1}{3}T_{\beta\gamma}^{(1)}A_{\gamma\delta\varepsilon}^{(2)}(T_{\delta\varepsilon\phi}^{(2)}\mu_{\phi}^{(1)} + \cdots) - \tfrac{1}{3}T_{\beta\gamma\delta}^{(1)}A_{\varepsilon\gamma\delta}^{(2)}\mathscr{E}_{0\varepsilon} \\ & - \tfrac{1}{3}T_{\beta\gamma\delta}^{(1)}A_{\varepsilon\gamma\delta}^{(2)}(T_{\varepsilon\phi}^{(2)}\mu_{\phi}^{(1)} \\ & - T_{\varepsilon\phi\lambda}^{(2)}\theta_{\phi\lambda}^{(1)}) - \tfrac{1}{3}T_{\beta\gamma\delta}^{(1)}C_{\gamma\delta\varepsilon\phi}^{(2)}(T_{\varepsilon\phi\lambda}^{(2)}\mu_{\lambda}^{(1)} + \cdots). \end{aligned} \tag{2.46}$$

Replacing the expressions of $\mu_{\alpha}^{(1)}$ and $\theta_{\alpha\beta}^{(1)}$ from equations (2.34) and (2.35) into (2.46) yields

$$\begin{aligned} F_{\beta}^{(1)} = {} & T_{\beta\gamma}^{(1)}\alpha_{\gamma\delta}^{(2)}\mathscr{E}_{0\delta} + T_{\beta\gamma}^{(1)}\alpha_{\gamma\delta}^{(2)}[T_{\delta\varepsilon}^{(2)}\{\alpha_{\varepsilon\phi}^{(1)}(\mathscr{E}_{0\phi} + F_{\phi}^{(1)}) \\ & + \tfrac{1}{3}A_{\varepsilon\phi\lambda}^{(1)}F_{\phi\lambda}^{(1)}\} - \tfrac{1}{3}T_{\delta\varepsilon\phi}^{(2)}\{A_{\gamma\varepsilon\phi}^{(1)}(\mathscr{E}_{0\lambda} + F_{\lambda}^{(1)}) + C_{\varepsilon\phi\lambda\eta}^{(1)}F_{\lambda\eta}^{(1)}\}] \\ & + \tfrac{1}{3}T_{\beta\gamma}^{(1)}A_{\gamma\delta\varepsilon}^{(2)}T_{\delta\varepsilon\phi}^{(2)}[\alpha_{\phi\lambda}^{(1)}(\mathscr{E}_{0\lambda} + F_{\lambda}^{(1)}) + \tfrac{1}{3}A_{\phi\lambda\eta}^{(1)}F_{\lambda\eta}^{(1)}] \\ & - \tfrac{1}{3}T_{\beta\gamma\delta}^{(1)}A_{\varepsilon\gamma\delta}^{(2)}\mathscr{E}_{0\varepsilon} - \tfrac{1}{3}T_{\beta\gamma\delta}^{(1)}A_{\varepsilon\gamma\delta}^{(2)}[T_{\varepsilon\phi}^{(2)}\{\alpha_{\phi\lambda}^{(1)}(\mathscr{E}_{0\lambda} + F_{\lambda}^{(1)}) \\ & + \tfrac{1}{3}A_{\phi\lambda\eta}^{(1)}F_{\lambda\eta}^{(1)}\} - \tfrac{1}{3}T_{\varepsilon\phi\lambda}^{(2)}\{A_{\eta\phi\lambda}^{(1)}(\mathscr{E}_{0\eta} + F_{\eta}^{(1)}) + C_{\phi\lambda\eta\upsilon}^{(1)}F_{\eta\upsilon}^{(1)}\}] \\ & - \tfrac{1}{3}T_{\beta\gamma\delta}^{(1)}C_{\gamma\delta\varepsilon\phi}^{(2)}T_{\varepsilon\phi\lambda}^{(2)}[\alpha_{\lambda\eta}^{(1)}(\mathscr{E}_{0\eta} + F_{\eta}^{(1)}) + \tfrac{1}{3}A_{\lambda\eta\upsilon}^{(1)}F_{\eta\upsilon}^{(1)}]. \end{aligned} \tag{2.47}$$

When successive substitutions of $F_{\beta}^{(1)}$, $F_{\gamma\delta}^{(1)}$, and of $F_{\beta}^{(2)}$ and $F_{\gamma\delta}^{(2)}$ are made, a lengthy series of terms is produced. It is difficult to know *a priori* after how many terms the series is to be truncated since little is known about the rate of convergence of the contributing terms.

However, Couling and Graham undertook a number of numerical calculations of these terms for gases of linear and quasi-linear molecules [9] and for non-linear molecules [14]. They established that the series $F_\beta^{(1)}$ could be truncated once the terms in the scattered intensities were of the order of α^5, $\alpha^2 A$, $\alpha^3 A$ and $\alpha^3 C$ since higher-order terms make negligible contributions, the series having converged adequately. Equation (2.47) becomes

$$\begin{aligned} F_\beta^{(1)} = {} & T_{\beta\gamma}^{(1)} \alpha_{\gamma\delta}^{(2)} \mathscr{E}_{0\delta} + T_{\beta\gamma}^{(1)} \alpha_{\gamma\delta}^{(2)} T_{\delta\varepsilon}^{(2)} \alpha_{\varepsilon\phi}^{(1)} \mathscr{E}_{0\delta} \\ & + T_{\beta\gamma}^{(1)} \alpha_{\gamma\delta}^{(2)} T_{\delta\varepsilon}^{(2)} \alpha_{\varepsilon\phi}^{(1)} T_{\phi\lambda}^{(1)} \alpha_{\lambda\eta}^{(2)} \mathscr{E}_{0\eta} - \tfrac{1}{3} T_{\beta\gamma\delta}^{(1)} A_{\varepsilon\gamma\delta}^{(2)} \mathscr{E}_{0\varepsilon} \\ & - \tfrac{1}{3} T_{\beta\gamma}^{(1)} \alpha_{\gamma\delta}^{(2)} T_{\delta\varepsilon}^{(2)} A_{\lambda\varepsilon\phi}^{(1)} \mathscr{E}_{0\lambda} + \tfrac{1}{3} T_{\beta\gamma}^{(1)} A_{\gamma\delta\varepsilon}^{(2)} T_{\delta\varepsilon\phi}^{(2)} \alpha_{\phi\lambda}^{(1)} \mathscr{E}_{0\lambda} \\ & - \tfrac{1}{3} T_{\beta\gamma\delta}^{(1)} A_{\varepsilon\gamma\delta}^{(2)} T_{\varepsilon\phi}^{(2)} \alpha_{\phi\lambda}^{(1)} \mathscr{E}_{0\lambda} - \tfrac{1}{3} T_{\beta\gamma\delta}^{(1)} C_{\gamma\delta\varepsilon\phi}^{(2)} T_{\varepsilon\phi\lambda}^{(2)} \alpha_{\lambda\eta}^{(1)} \mathscr{E}_{0\eta} + \cdots . \end{aligned} \tag{2.48}$$

To understand the physical meaning of the terms in equation (2.48), consider as an example the term $-\frac{1}{3} T_{\beta\gamma\delta}^{(1)} C_{\gamma\delta\varepsilon\phi}^{(2)} T_{\varepsilon\phi\lambda}^{(2)} \alpha_{\lambda\eta}^{(1)} \mathscr{E}_{0\eta}$ which can be interpreted as follows: the incident light wave field $\mathscr{E}_{0\eta}$ induces on molecule 1 an oscillating dipole moment $\alpha_{\lambda\eta}^{(1)} \mathscr{E}_{0\eta}$, which in turn gives rise to an oscillating field gradient at molecule 2 through the third rank T-tensor $T_{\varepsilon\phi\lambda}^{(2)}$. This field gradient results in an oscillating quadrupole on molecule 2 as described by $C_{\gamma\delta\varepsilon\phi}^{(2)}$, this quadrupole moment now making an additional oscillating field contribution at molecule 1.

Now that we have found the expression of the field $F_\beta^{(1)}$ at molecule1, the expression of the corresponding field gradient $F_{\beta\gamma}^{(1)}$ must be found. Using the approximation of Couling and Graham [9], where they concluded that by neglecting oscillating quadrupole moments and the higher multipole moments, and substituting the expression of $\mu_\alpha^{(2)}$ into equation (2.39) yields only two terms of $F_{\beta\gamma}^{(1)}$ whose contribution to B_ρ was found to be significant enough

for retention. Thus, we have

$$F^{(1)}_{\beta\gamma} = T^{(1)}_{\beta\gamma\delta}\alpha^{(2)}_{\delta\varepsilon}\mathcal{E}_{0\varepsilon} + T^{(1)}_{\beta\gamma\delta}\alpha^{(2)}_{\delta\varepsilon}T^{(1)}_{\varepsilon\phi}\alpha^{(1)}_{\phi\lambda}\mathcal{E}_{0\lambda} + \cdots. \tag{2.49}$$

Substituting equations (2.48) and (2.49) into equation (2.38) yields

$$\begin{aligned}\mu^{(1)}_{\alpha}(\mathcal{E}_0) = {} & \alpha^{(1)}_{\alpha\eta}\mathcal{E}_{0\eta} + \alpha^{(1)}_{\alpha\beta}T_{\beta\gamma}\alpha^{(2)}_{\gamma\eta}\mathcal{E}_{0\eta} + \alpha^{(1)}_{\alpha\beta}T_{\beta\gamma}\alpha^{(2)}_{\gamma\delta}T_{\delta\varepsilon}\alpha^{(1)}_{\varepsilon\eta}\mathcal{E}_{0\eta} \\ & + \alpha^{(1)}_{\alpha\beta}T_{\beta\gamma}\alpha^{(2)}_{\gamma\delta}T_{\delta\varepsilon}\alpha^{(1)}_{\varepsilon\eta}T_{\beta\lambda}\alpha^{(2)}_{\lambda\eta}\mathcal{E}_{0\eta} - \tfrac{1}{3}\alpha^{(1)}_{\alpha\beta}T_{\beta\gamma}A^{(2)}_{\eta\gamma\delta}\mathcal{E}_{0\eta} \\ & + \tfrac{1}{3}\alpha^{(1)}_{\alpha\beta}T_{\beta\gamma}\alpha^{(2)}_{\gamma\delta}T^{(1)}_{\delta\varepsilon\phi}A^{(1)}_{\eta\varepsilon\phi}\mathcal{E}_{0\eta} - \tfrac{1}{3}\alpha^{(1)}_{\alpha\beta}T_{\beta\gamma}A^{(2)}_{\gamma\delta\varepsilon}T^{(1)}_{\delta\varepsilon\phi}\alpha^{(1)}_{\phi\eta}\mathcal{E}_{0\eta} \\ & - \tfrac{1}{3}\alpha^{(1)}_{\alpha\beta}T^{(1)}_{\beta\gamma\delta}A^{(2)}_{\gamma\delta\varepsilon}T_{\varepsilon\phi}\alpha^{(1)}_{\phi\eta}\mathcal{E}_{0\eta} + \tfrac{1}{3}\alpha^{(1)}_{\alpha\beta}T^{(1)}_{\beta\gamma\delta}C^{(2)}_{\gamma\delta\varepsilon\phi}T^{(1)}_{\varepsilon\phi\lambda}\alpha^{(1)}_{\lambda\eta}\mathcal{E}_{0\eta} \\ & + \tfrac{1}{3}A^{(1)}_{\alpha\beta\gamma}T^{(1)}_{\beta\gamma\delta}\alpha^{(2)}_{\eta\delta}\mathcal{E}_{0\eta} + \tfrac{1}{3}A^{(1)}_{\alpha\beta\gamma}T^{(1)}_{\beta\gamma\delta}\alpha^{(2)}_{\delta\varepsilon}T_{\varepsilon\phi}\alpha^{(1)}_{\phi\eta}\mathcal{E}_{0\eta} + \cdots,\end{aligned} \tag{2.50}$$

which is the expression of the induced electric dipole moment on molecule 1 in terms of molecular property tensors. In order to obtain an expression of the differential polarizability $\pi^{(1)}_{\alpha\beta}$ which is defined in equation (2.12), we need to differentiate equation (2.50) with respect to $\mathcal{E}_{0\eta}$.

$$\begin{aligned}\pi^{(p)}_{\alpha\eta} = {} & \alpha^{(p)}_{\alpha\eta} + \alpha^{(p)}_{\alpha\beta}T_{\beta\gamma}\alpha^{(q)}_{\gamma\eta} + \alpha^{(p)}_{\alpha\beta}T_{\beta\gamma}\alpha^{(q)}_{\gamma\delta}T_{\delta\varepsilon}\alpha^{(p)}_{\varepsilon\eta} \\ & + \alpha^{(p)}_{\alpha\beta}T_{\beta\gamma}\alpha^{(q)}_{\gamma\delta}T_{\delta\varepsilon}\alpha^{(p)}_{\varepsilon\phi}T_{\phi\lambda}\alpha^{(q)}_{\lambda\eta} - \tfrac{1}{3}\alpha^{(p)}_{\alpha\beta}T^{(p)}_{\beta\gamma\delta}A^{(q)}_{\eta\gamma\delta} \\ & + \tfrac{1}{3}\alpha^{(p)}_{\alpha\beta}T_{\beta\gamma}\alpha^{(q)}_{\gamma\delta}T^{(p)}_{\delta\varepsilon\phi}A^{(p)}_{\eta\varepsilon\phi} - \tfrac{1}{3}\alpha^{(p)}_{\alpha\beta}T_{\beta\gamma}A^{(q)}_{\gamma\delta\varepsilon}T^{(p)}_{\delta\varepsilon\phi}\alpha^{(p)}_{\phi\eta} \\ & - \tfrac{1}{3}\alpha^{(p)}_{\alpha\beta}T^{(p)}_{\beta\gamma\delta}A^{(q)}_{\gamma\delta\varepsilon}T_{\varepsilon\phi}\alpha^{(p)}_{\phi\eta} + \tfrac{1}{3}\alpha^{(p)}_{\alpha\beta}T^{(p)}_{\beta\gamma\delta}C^{(q)}_{\gamma\delta\varepsilon\phi}T^{(p)}_{\varepsilon\phi\lambda}\alpha^{(p)}_{\lambda\eta} \\ & + \tfrac{1}{3}A^{(p)}_{\alpha\beta\gamma}T^{(p)}_{\beta\gamma\delta}\alpha^{(q)}_{\delta\eta} + \tfrac{1}{3}A^{(p)}_{\alpha\beta\gamma}T^{(p)}_{\beta\gamma\delta}\alpha^{(q)}_{\delta\varepsilon}T_{\varepsilon\phi}\alpha^{(p)}_{\phi\eta} + \cdots\end{aligned} \tag{2.51}$$

where p and q imply molecules p and q respectively. Now using equation (2.51) above in equation (2.32) yields

$$\rho = \frac{a_2 + a_3 + a_4 + a_5 + a_2 A_1 + a_3 A_1 + a_3 C_1 + \cdots}{b_2 + b_3} \tag{2.52}$$

where

$$a_2 = \left\langle \alpha^{(1)}_{zx} \alpha^{(1)}_{zx} \right\rangle + \left\langle \alpha^{(1)}_{zx} \alpha^{(2)}_{zx} \right\rangle, \tag{2.53}$$

$$a_3 = 2\left\langle \alpha^{(1)}_{zx} \alpha^{(1)}_{z\beta} T_{\beta\gamma} \alpha^{(2)}_{\gamma x} \right\rangle + 2\left\langle \alpha^{(1)}_{zx} \alpha^{(2)}_{z\beta} T_{\beta\gamma} \alpha^{(1)}_{\gamma x} \right\rangle, \tag{2.54}$$

$$\begin{aligned} a_4 = {} & \left\langle \alpha^{(1)}_{z\beta} T_{\beta\gamma} \alpha^{(2)}_{\beta x} \alpha^{(2)}_{z\delta} T_{\delta\varepsilon} \alpha^{(1)}_{\varepsilon x} \right\rangle + \left\langle \alpha^{(1)}_{z\beta} T_{\beta\gamma} \alpha^{(2)}_{\gamma x} \alpha^{(1)}_{z\delta} T_{\delta\varepsilon} \alpha^{(2)}_{\varepsilon x} \right\rangle \\ & + 2\left\langle \alpha^{(1)}_{zx} \alpha^{(2)}_{z\beta} T_{\beta\gamma} \alpha^{(1)}_{\gamma\delta} T_{\delta\varepsilon} \alpha^{(2)}_{\varepsilon x} \right\rangle + 2\left\langle \alpha^{(1)}_{zx} \alpha^{(1)}_{z\beta} T_{\beta\gamma} \alpha^{(2)}_{\gamma\delta} T_{\delta\varepsilon} \alpha^{(1)}_{\varepsilon x} \right\rangle, \end{aligned} \tag{2.55}$$

$$\begin{aligned} a_5 = {} & 2\left\langle \alpha^{(1)}_{zx} \alpha^{(1)}_{z\beta} T_{\beta\gamma} \alpha^{(2)}_{\gamma\delta} T_{\delta\varepsilon} \alpha^{(1)}_{\varepsilon\phi} T_{\phi\lambda} \alpha^{(2)}_{\lambda x} \right\rangle \\ & + 2\left\langle \alpha^{(1)}_{zx} \alpha^{(2)}_{z\beta} T_{\beta\gamma} \alpha^{(1)}_{\gamma\delta} T_{\delta\varepsilon} \alpha^{(2)}_{\varepsilon\phi} T_{\phi\lambda} \alpha^{(1)}_{\lambda x} \right\rangle \\ & + 2\left\langle \alpha^{(1)}_{z\beta} T_{\beta\gamma} \alpha^{(2)}_{\gamma x} \alpha^{(1)}_{z\delta} T_{\delta\varepsilon} \alpha^{(2)}_{\varepsilon\phi} T_{\phi\lambda} \alpha^{(1)}_{\lambda x} \right\rangle \\ & + 2\left\langle \alpha^{(1)}_{z\beta} T_{\beta\gamma} \alpha^{(2)}_{\gamma x} \alpha^{(2)}_{z\delta} T_{\delta\varepsilon} \alpha^{(1)}_{\varepsilon\phi} T_{\phi\lambda} \alpha^{(2)}_{\lambda x} \right\rangle, \end{aligned} \tag{2.56}$$

$$\begin{aligned} a_2 A_1 = {} & -\tfrac{2}{3}\left\langle \alpha^{(1)}_{zx} \alpha^{(1)}_{z\beta} T_{\beta\gamma\delta} A^{(2)}_{x\gamma\delta} \right\rangle + \tfrac{2}{3}\left\langle \alpha^{(1)}_{zx} \alpha^{(2)}_{z\beta} T_{\beta\gamma\delta} A^{(1)}_{x\gamma\delta} \right\rangle \\ & + \tfrac{2}{3}\left\langle \alpha^{(1)}_{zx} A^{(1)}_{z\beta\gamma} T_{\beta\gamma\delta} \alpha^{(2)}_{\delta x} \right\rangle - \tfrac{2}{3}\left\langle \alpha^{(1)}_{zx} A^{(2)}_{z\beta\gamma} T_{\beta\gamma\delta} \alpha^{(1)}_{\delta x} \right\rangle, \end{aligned} \tag{2.57}$$

$$
\begin{aligned}
a_3 A_1 = & -\tfrac{2}{3}\left\langle \alpha^{(1)}_{zx}\alpha^{(1)}_{z\beta} T_{\beta\gamma} A^{(2)}_{\gamma\delta\varepsilon} T_{\delta\varepsilon\phi}\alpha^{(1)}_{\phi x}\right\rangle + \tfrac{2}{3}\left\langle \alpha^{(1)}_{zx}\alpha^{(2)}_{z\beta} T_{\beta\gamma} A^{(1)}_{\gamma\delta\varepsilon} T_{\delta\varepsilon\phi}\alpha^{(2)}_{\phi x}\right\rangle \\
& -\tfrac{2}{3}\left\langle \alpha^{(1)}_{zx}\alpha^{(1)}_{z\beta} T_{\beta\gamma\delta} A^{(2)}_{\varepsilon\gamma\delta} T_{\varepsilon\phi}\alpha^{(1)}_{\phi x}\right\rangle + \tfrac{2}{3}\left\langle \alpha^{(1)}_{zx}\alpha^{(2)}_{z\beta} T_{\beta\gamma\delta} A^{(1)}_{\varepsilon\gamma\delta} T_{\varepsilon\phi}\alpha^{(2)}_{\phi x}\right\rangle \\
& +\tfrac{2}{3}\left\langle \alpha^{(1)}_{zx} A^{(1)}_{z\beta\lambda} T_{\beta\gamma\delta}\alpha^{(2)}_{\delta\varepsilon} T_{\varepsilon\phi}\alpha^{(1)}_{\phi x}\right\rangle - \tfrac{2}{3}\left\langle \alpha^{(1)}_{zx} A^{(2)}_{z\beta\lambda} T_{\beta\gamma\delta}\alpha^{(1)}_{\delta\varepsilon} T_{\varepsilon\phi}\alpha^{(2)}_{\phi x}\right\rangle \\
& +\tfrac{2}{3}\left\langle \alpha^{(1)}_{zx}\alpha^{(1)}_{z\beta} T_{\beta\gamma}\alpha^{(2)}_{\gamma\delta} T_{\delta\varepsilon\phi} A^{(1)}_{x\varepsilon\phi}\right\rangle - \tfrac{2}{3}\left\langle \alpha^{(1)}_{zx}\alpha^{(2)}_{z\beta} T_{\beta\gamma}\alpha^{(1)}_{\gamma\delta} T_{\delta\varepsilon\phi} A^{(2)}_{x\varepsilon\phi}\right\rangle \\
& -\tfrac{2}{3}\left\langle \alpha^{(1)}_{z\beta} T_{\beta\gamma}\alpha^{(2)}_{\gamma x}\alpha^{(1)}_{z\delta} T_{\delta\varepsilon\phi} A^{(2)}_{x\varepsilon\phi}\right\rangle + \tfrac{2}{3}\left\langle \alpha^{(1)}_{z\beta} T_{\beta\gamma}\alpha^{(2)}_{\gamma x}\alpha^{(2)}_{z\delta} T_{\delta\varepsilon\phi} A^{(1)}_{x\varepsilon\phi}\right\rangle \\
& +\tfrac{2}{3}\left\langle \alpha^{(1)}_{z\beta} T_{\beta\gamma}\alpha^{(2)}_{\gamma x} A^{(1)}_{z\delta\varepsilon} T_{\delta\varepsilon\phi}\alpha^{(2)}_{x\varepsilon\phi}\right\rangle - \tfrac{2}{3}\left\langle \alpha^{(1)}_{z\beta} T_{\beta\gamma}\alpha^{(2)}_{\gamma x} A^{(2)}_{z\delta\varepsilon} T_{\delta\varepsilon\phi}\alpha^{(1)}_{x\varepsilon\phi}\right\rangle,
\end{aligned}
\tag{2.58}
$$

$$
\begin{aligned}
a_3 C_1 = & -\tfrac{1}{3}\left\langle \alpha^{(1)}_{zx}\alpha^{(1)}_{z\beta} T_{\beta\gamma\delta} C^{(2)}_{\gamma\delta\varepsilon\phi} T_{\varepsilon\phi\lambda}\alpha^{(1)}_{\lambda x}\right\rangle \\
& +\tfrac{1}{3}\left\langle \alpha^{(1)}_{z\beta} T_{\beta\gamma\delta} C^{(2)}_{\gamma\delta\varepsilon\phi} T_{\varepsilon\phi\lambda}\alpha^{(1)}_{\lambda x}\alpha^{(1)}_{zx}\right\rangle \\
& +\tfrac{1}{3}\left\langle \alpha^{(1)}_{zx}\alpha^{(2)}_{z\beta} T_{\beta\gamma\delta} C^{(1)}_{\gamma\delta\varepsilon\phi} T_{\varepsilon\phi\lambda}\alpha^{(2)}_{\lambda x}\right\rangle \\
& +\tfrac{1}{3}\left\langle \alpha^{(1)}_{z\beta} T_{\beta\gamma\delta} C^{(2)}_{\gamma\delta\varepsilon\phi} T_{\varepsilon\phi\lambda}\alpha^{(1)}_{\lambda x}\alpha^{(2)}_{zx}\right\rangle,
\end{aligned}
\tag{2.59}
$$

$$
b_2 = \left\langle \alpha^{(1)}_{xx}\alpha^{(1)}_{xx}\right\rangle + \left\langle \alpha^{(1)}_{xx}\alpha^{(2)}_{xx}\cos\chi_{12}\right\rangle, \tag{2.60}
$$

and

$$
b_3 = \left\langle \alpha^{(1)}_{xx}\alpha^{(1)}_{x\beta} T_{\beta\gamma}\alpha^{(2)}_{\gamma x}\right\rangle + \left\langle \alpha^{(1)}_{xx}\alpha^{(2)}_{x\beta} T_{\beta\gamma}\alpha^{(1)}_{\gamma x}\right\rangle. \tag{2.61}
$$

The tensors in the above terms are expressed in the spaced-fixed axes (x,y,z). They must be projected into the molecule fixed axes (1,2,3) of molecule 1. To proceed, explicit forms of the tensors $T_{\alpha\beta}$, $T_{\alpha\beta\gamma}$, $\alpha_{\alpha\beta}$, $A_{\alpha\beta\gamma}$ and $C_{\alpha\beta\gamma\delta}$ are required.

2.3.2 The molecular tensor theory of B_ρ for linear molecules

The figure below indicates the parameters required to describe the relative configuration of two linear molecules. These are the four parameters R, θ_1, θ_2 and φ. R is the separation between centres of the two molecules (R is sometimes referred to as the line of centres) with λ being a unit vector along vector $\boldsymbol{R}$. Here 3 and 3' have been chosen as the principal axes of molecules 1 and 2 respectively, and θ_1 and θ_2 as the angles between 3-axis and the line of centres and the 3'-axis and the line of centres, respectively.

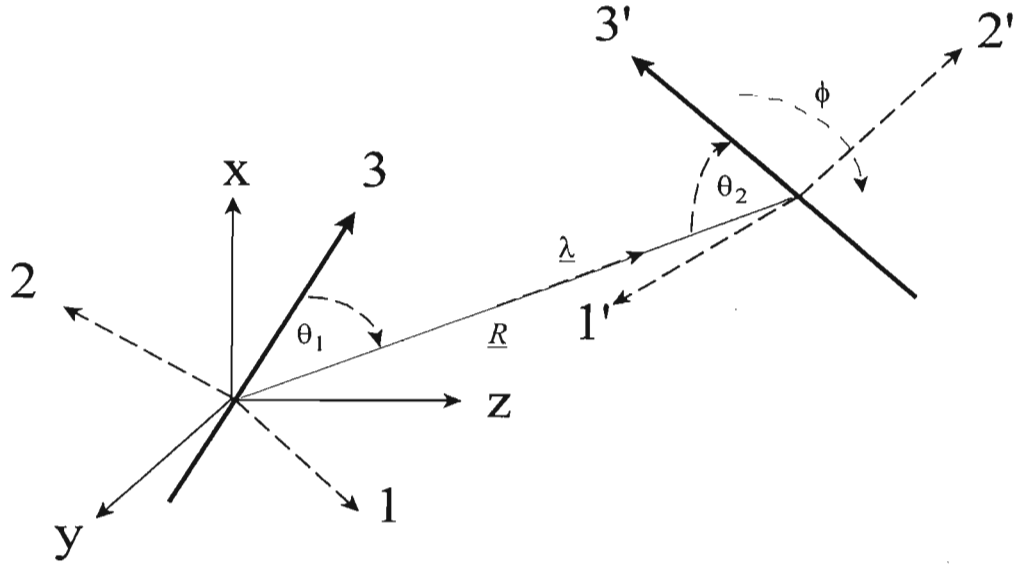

Figure 2.2. The coordinates R,θ_1, θ_2 and φ used to describe the relative configuration τ of two axially-symmetric molecules.

To exploit the symmetry of a molecule, its physical property tensors must be referred to a system of molecule-fixed axes. However, the experimental measurement of the depolarization ratio ρ is performed in the space-fixed system of axes which is oriented with

respect to the direction of propagation of the incident light beam. As a molecule in the gas sample tumbles in space, its set of molecule-fixed axes is continually changing with respect to the space-fixed axes. The average projection of the molecule's tensor properties in the space-fixed axes is obtained by (i) referring the molecular property tensors to molecule-fixed axes, (ii) projecting these tensors into the space-fixed axes, and (iii) averaging the projection over the orientational motion of the molecule.

The truncated virial expansion of the depolarization ratio ρ,

$$\rho = \rho_0 + \frac{B_\rho}{V_m}, \tag{2.63}$$

which describes the contribution of intermolecular pair interactions to ρ, requires us to obtain the explicit form of B_ρ. Initially we will consider only linear and quasi-linear molecules. Thereafter, the molecular tensor theory is extended to accommodate calculations of B_ρ for non-linear molecules.

The molecular property tensors such as $\alpha_{\alpha\beta}$ are referred to the space-fixed axes (x,y,z), and must now be projected into molecule 1's molecule-fixed axes (1,2,3). The procedure to be adopted has already been illustrated earlier in section 2.2: see equations (2.15) to (2.29). For example, the first term in the expression of a_2 that appears in equation (2.53) has its projected form given in equation (2.15), this result being obtained using the normal tensor projection procedure. In equation (2.15), a_i^α is the direction cosine between the α space-fixed axis and the i molecule-fixed axis.

For a molecule with a three-fold or higher rotation axis, let this axis coincide with the 3-axis

of the molecule-fixed system (1,2,3). The tensor $\alpha_{ij}^{(1)}$ is then diagonal, with components as given in equation (2.21):

$$\alpha_{ij}^{(1)} = \begin{bmatrix} \alpha_\perp & 0 & 0 \\ 0 & \alpha_\perp & 0 \\ 0 & 0 & \alpha_\parallel \end{bmatrix}. \tag{2.64}$$

Now recall equation (2.15):

$$\left\langle \alpha_{zx}^{(1)} \alpha_{zx}^{(1)} \right\rangle = \alpha_{ij}^{(1)} \alpha_{kl}^{(1)} \left\langle a_i^z a_k^z a_j^x a_l^x \right\rangle.$$

Here, $\left\langle \alpha_i^z \alpha_k^z \alpha_j^x \alpha_l^x \right\rangle$ is the average over all isotropic orientations of molecule 1 in the space-fixed axes, and this expression can be further simplified [18] to yield the results in equation (2.17) where δ_{ij} is the Kronecker delta.

Recall that mean polarizability for linear molecules is

$$\alpha = \tfrac{1}{3}\left(2\alpha_\perp + \alpha_\parallel\right). \tag{2.65}$$

Our goal is to obtain the explicit forms of all the averages appearing in equation (2.52) in terms of these diagonal elements and the interaction parameters R, θ_1, θ_2 and ϕ. These terms are all projected from the space-fixed system of axes (x,y,z) into molecule 1's molecule-fixed axes (1,2,3). This has already been achieved for the terms a_2 and b_2 in equations (2.19) and (2.26), respectively.

We use the first term of a_5 as an example in illustrating the tensor-projection procedure for the higher-order terms.

$$\begin{aligned}
&\left\langle \alpha^{(1)}_{zx}\alpha^{(1)}_{z\beta}T_{\beta\gamma}\alpha^{(2)}_{\gamma\delta}T_{\delta\varepsilon}\alpha^{(1)}_{\varepsilon\phi}T_{\phi\lambda}\alpha^{(2)}_{\lambda x}\right\rangle \\
&= \left\langle \alpha^{(1)}_{ij}a_i^z a_j^x \alpha^{(1)}_{kl}a_k^z a_l^z T_{mn}a_m^\beta a_n^\gamma \alpha^{(2)}_{pq}a_p^\gamma a_q^\delta T_{rs}a_r^\delta a_s^\varepsilon \alpha^{(1)}_{tu}a_t^\varepsilon a_u^\phi T_{\upsilon\omega}a_\upsilon^\phi a_\omega^\lambda \alpha^{(2)}_{gh}a_g^\lambda a_h^x \right\rangle \qquad (2.66)\\
&= \left\langle \alpha^{(1)}_{ij}\alpha^{(1)}_{km}T_{mn}\alpha^{(2)}_{nr}T_{rs}\alpha^{(1)}_{sv}T_{vw}\alpha^{(2)}_{wh}\right\rangle \left\langle a_i^z a_k^z a_j^x a_h^x \right\rangle .
\end{aligned}$$

The remaining terms are treated in a similar way. The term in the first pair of angular brackets in equation (2.66) is a constant as the interaction configuration is assumed fixed. Therefore, when allowing an isotropic rotation of the pair of molecules as a rigid whole, the projection into (x,y,z) of this pair property (referred to (1,2,3)) can be averaged over all orientations. Averaging over the interaction parameters may subsequently be carried out. We have

$$\begin{aligned}
&\left\langle \alpha^{(1)}_{zx}\alpha^{(1)}_{z\beta}T_{\beta\gamma}\alpha^{(2)}_{\gamma\delta}T_{\delta\varepsilon}\alpha^{(1)}_{\varepsilon\phi}T_{\phi\lambda}\alpha^{(2)}_{\lambda x}\right\rangle \\
&= \tfrac{1}{30}\left(4\delta_{ik}\delta_{jh} - \delta_{ij}\delta_{kh} - \delta_{ih}\delta_{jk}\right)\left\langle \alpha^{(1)}_{ij}\alpha^{(1)}_{km}T_{mn}\alpha^{(2)}_{nr}T_{rs}\alpha^{(1)}_{sv}T_{vw}\alpha^{(2)}_{wh}\right\rangle \qquad (2.67)\\
&= \tfrac{1}{30}\left\langle \alpha^{(1)}_{ij}\alpha^{(1)}_{im}T_{mn}\alpha^{(2)}_{nr}T_{rs}\alpha^{(1)}_{sv}T_{vw}\alpha^{(2)}_{wj} - \alpha^{(1)}_{ii}\alpha^{(1)}_{km}T_{mn}\alpha^{(2)}_{nr}T_{rs}\alpha^{(1)}_{sv}T_{vw}\alpha^{(2)}_{wk}\right\rangle
\end{aligned}$$

where the angular brackets indicate an average over the pair interaction coordinates R, θ_1, θ_2 and φ according to the general relationship

$$\langle X\rangle = \int_\tau X P(\tau)d\tau \, . \qquad (2.68)$$

Here the probability $P(\tau)$ at τ is related to the intermolecular potential energy $U_{12}(\tau)$ by

$$P(\tau) = \frac{N_A}{\Omega V_m}\exp\left\{-\frac{U_{12}(\tau)}{kT}\right\} \qquad (2.69)$$

where $\Omega = \frac{1}{V_m}\int d\tau$ is the integral over the orientational coordinates of the neighbouring

molecule 2. Substituting equation (2.69) into equation (2.68) yields

$$\langle X \rangle = \frac{N_A}{2V_m} \int_{R=0}^{\infty} \int_{\theta_1=0}^{\pi} \int_{\theta_2=0}^{\pi} \int_{\phi=0}^{2\pi} X \exp\left\{ -U_{12}(\tau) \Big/ kT \right\} R^2 dR \sin\theta_1 \sin\theta_2 d\theta_1 d\theta_2 d\phi . \qquad (2.70)$$

In order to further simplify equation (2.67), the explicit forms of $\alpha_{ij}^{(1)}$, $\alpha_{ij}^{(2)}$, $T_{ij}^{(1)}$ and $T_{ij}^{(2)}$ are required. These are found to contain redundant interaction parameters $l_1^{(1)}$, $l_2^{(2)}$, λ_1 and λ_2. However, there are well established relationships between this set of parameters and the direction cosines such that their elimination can be systematically achieved [11]:

$$a_i^{3'} = l_i^{(2)}, \qquad (2.71)$$

$$l_1^{(2)} l_2^{(2)} = l_3^{(2)} = \cos\theta_{12} = -\cos\theta_1 \cos\theta_2 + \sin\theta_1 \sin\theta_2 \cos\phi, \qquad (2.72)$$

$$l_i^{(1)} \lambda_i = \lambda_3 = \cos\theta_1, \qquad (2.73)$$

$$l_2^{(2)} \lambda_i = -\cos\theta_2, \qquad (2.74)$$

$$\begin{aligned} \alpha_{ij}^{(2)} &= \alpha_\perp \delta_{ij} + (\alpha_\parallel - \alpha_\perp) l_i^{(2)} l_j^{(2)} \\ &= \alpha(1-\kappa)\delta_{ij} + 3\kappa\alpha l_i^{(2)} l_j^{(2)}. \end{aligned} \qquad (2.75)$$

We mention again that the tensors $\alpha_{ij}^{(1)}$ and $\alpha_{i'j'}^{(2)}$ are diagonal in their own orthogonal axes (1,2,3) and (1',2',3') respectively, with elements, $\alpha_{11} = \alpha_{22} = \alpha_\perp$ and $\alpha_{33} = \alpha_\parallel$ for linear and quasi-linear molecules.

The second and the third rank T-tensors are [12]

$$T_{ij} = \frac{1}{4\pi\varepsilon_0}\frac{1}{R^3}(3\lambda_i\lambda_j - \delta_{\alpha\beta}), \tag{2.76}$$

and

$$T_{ijk} = \frac{1}{4\pi\varepsilon_0}\frac{1}{R^4}\left[5\lambda_i\lambda_j\lambda_k - (\lambda_i\delta_{jk} + \lambda_i\delta_{i\gamma} + \lambda_k\delta_{\alpha\beta})\right]. \tag{2.77}$$

Hence, Benoît and Stockmayer [26] were able to show that

$$\left\langle \alpha_{zx}^{(1)}\alpha_{zx}^{(2)} \right\rangle = \tfrac{1}{30}\left(\alpha_{\parallel} - \alpha_{\perp}\right)^2\left\langle 3\cos^2\theta_{12} - 1\right\rangle \tag{2.78}$$

and

$$\left\langle \alpha_{xx}^{(1)}\alpha_{xx}^{(2)}\cos\chi_{12} \right\rangle = \tfrac{1}{15}\tfrac{2}{3}\left(\alpha_{\parallel} - \alpha_{\perp}\right)^2\left\langle 3\cos^2\theta_{12} - 1\right\rangle + \alpha^2\left(\frac{-2B}{V_m}\right), \tag{2.79}$$

where B is the normal second pressure virial coefficient. It should be noted that equations (2.78) and (2.79) are the second terms of a_2 and b_2, respectively. We now have the explicit forms of the a_2 and b_2 terms of equation (2.52):

$$a_2 = \tfrac{1}{15}\left(\alpha_{\parallel} - \alpha_{\perp}\right)^2 + \tfrac{1}{30}\left(\alpha_{\parallel} - \alpha_{\perp}\right)^2\left\langle 3\cos^2\theta_{12} - 1\right\rangle, \tag{2.80}$$

and

$$b_2 = \alpha^2 + \tfrac{4}{45}\left(\alpha_{\parallel} - \alpha_{\perp}\right)^2 + \tfrac{2}{45}\left(\alpha_{\parallel} - \alpha_{\perp}\right)^2\left\langle 3\cos^2\theta_{12} - 1\right\rangle + \alpha^2\left(\frac{-2B}{V_m}\right). \tag{2.81}$$

To obtain the averages of all the terms in equations (2.53) to (2.61) according to equation

(2.69), we must eliminate $l_1^{(2)}, l_1^{(2)}, \lambda_1$ and λ_2 from the expanded forms of these expressions. This was achieved by using the Macsyma symbolic manipulation package, which performs piecemeal substitution of powers and multiples of the parameters [20]:

$$d = \lambda_1^2 + \lambda_2^2 = \left(1 - \cos^2\theta_1\right), \tag{2.82}$$

$$e = \left(l_1^{(2)}\right)^2 + \left(l_2^{(2)}\right)^2 = \left(1 - \cos^2\theta_{12}\right), \tag{2.83}$$

and

$$f = l_1^{(2)}\lambda_1 + l_2^{(2)}\lambda_2 = -\cos\theta_2 - \cos\theta_1\cos\theta_{12}. \tag{2.84}$$

Once the expressions for $a_2, a_3, a_4, a_5, a_2A_1, a_3A_1$ and a_3C_1 have been obtained (see Appendix B for examples of the explicit forms), they are gathered into equation (2.52) for ρ, which takes the form

$$\rho = \frac{\left[\begin{array}{l} \frac{1}{15}(\Delta\alpha)^2 + \frac{1}{30}(\Delta\alpha)^2\left\langle 3\cos^2\theta_{12} - 1\right\rangle + \dfrac{\alpha^3}{30(4\pi\varepsilon_0)}a_3' + \dfrac{\alpha^4}{30(4\pi\varepsilon_0)^2}a_4' \\ + \dfrac{\alpha^5}{30(4\pi\varepsilon_0)^3}a_5' + \dfrac{\alpha^2}{60(4\pi\varepsilon_0)}a_2A_1' + \dfrac{\alpha^3}{60(4\pi\varepsilon_0)}a_3A_1' + \dfrac{3\alpha^3}{30(4\pi\varepsilon_0)^2}a_3C_1' + \cdots \end{array}\right]}{\left[\frac{1}{15}\left(15\alpha^2 + \frac{4}{3}(\Delta\alpha)^2\right) + \frac{2}{45}(\Delta\alpha)^2\left\langle 3\cos^2\theta_{12} - 1\right\rangle + \dfrac{\alpha^3}{30(4\pi\varepsilon_0)}b_3' + \alpha^2\left(\dfrac{-2B}{V_m}\right)\right]}. \tag{2.85}$$

Here a_3' represents that part of a_3 which is contained within the angular brackets see equation (B.1), with similar definitions for $a_4', \cdots, a_3C_1'$. Equation (2.85) must now be expressed in the virial form of equation (2.31). For linear molecules, $\Delta\alpha = \alpha_\parallel - \alpha_\perp$, so

that from equations (2.22) and (2.27) we have

$$\rho_0 = \frac{3(\Delta\alpha)^2}{45\alpha^2 + 4(\Delta\alpha)^2}.$$

Equation (2.85) can now be further rearranged to yield

$$\rho = \rho_0 \frac{\left[1 + \frac{1}{2}\left\langle 3\cos^2\theta_{12} - 1\right\rangle + \frac{\alpha^3}{2(4\pi\varepsilon_0)(\Delta\alpha)^2} a_3' + \frac{\alpha^4}{2(4\pi\varepsilon_0)^2(\Delta\alpha)^2} a_4' + \frac{\alpha^5}{2(4\pi\varepsilon_0)^3(\Delta\alpha)^2} a_5' \right.}{\left. + \frac{\alpha^2}{2(4\pi\varepsilon_0)(\Delta\alpha)^2} a_2 A_1' + \frac{\alpha^3}{2(4\pi\varepsilon_0)^2(\Delta\alpha)^2} a_3 A_1' + \frac{3\alpha^3}{2(4\pi\varepsilon_0)^2} a_3 C_1' + O\left(\frac{1}{V_m^2}\right)\right]} \qquad (2.86)$$
$$\{1 + \frac{4}{3}\rho_0[\frac{1}{2}\left\langle 3\cos^2\theta_{12} - 1\right\rangle + \frac{3\alpha^3}{8(4\pi\varepsilon_0)(\Delta\alpha)^2} b_3' + \frac{2B}{V_m} + O\left(\frac{1}{V_m^2}\right)]\}$$

This reduces to

$$\rho = \rho_0 + \rho_0\left(1 - \frac{4}{3}\rho_0\right)\left[\begin{array}{l} \frac{2B}{V_m} + \frac{1}{2}\left\langle 3\cos^2\theta_{12} - 1\right\rangle + \frac{\alpha\left(1+\frac{4}{5}\kappa^2\right)}{18(4\pi\varepsilon_0)\kappa^2} a_3' + \frac{\alpha^2\left(1+\frac{4}{5}\kappa^2\right)}{18(4\pi\varepsilon_0)^2\kappa^2} a_4' \\ + \frac{\alpha^3\left(1+\frac{4}{5}\kappa^2\right)}{18(4\pi\varepsilon_0)^3\kappa^2} a_5' + \frac{\left(1+\frac{4}{5}\kappa^2\right)}{18(4\pi\varepsilon_0)\kappa^2} a_2' A_1' + \frac{\alpha\left(1+\frac{4}{5}\kappa^2\right)}{18(4\pi\varepsilon_0)^2\kappa^2} a_3' A_1' + \frac{\alpha\left(1+\frac{4}{5}\kappa^2\right)}{6(4\pi\varepsilon_0)^2\kappa^2} a_3' C_1' \\ - \frac{\alpha}{30(4\pi\varepsilon_0)} b_3' + O\left(\frac{1}{V_m^2}\right) \end{array}\right]. \qquad (2.87)$$

It follows from equations (2.87) and (2.31) that

$$B_\rho = \rho_0\left(1 - \frac{4}{3}\rho_0\right)(2B + G + a_3 + a_4 + a_5 + a_2 A_1 + a_3 A_1 + a_3 C_1 + b_3 + \cdots) \qquad (2.88)$$

where

$$G = \frac{1}{2}\left\langle 3\cos^2\theta_{12} - 1\right\rangle V_m, \qquad (2.89)$$

$$a_3 = \frac{\alpha\left(1 + \frac{4}{3}\kappa^2\right)}{18(4\pi\varepsilon_0)\kappa^2} V_m a_3', \qquad (2.90)$$

$$a_4 = \frac{\alpha^2\left(1+\frac{4}{5}\kappa^2\right)}{18(4\pi\varepsilon_0)^2\kappa^2}V_m a_4', \tag{2.91}$$

$$a_5 = \frac{\alpha^3\left(1+\frac{4}{5}\kappa^2\right)}{18(4\pi\varepsilon_0)^3\kappa^2}V_m a_5', \tag{2.92}$$

$$a_2 A_1 = \frac{\left(1+\frac{4}{3}\kappa^2\right)}{18(4\pi\varepsilon_0)\kappa^2}V_m a_2 A_1', \tag{2.93}$$

$$a_3 A_1 = \frac{\alpha(1+\frac{4}{5}\kappa^2)}{18(4\pi\varepsilon_0)^2}V_m a_3 A_1', \tag{2.94}$$

$$a_3 C_1 = \frac{\alpha\left(1+\frac{4}{5}\kappa^2\right)}{6(4\pi\varepsilon_0)^2\kappa^2}V_m a_3 C_1', \tag{2.95}$$

and

$$b_3 = -\frac{\alpha}{30(4\pi\varepsilon_0)}V_m b_3'. \tag{2.96}$$

From equation (2.88) it can be seen that experimental measurement of ρ allows a value of B_ρ to be extracted from a plot of ρ versus V_m^{-1}. Knowledge of ρ_0, which is the y-intercept of the plot, allows the value of

$$B_\rho' = \left(2B + G + a_3 + a_4 + a_5 + a_2 A_1 + a_3 A_1 + a_3 C_1 + b_3 + \cdots\right) \tag{2.97}$$

to be deduced. The presence of $2B$ in this expression for B_ρ' can mask the more interesting contributions from the remaining terms, which are summed to allow comparison with $2B$, giving

$$B_\rho' = \left(2B + S_\rho\right) \tag{2.98}$$

where the sum S_ρ arises purely from angular correlation and dipole-dipole, field-gradient, and induced quadrupole moment effects in the molecular interaction.

All known calculated and experimentally deduced values of B_ρ and S_ρ for linear and quasi-linear molecules are summarized in table 2.1.

2.3.3 The molecular tensor theory of B_ρ for nonlinear molecules

As for linear molecules, the physical property tensors of nonlinear molecules are referred to molecule-fixed axes in order to exploit molecular symmetry. There are seven parameters which are used to fully describe the relative configuration of a pair of interacting nonlinear molecules. These are R, α_1, β_1, γ_1, α_2, β_2 and γ_2, and they are now discussed in turn. R is the displacement between the two molecular centres, and is initially chosen to lie along the z-axis of the space-fixed axes for convenience. The parameters α_n, β_n and γ_n, (where n is 1 and 2 for molecules 1 and 2, respectively) are the three Euler angles which are used to specify the relative orientation of the molecule-fixed axes of molecule n relative to the space-fixed axes. To rotate molecule 1's molecule-fixed axes (1,2,3) into the space-fixed axes (x,y,z), for example, three successive rotations are required [14]:

(a) rotation about the 3-axis through an angle α_1 $\left(0 \le \alpha_1 \le 2\pi\right)$,

(b) rotation about the new 2'-axis through an angle β_1 $\left(0 \leq \beta_1 \leq \pi\right)$,

(c) rotation about the new 3"-axis (co-inciding with the z-axis) through an angle γ_1 $\left(0 \leq \gamma_1 \leq 2\pi\right)$.

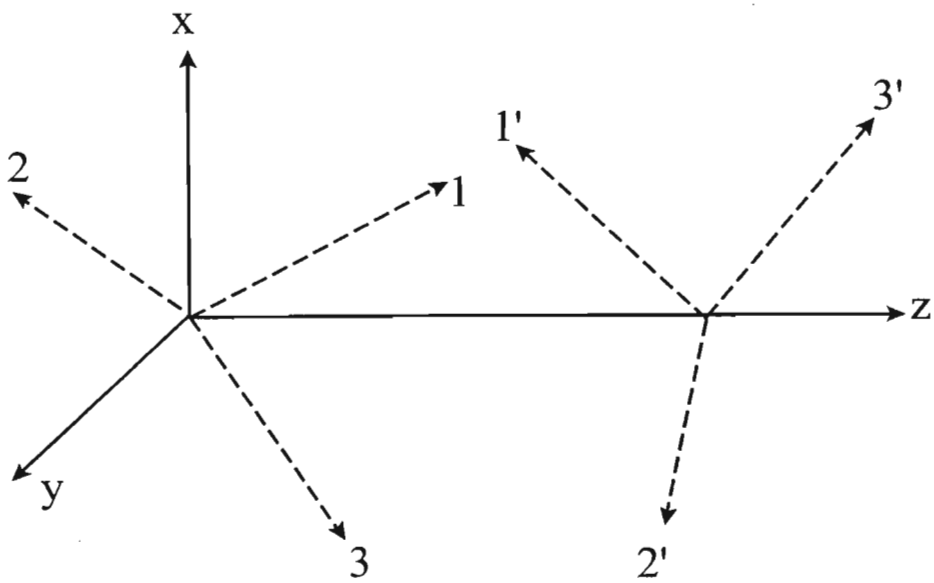

Figure 2.3. The molecule-fixed axes (1,2,3) and (1',2',3') of interacting molecules 1 and 2 respectively. The space-fixed axes are (x,y,z). The molecule-fixed axes generally change constantly in orientation with respect to the space-fixed axes as the molecules randomly tumble in space.

Hence, the *nine* direction cosines a_i^{α} which are required to fully describe the relative orientation of the molecule-fixed system of axes with respect to (x,y,z) can now be expressed as functions of the *three* Euler angles α_1, β_1 and γ_1. We have [22,35]

$$a_i^{\alpha} = \begin{bmatrix} \cos\gamma_1 & \sin\gamma_1 & 0 \\ -\sin\gamma_1 & \cos\gamma_1 & 0 \\ 0 & 0 & 1 \end{bmatrix} \begin{bmatrix} \cos\beta_1 & 0 & -\sin\beta_1 \\ 0 & 1 & 0 \\ \sin\beta_1 & 0 & \cos\beta_1 \end{bmatrix} \begin{bmatrix} \cos\alpha_1 & \sin\alpha_1 & 0 \\ -\sin\alpha_1 & \cos\alpha_1 & 0 \\ 0 & 0 & 1 \end{bmatrix}$$

$$= \begin{bmatrix} \cos\alpha_1\cos\beta_1\cos\gamma_1 - \sin\alpha_1\sin\gamma_1 & \sin\alpha_1\cos\beta_1\cos\gamma_1 + \cos\alpha_1\sin\gamma_1 & -\sin\beta_1\cos\gamma_1 \\ -\cos\alpha_1\cos\beta_1\sin\gamma_1 - \sin\alpha_1\cos\gamma_1 & -\sin\alpha_1\cos\beta_1\sin\gamma_1 + \cos\alpha_1\cos\gamma_1 & \sin\beta_1\sin\gamma_1 \\ \cos\alpha_1\sin\beta_1 & \sin\alpha_1\sin\beta_1 & \cos\beta_1 \end{bmatrix}. \quad (2.99)$$

The nine direction cosines a_i^{α} required to describe the relative orientations of the molecule-fixed axes of molecule 2, (1',2',3'), and the space-fixed system of axes (x,y,z) are written in an analogous manner, with subscript 1 replaced with subscript 2:

$$a_{i'}^{\alpha} = \begin{bmatrix} \cos\alpha_2\cos\beta_2\cos\gamma_2 - \sin\alpha_2\sin\gamma_2 & \sin\alpha_2\cos\beta_2\cos\gamma_2 + \cos\alpha_2\sin\gamma_2 & -\sin\beta_2\cos\gamma_2 \\ -\cos\alpha_2\cos\beta_2\sin\gamma_2 - \sin\alpha_2\cos\gamma_2 & -\sin\alpha_2\cos\beta_2\sin\gamma_2 + \cos\alpha_2\cos\gamma_2 & \sin\beta_2\sin\gamma_2 \\ \cos\alpha_2\sin\beta_2 & \sin\alpha_2\sin\beta_2 & \cos\beta_2 \end{bmatrix} \quad (2.100)$$

In their calculations of B_ρ for the nonlinear molecule SO_2, Couling and Graham omitted the A- and C- tensor components [23]. This was because there were no available literature values for these tensor components. The contribution arising from $a_3 C_1$ term towards B_ρ was found to be less than 1% for all linear molecules studied thus far [20], and so it appears that this term can be safely omitted for nonlinear molecules as well. However, the $a_2 A_1$ term, which exists only for polar molecules, was found to sometimes make significant contributions to B_ρ for linear molecules of as much as 9% [20], and ought to be included in a full treatment. The higher order $a_3 A_1$ term contributes less than 1% to B_ρ for all the linear molecules investigated

[20], the A-tensor series having rapidly converged. In this work, we were fortunate to have obtained from Professor Mark Spackman [40] *ab initio* calculated estimates of the A-tensor components of the non-linear polar molecule under investigation, namely dimethyl ether. The inclusion of this additional contribution to B_ρ will ensure a better theoretical estimation of this second virial coefficient. The a_3C_1 and a_3A_1 terms have been omitted since, as already discussed above, their contributions to B_ρ are negligible compared to those of the other terms.

The analysis is quite similar to the treatment of the linear and quasi-linear molecules. The averages of $a_2, a_3, a_4, a_5, a_2A_1, b_2$ and b_3 must be expressed both in terms of the components of the diagonal tensors $\alpha_{ij}^{(1)} = \alpha_{i'j'}^{(2)}$ and the seven interaction parameters R, α_1, α_2, β_1, β_2, γ_1 and γ_2 as in figure 2.3 on page 31.

As with linear-molecules, all tensors are initially referred to the molecule-fixed axes (1,2,3) of molecule 1. This ensures that for a given relative configuration of the pair of molecules, the tensor product in (1,2,3) is fixed. Then, when the pair of molecules is allowed to rotate isotropically as a rigid whole in the space-fixed axes (x,y,z), the average projection into (x,y,z) of this pair property (referred to (1,2,3)) can be averaged over all orientations, the average $\langle X \rangle$ of the pair property X over the interaction coordinates following from the probability $P(\tau)$ as defined in equation (2.69):

$$\langle X \rangle = \frac{N_A}{16\pi^3 V_m} \int_{R=0}^{\infty} \int_{\alpha_1=0}^{2\pi} \int_{\beta_1=0}^{\pi} \int_{\gamma_1=0}^{2\pi} \int_{\alpha_2=0}^{2\pi} \int_{\beta_2=0}^{\pi} \int_{\gamma_2=0}^{2\pi} X e^{-\frac{U_{12}(\tau)}{kT}} R^2 \sin\beta_1 \sin\beta_2 dR d\alpha_1 d\beta_1 d\gamma_1 d\alpha_2 d\beta_2 d\gamma_2 . \quad (2.101)$$

The term $\langle \alpha_{zx}^{(1)} \alpha_{zx}^{(2)} \rangle$ from equation (2.53) is now referred to molecule-fixed axes:

$$\left\langle \alpha_{zx}^{(1)} \alpha_{zx}^{(2)} \right\rangle = \left\langle \alpha_{ij}^{(1)} \alpha_{kl}^{(2)} \right\rangle \left\langle a_i^z a_j^x a_k^z a_l^x \right\rangle = \tfrac{1}{30} \left\langle 3\alpha_{ij}^{(1)} \alpha_{ij}^{(2)} - 9\alpha^{2} \right\rangle \tag{2.102}$$

where $\alpha_{ij}^{(2)}$ is the polarizability tensor of molecule 2 expressed in the molecule-fixed axes of molecule 1. In order to obtain the explicit form of what is contained within the angular brackets in equation (2.102), use must be made of the definitions of a_i^{α} and $a_{i'}^{\alpha}$, the notation of which is abbreviated by writing

$$a_i^{\alpha} = \begin{bmatrix} A_1 & A_2 & A_3 \\ A_4 & A_5 & A_6 \\ A_7 & A_8 & A_9 \end{bmatrix} \quad \text{and} \quad a_{i'}^{\alpha} = \begin{bmatrix} B_1 & B_2 & B_3 \\ B_4 & B_5 & B_6 \\ B_7 & B_8 & B_9 \end{bmatrix}, \tag{2.103}$$

where

$$A_1 = \cos\alpha_1 \cos\beta_1 \cos\gamma_1 - \sin\alpha_1 \sin\gamma_1, \tag{2.104}$$

$$B_1 = \cos\alpha_2 \cos\beta_2 \cos\gamma_2 - \sin\alpha_2 \sin\gamma_2, \tag{2.105}$$

$$A_2 = \sin\alpha_1 \cos\beta_1 \cos\gamma_1 + \cos\alpha_1 \sin\gamma_1, \tag{2.106}$$

$$B_2 = \sin\alpha_2 \cos\beta_2 \cos\gamma_2 + \cos\alpha_2 \sin\gamma_2, \tag{2.107}$$

$$A_3 = -\sin\beta_1 \cos\gamma_1, \tag{2.108}$$

$$B_3 = -\sin\beta_2 \cos\gamma_2, \tag{2.109}$$

$$A_4 = -\cos\alpha_1 \cos\beta_1 \sin\gamma_1 - \sin\alpha_1 \cos\gamma_1, \tag{2.110}$$

$$B_4 = -\cos\alpha_2 \cos\beta_2 \sin\gamma_2 - \sin\alpha_2 \cos\gamma_2, \tag{2.111}$$

$$A_5 = -\sin\alpha_1 \cos\beta_1 \sin\gamma_1 + \cos\alpha_1 \cos\gamma_1, \tag{2.112}$$

$$B_5 = -\sin\alpha_2 \cos\beta_2 \sin\gamma_2 + \cos\alpha_2 \cos\gamma_2, \tag{2.113}$$

$$A_6 = \sin\beta_1 \sin\gamma_1, \tag{2.114}$$

$$B_6 = \sin\beta_2 \sin\gamma_2, \tag{2.115}$$

$$A_7 = \cos\alpha_1 \sin\beta_1, \tag{2.116}$$

$$B_7 = \cos\alpha_2 \sin\beta_2, \tag{2.117}$$

$$A_8 = \sin\alpha_1 \sin\beta_1, \tag{2.118}$$

$$B_8 = \sin\alpha_2 \sin\beta_2, \tag{2.119}$$

$$A_9 = \cos\beta_1, \tag{2.120}$$

$$B_9 = \cos\beta_2. \tag{2.121}$$

It follows from the above that the dynamic polarizability tensor of molecule 2 in molecule 1's

molecule fixed axes (1,2,3), namely $\alpha_{ij}^{(2)}$, is

$$\alpha_{ij}^{(2)} = a_{\alpha}^{i} a_{\beta}^{j} a_{i'}^{\alpha} a_{j'}^{\beta} \alpha_{i'j'}^{(2)} = \begin{bmatrix} Z_{11} & Z_{12} & Z_{13} \\ Z_{12} & Z_{22} & Z_{23} \\ Z_{13} & Z_{23} & Z_{33} \end{bmatrix} \tag{2.122}$$

where a_{α}^{i} may be viewed as the transpose of equation (2.103), but this is taken care of by the summation indices. Now since the

$$\alpha_{i'j'}^{(2)} = \alpha_{ij}^{(1)} = \begin{bmatrix} \alpha_{11} & 0 & 0 \\ 0 & \alpha_{22} & 0 \\ 0 & 0 & \alpha_{33} \end{bmatrix}, \tag{2.123}$$

coefficients Z_{11}, Z_{12}, Z_{13}, $\cdots$, Z_{33} are:

$$\begin{aligned} Z_{11} = \alpha_{11}[&A_1^2 B_1^2 + A_4^2 B_4^2 + A_7^2 B_7^2 + 2A_1 A_4 B_1 B_4 + 2A_7 B_7 (A_4 B_4 + A_1 B_1)] \\ +\alpha_{22}[&A_1^2 B_2^2 + A_4^2 B_5^2 + A_7^2 B_8^2 + 2A_1 A_4 B_2 B_5 + 2A_7 B_8 (A_4 B_5 + A_1 B_2)] \\ +\alpha_{33}[&A_1^2 B_3^2 + A_4^2 B_6^2 + A_7^2 B_9^2 + 2A_1 A_4 B_3 B_6 + 2A_7 B_9 (A_4 B_6 + A_1 B_3)], \end{aligned} \tag{2.124}$$

$$\begin{aligned} Z_{22} = \alpha_{11}[&A_2^2 B_1^2 + A_5^2 B_4^2 + A_8^2 B_7^2 + 2A_2 A_5 B_1 B_4 + 2A_8 B_7 (A_5 B_4 + A_2 B_1)] \\ +\alpha_{22}[&A_2^2 B_2^2 + A_5^2 B_5^2 + A_8^2 B_8^2 + 2A_2 A_5 B_2 B_5 + 2A_8 B_8 (A_5 B_5 + A_2 B_2)] \\ +\alpha_{33}[&A_2^2 B_3^2 + A_5^2 B_6^2 + A_8^2 B_9^2 + 2A_2 A_5 B_3 B_6 + 2A_8 B_9 (A_5 B_6 + A_2 B_3)], \end{aligned} \tag{2.125}$$

$$
\begin{aligned}
Z_{33} = \alpha_{11}[&A_3^2B_1^2 + A_6^2B_4^2 + A_9^2B_7^2 + 2A_3A_6B_1B_4 + 2A_9B_7\left(A_6B_4 + A_3B_1\right)] \\
&+\alpha_{22}[A_3^2B_2^2 + A_6^2B_5^2 + A_9^2B_8^2 + 2A_3A_6B_2B_5 + 2A_9B_8\left(A_6B_5 + A_3B_2\right)] \\
&+\alpha_{33}[A_3^2B_3^2 + A_6^2B_6^2 + A_9^2B_9^2 + 2A_3A_6B_3B_6 + 2A_9B_9\left(A_6B_6 + A_3B_3\right)],
\end{aligned}
\tag{2.126}
$$

$$
\begin{aligned}
Z_{12} = \alpha_{11}[&A_1A_2B_1^2 + A_4A_5B_4^2 + A_7A_8B_7^2 + B_1B_4\left(A_1A_5 + A_2A_4\right) \\
&+B_7(B_4(A_4A_8 + A_5A_7) + B_1(A_1A_8 + A_2A_7))] + \alpha_{22}[A_1A_2B_2^2 \\
&+A_4A_5B_5^2 + A_7A_8B_8^2 + B_2B_5\left(A_1A_5 + A_2A_4\right) + B_8(B_5(A_4A_8 + A_5A_7) \\
&+B_2(A_1A_8 + A_2A_7))] + \alpha_{33}[A_1A_2B_3^2 + A_4A_5B_6^2 + A_7A_8B_9^2 \\
&+B_3B_6\left(A_1A_5 + A_2A_4\right) + B_9(B_6(A_4A_8 + A_5A_7) \\
&+B_3(A_1A_8 + A_2A_7))],
\end{aligned}
\tag{2.127}
$$

$$
\begin{aligned}
Z_{13} = \alpha_{11}[&A_1A_3B_1^2 + A_4A_6B_4^2 + A_7A_9B_7^2 + B_1B_4\left(A_1A_6 + A_3A_4\right) \\
&+B_7(B_4(A_4A_9 + A_6A_7) + B_1(A_1A_9 + A_3A_7))] + \alpha_{22}[A_1A_3B_2^2 \\
&+A_4A_6B_5^2 + A_7A_9B_8^2 + B_2B_5\left(A_1A_6 + A_3A_4\right) + B_8(B_5(A_4A_9 + A_6A_7) \\
&+B_2(A_1A_9 + A_3A_7))] + \alpha_{33}[A_1A_3B_3^2 + A_4A_6B_6^2 + A_7A_9B_9^2 \\
&+B_3B_6\left(A_1A_6 + A_3A_4\right) + B_9(B_6(A_4A_9 + A_6A_7) \\
&+B_3(A_1A_9 + A_3A_7))],
\end{aligned}
\tag{2.128}
$$

$$
\begin{aligned}
Z_{23} = \alpha_{11}[&A_2A_3B_1^2 + A_5A_6B_4^2 + A_8A_9B_7^2 + B_1B_4\left(A_2A_6 + A_3A_5\right) \\
&+B_7(B_4(A_5A_9 + A_6A_8) + B_1(A_2A_9 + A_3A_8))] + \alpha_{22}[A_2A_3B_2^2 \\
&+A_5A_6B_5^2 + A_8A_9B_8^2 + B_2B_5\left(A_2A_6 + A_3A_5\right) + B_8(B_5(A_5A_9 + A_6A_8) \\
&+B_2(A_2A_9 + A_3A_8))] + \alpha_{33}[A_2A_3B_3^2 + A_5A_6B_6^2 + A_8A_9B_9^2 \\
&+B_3B_6\left(A_2A_6 + A_3A_5\right) + B_9(B_6(A_5A_9 + A_6A_8) + B_3(A_2A_9 + A_3A_8))].
\end{aligned}
\tag{2.129}
$$

Now the term $\left\langle 3\alpha_{ij}^{(1)}\alpha_{ij}^{(2)} - 9\alpha^2 \right\rangle$ that appears in equation (2.102) is expressed in terms of those tensor components of equation (2.122) and (2.123) to yield

$$\left\langle 3\alpha_{ij}^{(1)}\alpha_{ij}^{(2)} - 9\alpha^2 \right\rangle = \left\langle 3\left(\alpha_{11}Z_{11} + \alpha_{22}Z_{22} + \alpha_{33}Z_{33}\right) - 9\alpha^2 \right\rangle. \tag{2.130}$$

Therefore equation (2.102) becomes

$$\left\langle \alpha_{zx}^{(1)}\alpha_{zx}^{(2)} \right\rangle = \frac{1}{30}\left\langle 3\left(\alpha_{11}Z_{11} + \alpha_{22}Z_{22} + \alpha_{33}Z_{33}\right) - 9\alpha^2 \right\rangle \tag{2.131}$$

which is the second term of a_2 in equation (2.53). The second term, $\left\langle \alpha_{xx}^{(1)}\alpha_{xx}^{(2)} \cos\chi_{12} \right\rangle$, of b_2 in equation (2.60) was treated by Couling and Graham [25] in an analogous manner to that of Bonoît and Stockmayer [26], yielding

$$\left\langle \alpha_{xx}^{(1)}\alpha_{xx}^{(2)} \cos\chi_{12} \right\rangle = \frac{2}{45}\left\langle \alpha_{ij}^{(1)}\alpha_{ij}^{(2)} - 9\alpha^2 \right\rangle + \alpha^2\left(-\frac{2B}{V_m}\right) \tag{2.132}$$

where B is the normal pressure virial coefficient.

Since the explicit forms of $\alpha_{ij}^{(1)}$ and $\alpha_{ij}^{(2)}$ are available in equation (2.123) and (2.122) respectively, we can invoke the Macsyma symbolic manipulation package to simplify equation (2.132). The higher-order terms can also be referred to (1,2,3) in a similar manner, as is now illustrated with a particular example, namely the first term of equation (2.56):

$$\begin{aligned}&\left\langle \alpha_{zx}^{(1)}\alpha_{z\beta}^{(1)}T_{\beta\gamma}\alpha_{\gamma\delta}^{(2)}T_{\delta\varepsilon}\alpha_{\varepsilon\phi}^{(1)}T_{\phi\lambda}\alpha_{\lambda x}^{(2)} \right\rangle \\ &= \frac{1}{30}\left\langle 3\alpha_{ij}^{(1)}\alpha_{im}^{(1)}T_{mn}\alpha_{nr}^{(2)}T_{rs}\alpha_{sv}^{(1)}T_{vw}\alpha_{wj}^{(2)} - 3\alpha_{ii}^{(1)}\alpha_{km}^{(1)}T_{mn}\alpha_{nr}^{(2)}T_{rs}\alpha_{sv}^{(1)}T_{vw}\alpha_{wk}^{(2)} \right\rangle\end{aligned} \tag{2.133}$$

where the angular brackets indicate an average over the pair interaction coordinates $R,\alpha_1,\beta_1,\gamma_1,\alpha_2,\beta_2$ and γ_2. The T-tensor $T_{\alpha\beta}$ is given in equation (2.40), where it is referred to the space-fixed axes (x,y,z). Projecting this T-tensor into molecule-fixed axes yields

$$T_{ij} = \alpha^i_\alpha \alpha^j_\beta T_{\alpha\beta} = \frac{1}{4\pi\varepsilon_0}\frac{1}{R^3}\begin{bmatrix} T_{11} & T_{12} & T_{13} \\ T_{12} & T_{22} & T_{23} \\ T_{13} & T_{23} & T_{33} \end{bmatrix} \tag{2.134}$$

where

$$\left.\begin{aligned} T_{11} &= 2A_7^2 - A_4^2 - A_1^2, \\ T_{22} &= 2A_8^2 - A_5^2 - A_2^2, \\ T_{33} &= 2A_9^2 - A_6^2 - A_3^2, \\ T_{12} &= 2A_7A_8 - A_4A_5 - A_1A_2, \\ T_{13} &= 2A_7A_9 - A_4A_6 - A_1A_3, \\ T_{23} &= 2A_8A_9 - A_5A_6 - A_2A_3. \end{aligned}\right\} \tag{2.135}$$

Using these results, the Macsyma tensor manipulation facilities are able to evaluate the averages of b_2, b_3, a_3, a_4, a_5 and a_2A_1. The simplified expressions of these terms are not quoted in this work because some of them are extremely lengthy, taking several pages each. Nevertheless, once they are substituted into equation (2.52), the following general expression is obtained:

$$\rho = \frac{\left(\begin{array}{l} \frac{1}{15}(\Delta\alpha)^2 + \frac{1}{30}g' + \frac{1}{30}(4\pi\varepsilon_0)^{-1}a_3' + \frac{1}{30}(4\pi\varepsilon_0)^{-2}a_4' + \frac{1}{30}(4\pi\varepsilon_0)^{-3}a_5' \\ + \frac{3}{90}(4\pi\varepsilon_0)^{-1}a_2A_1' + \ldots \end{array}\right)}{\left(\alpha^2 + \frac{4}{45}(\Delta\alpha)^2 + \frac{1}{15}\frac{2}{3}g' + \alpha^2\left[\frac{-2B}{V_m}\right] + \frac{1}{15}(4\pi\varepsilon_0)^{-1}b_3'\right)}. \tag{2.136}$$

Now, recalling that

$$\rho_0 = \frac{3(\Delta\alpha)^2}{45\alpha^2 + 4(\Delta\alpha)^2},$$

equation (2.136) can be written as

$$\rho = \frac{\rho_0\left\{1 + \frac{1}{2(\Delta\alpha)^2}g' + \frac{(4\pi\varepsilon_0)^{-1}}{2(\Delta\alpha)^2}a_3' + \frac{(4\pi\varepsilon_0)^{-2}}{2(\Delta\alpha)^2}a_4' + \frac{(4\pi\varepsilon_0)^{-3}}{2(\Delta\alpha)^2}a_5' + \frac{(4\pi\varepsilon_0)^{-1}}{2(\Delta\alpha)^2}a_2A_1' + \frac{2B}{V_m} + O\left(\frac{1}{V_m^2}\right)\right\}}{1 + \frac{4}{3}\rho_0\left\{\frac{1}{2(\Delta\alpha)^2}g' + \frac{3(4\pi\varepsilon_0)^{-1}}{2(\Delta\alpha)^2}b_3' + \frac{2B}{V_m}\right\}}, \quad (2.137)$$

which reduces to

$$\rho = \rho_0 + \rho_0(1 - \tfrac{4}{3}\rho_0)(2B + g + a_3 + a_4 + a_5 + a_2A_1 + b_3 + \ldots),$$

this being in the form of virial expansion. Extraction of the second light-scattering virial coefficient B_ρ is a simple matter:

$$B_\rho = \rho_0\left(1 - \tfrac{4}{3}\rho_0\right)(2B + g + a_3 + a_4 + a_5 + a_2A_1 + b_3 + \ldots), \quad (2.138)$$

where B is the normal pressure virial coefficient, and where

$$g = \frac{1}{2(\Delta\alpha)^2}V_m g', \quad (2.139)$$

$$a_3 = \left\{\frac{1}{2(\Delta\alpha)^2} + \frac{2}{48\alpha^2}\right\}(4\pi\varepsilon_0)^{-1}V_m a_3', \quad (2.140)$$

$$a_4 = \left\{\frac{1}{2(\Delta\alpha)^2} + \frac{2}{45\alpha^2}\right\}(4\pi\varepsilon_0)^{-2} V_m a_4', \tag{2.141}$$

$$a_5 = \left\{\frac{1}{2(\Delta\alpha)^2} + \frac{2}{45\alpha^2}\right\}(4\pi\varepsilon_0)^{-3} V_m a_5', \tag{2.142}$$

$$a_2 A_1 = \left\{\frac{1}{2(\Delta\alpha)^2} + \frac{2}{45\alpha^2}\right\}(4\pi\varepsilon_0)^{-1} V_m A_2 a_1', \tag{2.143}$$

and

$$b_3 = -\tfrac{1}{15}\tfrac{1}{\alpha^2}(4\pi\varepsilon_0)^{-1} V_m b_3'. \tag{2.144}$$

As with the normal second pressure virial coefficient B, the coefficients in equations (2.139) to (2.144) are independent of the molar volume but dependent on temperature. g' in equation (2.139) is the expression given by equation (2.130), while b_3' is that part of b_3 that is contained within the angular brackets (see Appendix C), with similar definitions for a_2', a_3', a_4', a_5' and a_2A_1'. Plotting a graph of ρ versus V_m^{-1} from experimentally measured values of ρ and V_m for a particular molecular species will enable us to extract the value of ρ_0, and hence deduce from equation (2.138) a value for

$$B_\rho' = (2B + g + a_3 + a_4 + a_5 + a_2 A_1 + b_3 + \cdots). \tag{2.145}$$

It is the sum of terms arising purely from angular correlation and collision-induced

polarizability anisotropy, namely

$$S_\rho = \left(g + a_3 + a_4 + a_5 + a_2 A_1 + b_3 + \cdots\right). \tag{2.146}$$

which is of interest; and to extract a precise value of this sum from the value of $B_\rho^{'}$ requires the ratio $\left(\frac{S_\rho}{2B}\right)$ to be of the order of unity or greater.

2.4 Evaluation of B_ρ by Numerical Integration

Evaluation of the average $\langle X \rangle$ of a quantity X over the pair interaction co-ordinates according to equations (2.70) and (2.101) has been achieved in this work by using the numerical integration method of Gaussian Quadrature. (For a detailed discussion of integration by Gaussian Quadrature, see [43]). The averaging requires the classical intermolecular potential energy $U_{12}(\tau)$. General tensor expressions for $U_{12}(\tau)$ have been derived by Buckingham [12], who evaluated them for the special case of interacting linear molecules in the configuration of figure 2.2. Couling and Graham [14] have subsequently evaluated them for the case of interacting nonlinear molecules as shown in figure 2.3. These interaction energies are now reviewed in full.

Buckingham and Utting [10] showed that for intermolecular separations R which are large relative to molecular dimensions, the pair interaction energy $U_{12}(\tau)$ has three components: the *electrostatic*, *induction* and London *dispersion* energies. The electrostatic energy arises from the interactions of the zero-field electric moments (charge, dipole, quadrupole, *etc.*) of

the two molecules. The induction energy arises from the distortion of the electronic structure of a molecule due to the permanent electric moments on the neighbouring molecule. The London dispersion energy arises from interactions of the electric moments due to fluctuations in the charge distributions of the two molecules.

These interaction energies are the result of long-range forces which are well understood [10,12,17], and which are evaluated on the assumption that the overlap of the molecular wave functions is small. Now, at small ranges of interaction where the electron clouds of the molecules do overlap significantly, the *ab initio* quantum-mechanical calculations [36] which would be required to take into account the intermediate-range exchange forces are prohibitively complicated (especially for many-electron atoms); and so it has been customary [4,16] to assume that the three interaction components mentioned above are applicable also to short-range interactions provided that an additional overlap energy term is added to account for the repulsive short-range interactions.

The general form of $U_{12}(\tau)$ used in our calculations is [11,12,14]

$$U_{12}(\tau) = U_{LJ} + U_{\mu,\mu} + U_{\mu,\theta} + U_{\theta,\theta} + U_{\mu,\mathrm{ind}\mu} + U_{\theta,\mathrm{ind}\mu} + U_{\mathrm{ind}\mu,\mathrm{ind}\mu} + U_{\mathrm{shape}} \qquad (2.147)$$

Here, U_{LJ} is the familiar Lennard-Jones 6:12 potential

$$U_{LJ} = 4\varepsilon\left[\left(\frac{R_0}{R}\right)^{12} - \left(\frac{R_0}{R}\right)^{6}\right], \qquad (2.148)$$

which is used to represent the dispersion and overlap energies. R is the intermolecular separation, R_0 and ε are the well-known Lennard-Jones parameters, the term $\left(\frac{R_0}{R}\right)^6$ describes

the attractive part of the potential, while $\left(\frac{R_0}{R}\right)^{12}$ describes the short-range repulsive part. $U_{\mu,\mu}, U_{\mu,\theta}$ and $U_{\theta,\theta}$ are the electrostatic dipole-dipole, dipole-quadrupole and quadrupole-quadrupole interaction energies of the two molecules, respectively, while $U_{\mu,ind\mu}$ and $U_{\theta,ind\mu}$ are the dipole-induced-dipole and quadrupole-induced-dipole interaction energies, respectively. Finally, U_{shape} is the shape energy which accounts for the angular dependence of short-range repulsive forces for non-spherical molecules. We have from Buckingham [12]

$$U_{\mu,\mu} = \mu_\alpha^{(1)} T_{\alpha\beta}^{(1)} \mu_\beta^{(2)}, \tag{2.149}$$

$$U_{\mu,\theta} = \tfrac{1}{3}\left(\mu_\alpha^{(1)} T_{\alpha\beta\gamma}^{(1)} \theta_{\beta\gamma}^{(2)} - \mu_\alpha^{(2)} T_{\alpha\beta\gamma}^{(1)} \theta_{\beta\gamma}^{(1)}\right), \tag{2.150}$$

$$U_{\theta,\theta} = \tfrac{1}{9}\theta_{\alpha\beta}^{(1)} T_{\alpha\beta\gamma\delta}^{(1)} \theta_{\gamma\delta}^{(2)}, \tag{2.151}$$

$$U_{\mu,\mathrm{ind}\mu} = -\tfrac{1}{2}\alpha\left(T_{\alpha\beta}^{(1)} \mu_\beta^{(2)} T_{\alpha\gamma}^{(1)} \mu_\gamma^{(2)} + T_{\alpha\beta}^{(1)} \mu_\beta^{(1)} T_{\alpha\gamma}^{(1)} \mu_\gamma^{(1)}\right), \tag{2.152}$$

$$U_{\theta,\mathrm{ind}\mu} = -\tfrac{1}{18}\alpha\left(T_{\alpha\beta\gamma}^{(1)} \theta_{\beta\gamma}^{(1)} T_{\alpha\delta\varepsilon}^{(1)} \theta_{\delta\varepsilon}^{(1)} + T_{\alpha\beta\gamma}^{(1)} \theta_{\beta\gamma}^{(2)} T_{\alpha\delta\varepsilon}^{(1)} \theta_{\delta\varepsilon}^{(2)}\right), \tag{2.153}$$

and

$$U_{\mathrm{ind}\mu,\mathrm{ind}\mu} = -\alpha^2 T_{\alpha\gamma}^{(1)} \mu_\gamma^{(1)} T_{\alpha\beta}^{(1)} T_{\beta\delta}^{(1)} \mu_\delta^{(2)}. \tag{2.154}$$

Below are given the explicit forms of these potential energies for two specific cases, namely interacting linear molecules, and interacting nonlinear molecules of either C_{2v} or D_{2h} symmetry.

2.4.1 The potential energy expressions for interacting linear molecules in the coordinate system shown in figure 2.2

$$U_{\mu,\mu} = \frac{1}{4\pi\varepsilon_0}\left\{\mu^2 R^{-3}\left(2\cos\theta_1\cos\theta_2 + \sin\theta_1\sin\theta_2\cos\phi\right)\right\}, \tag{2.155}$$

$$\begin{aligned} U_{\mu,\theta} = \frac{1}{4\pi\varepsilon_0}\{\tfrac{3}{2}\mu\theta R^{-4}[&\cos\theta_1\left(3\cos^2\theta_2 - 1\right) + \cos\theta_2\left(3\cos^2\theta_1 - 1\right) \\ &+2\sin\theta_1\sin\theta_2\cos\theta_2\cos\phi + 2\sin\theta_1\sin\theta_2\cos\theta_1\cos\phi]\}, \end{aligned} \tag{2.156}$$

$$\begin{aligned} U_{\theta,\theta} = \frac{1}{4\pi\varepsilon_0}\{\tfrac{3}{4}\theta^2 R^{-5}[&1 - 5\cos^2\theta_1 - 5\cos^2\theta_2 + 17\cos^2\theta_1\cos^2\theta_2 \\ &+2\sin^2\theta_1\sin^2\theta_2\cos^2\phi + 16\sin\theta_1\cos\theta_1\sin\theta_2\cos\theta_2\cos\phi]\}, \end{aligned} \tag{2.157}$$

$$U_{\mu,ind\mu} = \left(4\pi\varepsilon_0\right)^{-2}\{-\tfrac{1}{2}\alpha\mu^2 R^{-6}[\left(3\cos^2\theta_1 - 1\right) + \left(3\cos^2\theta_2 - 1\right)]\}, \tag{2.158}$$

$$U_{\theta,ind\mu} = \left(4\pi\varepsilon_0\right)^{-2}\{-\tfrac{9}{8}\alpha\theta^2 R^{-8}(4\cos^4\theta_1 + 4\cos^4\theta_2 + \sin^4\theta_1 + \cos^4\theta_2)\}, \tag{2.159}$$

$$U_{ind\mu,ind\mu} = (4\pi\varepsilon_0)^{-3}\{-\tfrac{1}{2}\alpha^2\mu^2 R^{-9}\{8\cos\theta_1\cos\theta_2 + \sin\theta_1\sin\theta_2\cos\phi\}, \quad (2.160)$$

and

$$U_{\text{shape}} = 4D\varepsilon\left(\frac{R_0}{R}\right)^{12}\left[3\cos^2\theta_1 + 3\cos^2\theta_2 - 2\right], \quad (2.161)$$

where D is a dimensionless parameter called the shape factor, and which lies in the range -0.25 to 0.5 to ensure that the R^{-12} term is always repulsive at short range [14].

2.4.2 The potential energy expressions for interacting nonlinear molecules in the coordinate system shown in figure 2.3

Since we will be considering the dimethyl ether molecule, which is of C_{2v} symmetry, we only present expressions for this particular symmetry point group. The 3-axis is taken to be the principal molecular axis, and so the dipole moment has only one independent component

$$\mu_i^{(1)} = \mu_{j'}^{(2)} = [0 \quad 0 \quad \mu_3], \quad (2.162)$$

while the traceless quadrupole moment has two independent components [12]

$$\theta_{ij}^{(1)} = \theta_{i'j'}^{(2)} = \begin{bmatrix} \theta_1 & 0 & 0 \\ 0 & \theta_2 & 0 \\ 0 & 0 & -\theta_1 - \theta_2 \end{bmatrix}. \quad (2.163)$$

The transformation from space-fixed axes (x,y,z) into molecule-fixed axes (1,2,3) or (1',2',3') is carried out as follows:

$$\mu_\alpha^{(1)} = a_i^\alpha \mu_i^{(1)}, \quad \mu_\alpha^{(2)} = a_{i'}^\alpha \mu_{i'}^{(2)}, \quad \theta_{\alpha\beta}^{(1)} = a_i^\alpha a_j^\beta \theta_{ij}^{(1)}, \quad \text{and} \quad \theta_{\alpha\beta}^{(2)} = a_{i'}^\alpha a_{j'}^\beta \theta_{i'j'}^{(2)}. \tag{2.164}$$

Invoking the tensor facilities of the Macsyma algebraic manipulation package, we obtain the following expressions:

$$U_{\mu,\mu} = \frac{1}{4\pi\varepsilon_0}\left\{\mu_3^2 R^{-3}\left(A_3B_3 + A_6B_6 - 2A_9B_9\right)\right\}, \tag{2.165}$$

$$\begin{aligned} U_{\mu,\theta} = \frac{1}{4\pi\varepsilon_0}\{&\mu_3 R^{-4}[\theta_1(A_9\left(-B_1^2 + B_3^2 - B_4^2 + B_6^2 + 2B_7^2 - 2B_9^2\right) \\ &+2B_3(A_1A_7 - A_3A_9) + 2B_6(A_4A_7 - A_6A_9) \\ &-2B_7(A_3B_1 - A_6B_4) + B_9(A_1^2 - A_3^2 + A_4^2 - A_6^2 - 2A_7^2 + 2A_9^2 \\ &+2A_3B_3 + 2A_6B_6)) + \theta_2(A_9(-B_2^2 + B_3^2 - B_5^2 + B_6^2 + 2B_8^2 \\ &-B_9^2) + 2B_3(A_2A_8 - A_3A_9) + 2B_6(A_5A_8 - A_6A_9) - 2B_8(A_3B_2 \\ &+A_6B_5) + B_9(A_2^2 - A_3^2 + A_5^2 - A_6^2 - 2A_8^2 + 2A_9^2 + 2A_3B_3 \\ &+2A_6B_6))]\}, \end{aligned} \tag{2.166}$$

$$\begin{aligned} U_{\theta,ind\mu} = (4\pi\varepsilon_0)^{-2}\{&-\tfrac{1}{2}\alpha R^{-8}[\theta_1^2(A_1^4 - 2A_1^2A_3^2 + A_3^4 + 2A_4^2\left(A_1^2 - A_3^2\right) + A_4^4 \\ &+2A_6^2(-A_1^2 + A_3^2 - A_4^2) + A_6^2 + 4A_7^2\left(A_3^2 + A_6^2\right) + 4A_7^4 - 8A_7A_9(A_1A_3 \\ &+A_4A_6) + 4A_9^2(A_1^2 + A_4^2 - 2A_7^2) + 4A_9^4) + \theta_2^2[A_2^4 - 2A_2^2A_3^2 + A_3^4 \\ &+2A_5^2\left(A_2^2 - A_3^2\right) + A_5^4 + 2A_6^2(-A_2^2 + A_3^2 - A_5^2) + A_6^4 + 4A_8^2\left(A_3^2 + A_6^2\right) \\ &+4A_8^4 - 8A_8A_9(A_2A_3 + A_5A_6) + 4A_9^2(A_2^2 + A_5^2 - 2A_8^2) + 4A_9^4) \\ &2\theta_1\theta_2(A_1^2A_2^2 - A_3^2(A_1^2 + A_2^2) + A_3^4 + A_4^2(A_2^2 - A_3^2) + A_5^4(A_1^2 - A_3^2 \\ &+A_4^2) - A_6^2(A_1^2 + A_2^2 - 2A_3^2 + A_4^2 + A_5^2) + A_6^4 + 2A_7^2(-A_2^2 + A_3^2 \\ &-A_5^2 + A_6^2) + 4A_7A_8(A_1A_2 + A_4A_5) + 2A_8^2(-A_1^2 + A_3^2 - A_4^2 + A_6^2 \\ &+2A_7^2) - 4A_9[A_7(A_1A_3 + A_4A_6) + A_8(A_2A_3 + A_5A_6)] + 2A_9^2(A_1^2 \\ &+A_2^2 + A_4^2 + A_5^2 - 2A_7^2 - 2A_8^2) + 4A_9^2)]\}, \end{aligned} \tag{2.167}$$

$$
\begin{aligned}
U_{\theta,\theta} = {} & \tfrac{1}{3}\tfrac{1}{4\pi\varepsilon_0}\{R^{-5}[\theta_1^2[B_1^2(3A_1^2-3A_3^2+A_4^2-A_6^2-4A_7^2+4A_9^2)+B_3^2(-3A_1^2 \\
& +3A_3^2-A_4^2+A_6^2+4A_7^2-4A_9^2)+B_4^2(A_1^2-A_3^2+3A_4^2-3A_6^2-4A_7^2 \\
& +4A_9^2)+4(A_3A_6-A_1A_4)(B_3B_6-B_1B_4)+B_6^2(-A_1^2+A_3^2-3A_4^2+3A_6^2 \\
& +4A_7^2-4A_9^2)+4(A_1^2-A_3^2+A_4^2-A_6^2-2A_7^2+2A_9^2)(B_9-B_7)(B_9+B_7) \\
& -16(A_3A_9-A_1A_7)(B_3B_9-B_1B_7)-16(A_6A_9-A_4A_7)(B_6B_9-B_4B_7)] \\
& +\theta_2^2[B_2^2(3A_2^2-3A_3^2+A_5^2-A_6^2-4A_8^2+4A_9^2)+B_3^2(-3A_2^2+3A_3^2-A_5^2 \\
& +A_6^2+4A_8^2-4A_9^2)+B_5^2(A_2^2-A_3^2+3A_5^2-3A_6^2-4A_8^2+4A_9^2) \\
& +4(A_3A_6-A_2A_5)(B_3B_6-B_2B_5)+B_6^2(-A_2^2+A_3^2-3A_5^2+3A_6^2+4A_8^2 \\
& -4A_9^2)+4(A_2^2-A_3^2+A_5^2-A_6^2-2A_8^2+2A_9^2)(B_9-B_8)(B_9+B_8) \\
& -16(A_3A_9-A_2A_8)(B_3B_9-B_2B_8)-16(A_6A_9-A_5A_8)(B_6B_9-B_5B_8)] \\
& +\theta_1\theta_2[B_1^2(3A_2^2-3A_3^2+A_5^2-A_6^2-4A_8^2+4A_9^2)+B_2^2(3A_1^2-3A_3^2+A_4^2 \\
& -A_6^2-4A_7^2+4A_9^2)+B_3^2[-3(A_1^2+A_2^2)+6A_3^2-A_4^2-A_5^2+2A_6^2 \\
& +4(A_7^2+A_8^2)-8A_9^2]-4B_1B_4(A_3A_6-A_2A_5)+B_4^2(A_2^2-A_3^2+3A_5^2 \\
& -3A_6^2-4A_8^2+4A_9^2)-4B_2B_5(A_3A_6-A_1A_4)+B_5^2(A_1^2-A_3^2+3A_4^2-3A_6^2 \\
& -4A_7^2+4A_9^2)+4B_3B_6(2A_3A_6-A_2A_5-A_1A_4)+B_6^2(-A_1^2-A_2^2+2A_3^2 \\
& -3(A_4^2+A_5^2)+6A_6^2+4(A_7^2+A_8^2)-8A_9^2]+16B_1B_7(A_3A_9-A_2A_8) \\
& +16B_4B_7(A_6A_9-A_5A_8)-4B_7^2(A_2^2-A_3^2+A_5^2-A_6^2-2A_8^2+2A_9^2) \\
& +16B_2B_8(A_3A_9-A_1A_7)+16B_5B_8(A_6A_9-A_4A_7)-4B_8^2(A_1^2-A_3^2+A_4^2 \\
& -A_6^2-2A_7^2+2A_9^2)-16B_3B_9(2A_3A_9-A_2A_8-A_1A_7) \\
& -16B_6B_9(2A_6A_9-A_5A_8-A_4A_7)+4B_9^2[A_1^2+A_2^2+A_5^2-2(A_3^2+A_6^2 \\
& +A_7^2+A_8^2)+4A_9^2))]\},
\end{aligned}
\tag{2.168}
$$

$$
U_{\mu,ind\mu} = \frac{1}{(4\pi\varepsilon_0)^2}\left\{-\tfrac{1}{2}\alpha\mu_3^2R^{-6}\left(3A_9^2+3B_9^2-2\right)\right\}, \tag{2.169}
$$

$$
\begin{aligned}
U_{ind\mu,ind\mu} = \tfrac{1}{2}\frac{1}{(4\pi\varepsilon_0)^2}\alpha R^{-8}\{&\theta_1^2[A_1^4 - 2A_1^2A_3^2 + 2A_4^2(A_1^2 - A_3^2) + A_4^4 + 2A_6^2(-A_1^2 \\
&A_3^2 - A_4^2) + A_6^4 + 4A_7^2(A_3^2 + A_6^2) + 4A_7^4 - 8A_7A_9(A_1A_3 - A_4A_6) \\
&+4A_9^2(A_1^2 + A_4^2 - 2A_7^2 + 4A_9^4] \\
&\theta_2^2[A_2^4 - 2A_2^2A_3^2 + A_3^4 + 2A_5^2(A_2^2 - A_3^2) \\
&+A_5^4 + 2A_6^2(-A_2^2 + A_3^2 - A_5^2) + A_6^4 + 4A_8^2(A_3^2 + A_6^2) + 4A_8^4 \\
&-8A_8A_9(A_2A_3 + A_5A_6) + 4A_9^2(A_2^2 + A_5^2 - 2A_8^2) + 4A_9^4] \\
&+2\theta_1\theta_2[A_1^2A_2^2 - A_3^2(A_1^2 + A_2^2) + A_3^4 + A_4^2(A_2^2 - A_3^2) + A_5^2(A_1^2 - A_3^2 \\
&+A_4^2) - A_6^2(A_2^2 - 2A_3^2 + A_4^2 + A_5^2) + A_6^2 + 2A_7^2(-2A_2^2 + A_3^2 \\
&-A_5^2 + A_6^2) + 4A_7A_8(A_1A_2 + A_4A_5) + 2A_8^2(-A_1^2 + A_3^2 - A_4^2 + A_6^2 \\
&+2A_7^2) - 4A_9[A_7(A_1A_3 + A_4A_6) + A_8(A_2A_3 + A_5A_6)] \\
&+2A_9^2(A_1^2 + A_2^2 + A_4^2 + A_5^2 - 2A_7^2 - 2A_8^2) + 4A_9^2]\},
\end{aligned}
\tag{2.170}
$$

and

$$
U_{\text{shape}} = 4\varepsilon\left(\frac{R_0}{R}\right)^{12}\left\{D_1\left[3\cos^2\beta_1 + 3\cos^2\beta_2 - 2\right] + D_2\left[3\sin^2\beta_1\cos^2\gamma_1 + 3\sin^2\beta_2\cos^2\gamma_2 - 2\right]\right\}, \tag{2.171}
$$

where D_1 and D_2 are dimensionless parameters called the shape factors: for axially-symmetric molecules, we set $D_2 = 0$ and recover Buckingham's shape potential. The above expressions are substituted into $U_{12}(\tau)$ in equation (2.147) for use in the averaging process, this being achieved using Macsyma: the A_n and B_n (where n is 1 to 9) were replaced by the explicit expressions as they appear in equations (2.104) to (2.121). Upon obtaining the final explicit form of $U_{12}(\tau)$, the resulting expression was translated directly into Fortran code using Macsyma itself. The programs for performing the numerical integration were written in Fortran. The integration limits for the orientation angles are given by the ranges of α_1, α_2, β_1, β_2, γ_1 and γ_2 as in equation (2.101). These ranges were divided into sixteen intervals each, while R was given a range of 0.1 nm to 3.0 nm divided into sixty four intervals.

The Fortran programs, an example of which is given in Appendix D, were run in double precision either on a Pentium II 450 MHz PC with 256 Mb of RAM using the fast University of Salford FTN95 compiler, or our Silicon Graphics Origin 200 workstation with twin MIPS R10 000 processors and 256 Mb of RAM. Program run times were typically of the order of 30 minutes each.

Through this process it was possible to determine all of the required numerical averages for the series of contributing terms to B_p.

2.5 Results of Calculations of B_p for Dimethyl Ether

2.5.1 Molecular properties of dimethyl ether

The molecular data used in the calculations of B_p of dimethyl ether are listed in table 2.2. This molecule belongs to the C_{2V} symmetry point group, and is taken to lie in the 1-3 plane of the molecule-fixed axes O(1,2,3), with 3 along the principal molecular axis.

In previous work on the non-linear molecule C_2H_4 [14], and for various non-linear molecules of C_{2v} symmetry [25], optimized values for the Lennard-Jones force constants R_0 and ε/k, and the shape factors D_1 and D_2, were obtained by fitting values of the second pressure virial coefficient $B(T)$ calculated according to

$$B(T) = \frac{N_A}{2} \int_{\tau} \left[1 - \exp\left(-U_{12}(\tau)/kT\right)\right] d\tau, \qquad (2.172)$$

to experimental data over a range of temperature. We have adopted the same procedure in this work for dimethyl ether, using the measured $B(T)$ data of Tripp and Dunlap [37] as a basis for the fitting procedure. The optimized force constants and shape factors are reported in table 2.2, while values of $B(T)$ calculated using these parameters are compared with the experimental data in table 2.3.

Table 2.2. Molecular properties used in the calculation of B_ρ for $(CH_3)_2O$. Dynamic polarizability tensor components are all at the wavelength of 514.5 nm.

Property	Value
R_0(nm)	0.47[a]
ε / k(K)	290.0[a]
D_1	-0.04926[a]
D_2	0.29666[a]
$10^{30}\mu_3$(Cm)	-4.37 ± 0.03 [30]
$10^{40}\theta_{11}$(Cm^2)	11.0 ± 2.0 [38]
$10^{40}\theta_{22}$(Cm^2)	-4.3 ± 2.0 [38]
$10^{40}\theta_{33}$(Cm^2)	-6.7 ± 1.7 [38]
$10^{40}\alpha_{11}$(C^{2}m^{2}J^{-1})	6.72[b]
$10^{40}\alpha_{22}$(C^{2}m^{2}J^{-1})	5.51[b]
$10^{40}\alpha_{33}$(C^{2}m^{2}J^{-1})	5.32[b]
$10^{40}a_{11}$(C^{2}m^{2}J^{-1})	7.278[c]
$10^{40}a_{22}$(C^{2}m^{2}J^{-1})	5.744[c]
$10^{40}a_{33}$(C^{2}m^{2}J^{-1})	5.968[c]
$10^{40}a$(C^{2}m^{2}J^{-1})	6.33[c]
$10^{50}A_{113}$(C^{2}m^{3}J^{-1})	-0.6939834[d]
$10^{50}A_{223}$(C^{2}m^{3}J^{-1})	-3.5661792[d]
$10^{50}A_{311}$(C^{2}m^{3}J^{-1})	2.7869264[d]
$10^{50}A_{322}$(C^{2}m^{3}J^{-1})	-0.7622253[d]

[a]Obtained by fitting pressure virial coefficients (see text)
[b]*ab initio* MP2 calculated values at λ = 514.5 nm [40]. We note the excellent agreement (within 3%) between the calculated [39,40] and measured [39,41] polarizability values at λ = 632.8 nm, and so use the calculated values at λ = 514.5 nm with confidence.
[c]*ab initio* MP2 calculated values [40] scaled according to the experimentally deduced mean static polarizability [42].
[d]*ab initio* SCF calculated values [40].

Table 2.3. A comparison of experimental values of $B(T)$ for dimethyl ether, together with our calculated values. See table 2.2 for the force constants and shape factors.

	$10^6\ B(T)/\mathrm{m^3mol^{-1}}$	
T/K	Tripp and Dunlap [38]	Calculated in this work
283.25	-542 ± 4	-542.29
303.15	-466 ± 11	-468.4
323.15	-411 ± 9	-409.69

2.5.2 Results of calculations for dimethyl ether

Table 2.4 gives the relative magnitudes of the various contributions to B_ρ calculated for dimethyl ether at T = 299.68 K and λ = 514.5 nm, this being the mean temperature and wavelength at which our experimental determination of B_ρ was undertaken, as reported in chapter 3. Also included in chapter 3 is a comparison of the measured and calculated B_ρ values for this molecule.

We note that, as found for previously studied molecules [14], the a_4 term makes the dominant contribution to S_ρ, while the a_5 term makes a much smaller, although still significant contribution. This series of terms is now rapidly converging, so that the a_6 and higher-order terms in the dipole-dipole interaction should contribute negligibly. Notice also how the a_2A_1 term, which has, in this project, been evaluated for the first time for a non-linear molecule, makes a small but significant contribution of some 3.6% to B_ρ.

Table 2.5 lists the temperature dependence of the calculated S_ρ and B_ρ values for dimethyl ether, while table 2.6 summarizes the calculated and experimentally deduced values of S_ρ and B_ρ for the other two non-linear molecules already investigated, namely ethene and sulphur dioxide [14].

Table 2.4. The relative magnitudes of the various contributions to B_ρ of dimethyl ether calculated at $T = 299.68$K and $\lambda = 514.5$ nm. B_ρ is obtained using the experimental $\rho_0 = 0.00377$, as reported in chapter 3.

Contributing term	$\frac{10^6 \times value}{m^3 mol^{-1}}$	% contribution to B_ρ
g	17.593	-3.97
b_3	2.987	-0.67
a_3	-240.558	54.32
a_4	691.356	-156.12
a_5	47.967	-10.83
$a_2 A_1$	-15.99	3.61
S_ρ	503.355	-113.66
$2B$	-946.194	213.66

$$2B + S_\rho = -442.839 \times 10^{-6} m^3 mol^{-1}$$

$$B_\rho = -1.661 \times 10^{-6} m^3 mol^{-1}{}^a$$

[a] obtained using $B_\rho = \rho_0(1 - \frac{4}{3}\rho_0)(2B + S_\rho)$

Table 2.5. Temperature dependence of the calculated S_ρ and B_ρ values of dimethyl ether at $\lambda = 514.5$ nm.

T/K	$\frac{10^6 S_\rho}{m^3 mol^{-1}}$	$\frac{10^6 B}{m^3 mol^{-1}}$	$\frac{S_\rho}{2B}$	$\frac{10^6 B_\rho}{m^3 mol^{-1}}$
283.25	531.49	-542	-0.49	-2.072
299.68	503.355	-473.097	-0.53	-1.661
303.15	498.185	-466	-0.53	-1.627
323.15	471.925	-411	-0.57	-1.313

Table 2.6. A summary of all measured B_ρ and S_ρ values for nonlinear molecules. Comparison is made with the theoretical values obtained using the molecular-tensor light-scattering theory of B_ρ described in section 2.3.3.

Molecule	Reference	λ/nm	T/K	$\frac{10^6 B_\rho^{(\mathrm{exp})}}{\mathrm{m^3 mol^{-1}}}$	$\frac{10^6 B_\rho^{(\mathrm{theory})}}{\mathrm{m^3 mol^{-1}}}$	$\frac{B_\rho^{(\mathrm{exp})}}{B_\rho^{(\mathrm{theory})}}$	$\frac{10^6 S_\rho^{(\mathrm{exp})}}{\mathrm{m^3 mol^{-1}}}$	$\frac{10^6 S_\rho^{(\mathrm{theory})}}{\mathrm{m^3 mol^{-1}}}$	$\frac{S_\rho^{(\mathrm{exp})}}{S_\rho^{(\mathrm{theory})}}$
C_2H_4	Couling *et al.* [25]	514.5	294.92	-2.384 ± 0.027	-2.357	1.011	92.2 ± 4.8	94.36	0.977
	Berrue *et al.* [8]	514.5	328.0	-1.78 ± 0.07	-1.671	1.065	85.0 ± 8.0	91.87	0.925
SO_2	Couling *et al.* [21]	514.5	338.35	-5.74 ± 0.37	-5.951	0.965	270 ± 47	257.70	1.048
$(CH_3)_2O$	this work	514.5	299.68	-1.78 ± 0.13	-1.661	1.072	480 ± 44	503.36	0.955

2.6 References

[1] Landau, L. D., and Lifshitz, E. M., 1962, *The Classical Theory of Fields* (Oxford: Pergamon).

[2] Buckingham, A. D., and Raab, R. E., 1975, *Proc. Roy. Soc. Lond.* A, **345**, 365.

[3] Dayan, E., Dunmur., D. A., and Manterfield, M. R., 1980, *J. chem. Soc. Faraday Trans.* II,**76**, 309.

[4] Buckingham, A. D., and Pople, J. A., 1955, *Proc. Phys. Soc. A*, **68**, 905.

[5] Maroulis, G., 1993, *J. Phys.* B, **26**, 775.

[6] Bridge, N. J., and Buckingham, A. D., 1966, *Proc. Roy. Soc. Lond.* A, **295**, 334.

[7] Buckingham, A. D., and Pople, J. A., 1956, *Disc. Faraday Soc.*, **22**, 17.

[8] Berrue, J. Chave, A., Dumon, B., and Thibeau, M., 1978, *J. Phys.*, **39**, 815.

[9] Couling, V. W., and Graham, C., 1993, *Molec. Phys.*, **92**, 235.

[10] Buckingham, A. D., and Utting, B. D., 1970, *Annu. Rev. phys. Chem.*, **21**, 287.

[11] Graham, C., 1971, Ph D thesis, University of Cambridge.

[12] Buckingham, A. D., 1967, *Adv. chem. Phys.*, **12**, 107.

[13] Strutt, R. J., (Fourth Baron Rayleigh), 1920, *Proc. Roy. Soc. Lond.* A, **97**, 435.

[14] Couling, V. W., 1995, Ph D thesis, University of Natal (Pietermaritzburg).

[15] Graham, C., 1992, *Molec. Phys.*, **77**, 291.

[16] Copleland, T. G., and Cole, R. H., 1976, *J. chem. Phys.*, **64,** 1741.

[17] Buckingham, A. D., and Stephen, M. J., 1957, *Trans. Faraday Soc.*, **53**, 884.

[18] Raab, R. E., 1975, *Molec. Phys.*, **29**, 1323.

[19] Bridge, N. J., and Buckingham, A. D., 1964, *J. chem. Phys.*, **40**, 2733.

[20] Couling, V. W., 1993, M Sc thesis, University of Natal (Pietermaritzburg).

[21] Couling, V. W., and Graham, C., 1999, *Molec. Phys.*, **96**, 921.

[22] Margenau, H., and Murphy, G. M., 1992, *The Mathematics of Physics and Chemistry*, (New York: Van Nostrand).

[23] Couling, V. W., and Graham, C., 1994, *Molec. Phys.*, **82**, 235.

[24] Hohls, J., 1997, Ph D thesis, University of Natal (Pietermaritzburg).

[25] Couling, V. W., and Graham, C., 1996, *Molec. Phys.*, **87**, 779.

[26] Benoît, H., and Stockmayer, W. H., 1956, *J. Phys. Radium*, **17**, 21.

[27] Levelt Sengers, J. M. H., and Hastings, J. R., 1982, *Proceedings of the 8th Symposium on Thermophysical Properties*, **1**, 66.

[28] Waxman, M., and Davis, H. A., 1979, *Equations of state in Engineering and Research, Advances in Chemistry Series* (American Chemical Society: New York), **182**, 285.

[29] Couling, V. W., and Graham, C., 1998, *Molec. Phys.*, **93**, 31.

[30] Blukis, U., Kasai, P. H., and Myers, R. J., 1963, *J. chem. Phys.*, **38**, 2753.

[31] Graham, C., 1992, *Molec. Phys.*, **77**, 291.

[32] Andrews, A. L., and Buckingham, A. D., 1960, *Molec. Phys.*, **3**, 183.

[33] Spackman, M. A., 1989, *J. phys. Chem.*, **93**, 7594.

[34] Bogaard, M. P., Buckingham, A. D., Pierens, R. K., and White, A. H., 1978, *Trans. Faraday Soc.* I, **74**, 3008.

[35] Varshalovich, D. A., Moskalev, A. N., and Kharsonkii, V, K., 1988, *Quantum Theory of Angular Momentum*, (Teaneck: World Scientific).

[36] Buckingham, A. D., and Watts, R. S., 1973, *Molec. Phys.*, **26**, 7.

[38] Tripp, T. B., and Dunlap, R. D., 1962, *J. phys. Chem.*, **66,** 635.

[38] Benson, R. C., and Flygare, W. H., 1970, *J. phys. Chem.*, **52,** 5291.

[39] Coonan, M. H., Craven, I. E., Hesling, M. R., Ritchie, G. L. D., and Spackman, M. A., *J. phys. Chem.*, **96**, 7301.

[40] Spackman, M. A., 1999, *Private Communication.*

[41] Bogaard, M. P., Buckingham, A. D., and Ritchie, G. L. D., 1981, *J. chem. Soc. Faraday* Trans. *II, 77, 1547.*

[42] Barnes, A. N. M., Turner, D. J., and Sutton, L. E., *Trans. Faraday Soc.*, 1971, **67**, 2902.

[43] Arfken, G. B., and Weber, H. J., 1995, *Mathematical Methods for Physicists, 4th Ed.* (London: Academic Press).

Chapter 3

Experimental Measurement of the Second Light-scattering Virial Coefficient of Dimethyl Ether

3.1 The Light-scattering Apparatus

Determining experimental values of the second light-scattering virial coefficient B_ρ of a gas requires apparatus which can measure the depolarization ratio ρ of the light scattered at right angles to the direction of propagation of the incident beam in the gas sample for a wide range of pressures. The initial development of the light-scattering apparatus used in this work was carried out in the period 1991-1995, and has been extensively discussed in [1]. Hence we only give a brief review here.

The optical system used for our experiment is shown schematically in figure 3.1. The output beam of the argon-ion laser is nominally polarized vertical to the optical bench, and pure polarized light is obtained by a polarizing prism. The polarized beam then passes through the scattering cell, finally striking a light transducer which allows for continuous monitoring of the incident beam intensity. The 90° scattered beam passes through an analyzing prism which allows for selection of the horizontally and vertically polarized components. The neutral density filter is used to attenuate the more intense vertically polarized component, so overcoming the problems associated with the slight nonlinearity in the photomultiplier

response at higher count rates. The output signal from the photomultiplier is amplified and fed into an electronic photon counting system housed in an IBM compatible personal computer. Supporting software allows the computer to count discrete photons reaching the photomultiplier photocathode. ρ is then calculated from measured count rates of the horizontally and vertically polarized components of the scattered beam.

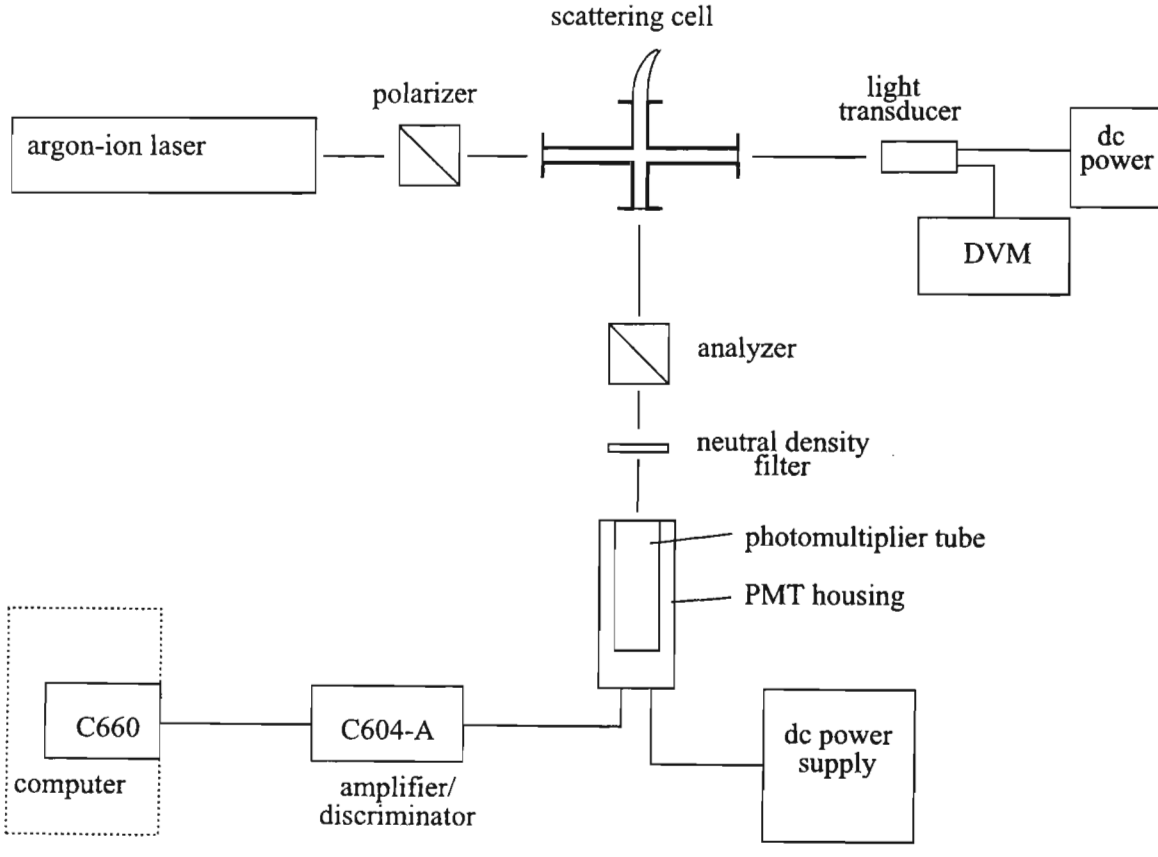

Figure 3.1. The optical system used for measurement of the depolarization ratio ρ of the light scattered by dimethyl ether.

We now discuss each of the various components in a little more detail.

3.1.1 The optical bench

The various optical components have to be aligned as precisely as possible to reduce the presence of geometrical errors in ρ. Bridge and Buckingham [2] have shown that the error in ρ will be negligible (*i.e.* less than 1/500) provided that the vertical of the main optical rail supporting the polarizer and scattering cell, and that of the 90° optical rail supporting the analyzer and photomultiplier, coincide to within 1°. This requires a stable, vibration free optical bench to support the optical rails, which themselves need to be easily adjustable for obtaining the vertical position.

Use was made of an optical bench (a heavy L-shaped steel C-bar 2.3 m long, 25 cm wide and 9 cm high, with a 0.5 m L-piece) having three adjustable feet with anti-vibration pads, resting on a granite slab supported by brick pillars. The two steel optical rails were each mounted onto this optical bench by resting upon the tips of three bolts screwed into the bench, hence providing a tripod support. Using an engineering spirit level and a T-square, these rails were set to be exactly perpendicular to each other, and exactly level. A plumb-bob enabled the rails to be set vertical to less than 1°, hence keeping geometrical errors negligible.

3.1.2 The laser

The argon-ion (Ar^+) laser is preferable to the helium-neon (He-Ne) laser as a light source for light-scattering experiments for three reasons. Firstly, the output intensity of the 514.5 nm green line of the Ar^+ laser is generally ten times that of the He-Ne 632.8 nm line. Secondly, the intensity of Rayleigh scattered light is inversely proportional to the fourth power of the wavelength of the incident beam. Finally, most photomultipliers operate more efficiently in the blue-green spectral range than in the red.

The Spectra Physics model 165 Ar^+ laser was used in this work. It was operated on the 514.5 nm line, which has an adjustable output power up to a maximum of 0.8 W. The beam diameter is 1.5 mm at its $1/e^2$ points, with a divergence of 0.5 milliradians. For a slightly divergent linearly polarized incident beam, the observed depolarization ratio ρ deviates from the true ρ by an amount [2]

$$\rho_{observed} = \rho_{true} + \tfrac{1}{4}B^2 \qquad (3.1)$$

where B is the maximum angle of divergence of the beam in radians. For the Ar^+ laser beam used in these experiment the beam divergence of 0.5 milliradians leads to a $\frac{1}{4}B^2$ of the order of 10^{-7}, which is a completely negligible error for a ρ value of down to about 10^{-4}. Therefore we can confidently state that the geometrical error of our experimental setup cannot affect our measured depolarization ratios, since they are of the order 10^{-2} for dimethyl ether.

Since the laser output beam may fluctuate in intensity from time to time, thereby causing instability in the measurement of ρ, the intensity had to be monitored continuously. This was achieved by using a Photoamp model A-1805 light transducer. The incident light emerging from the scattering cell fell onto this device, its output voltage, as measured by a digital multimeter, being continuously monitored. Any drift in voltage could be countered by adjusting the plasma current, the beam intensity thus being held constant. The output was typically kept constant to one part in a thousand throughout any one experimental determination of ρ.

3.1.3 The scattering cell

Figure 3.2 gives a cross-sectional view of the scattering cell. The cell must contain the gas samples introduced into it in a pure and dust-free state. Our scattering cell was made up of

two stainless-steel cylinders: the one parallel to the incident beam and the other one parallel to the direction of observation. It was designed to withstand a pressure of several MPa, and to keep stray background light to a bare minimum, this being achieved by having a highly polished aluminium Rayleigh horn positioned at the far end of the scattered light tube as seen by the detector. The use of stainless steel and aluminium, and teflon O-rings as seals, ensured that the cell would be inert to many of the corrosive chemical gases which may be used in the measurement of ρ.

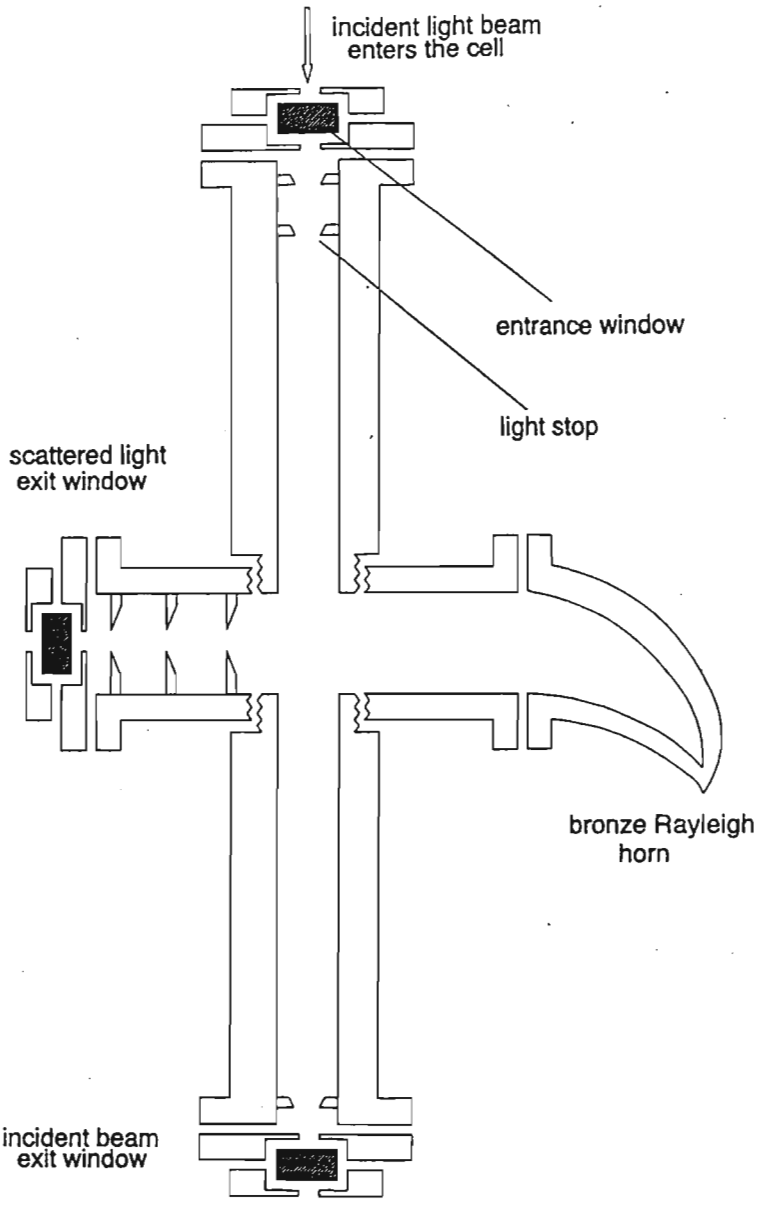

Figure 3.2. A Cross-sectional view of the scattering cell.

The measurement of ρ requires that the entrance window and 90° exit window of the cell do not introduce significant spurious depolarization of the incident and scattered beams. Pockels glass windows were chosen because of their inherent low strain, and their low stress coefficient.

3.1.4 The gas line

Figure 3.3 shows a schematic representation of the gas line which was assembled to allow dust-free gas samples to be introduced into the scattering cell. The line was constructed out of standard Hoke high-pressure stainless steel tubing and valves, enabling it to withstand pressures in excess of 15MPa. Both the gas line and the cell itself had to be leak free to prevent dust particles entering the system through leaks. The presence of a single dust particle can lead to light scattered out of the incident beam which is far more intense than the light scattered by the gas sample itself. This results in the light detector producing a large and strongly fluctuating signal.

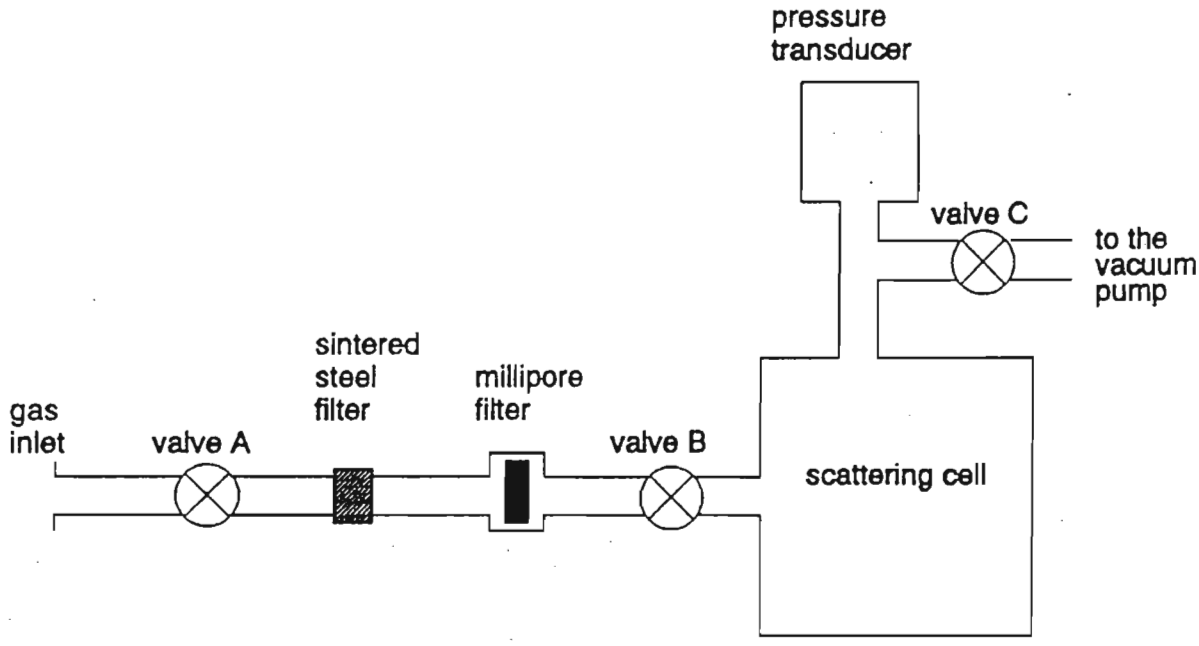

Figure 3.3. A schematic representation of the gas line

Before introducing gas samples to the cell, they were passed through a millipore plastic membrane with an average pore size of 0.2μm. A visual test to ascertain that the gas sample is dust free was to increase the power of the incident beam to its full 0.8 W, and to observe the 90° scattered beam with a travelling microscope. Any dust particles are readily detected as bright specks of light drifting about randomly.

The scattering cell was initially dedusted by flushing with a constant stream of dry air which had been sucked through the millipore filter by the rotary oil pump. After a few minutes of flushing, no dust particles could be detected with use of the travelling microscope. The cell was then evacuated by closing the Hoke Micromite fine-metering valve while leaving the vacuum pump running. The entire line was then tested for leaks with the Edwards Spectron model 300E leak detection system, both when under vacuum and when filled with a helium-oxygen mixture to about 5 MPa.

Since the dimethyl ether used in our experiments is flammable, and can produce anaesthesia if inhaled, it had to be handled and disposed of with caution. The light-scattering laboratory was well ventilated, with a spark-proof extractor fan. After measurements had been taken, the excess dimethyl ether was burnt off in a controlled way.

3.1.5 The analyzer

The 90° scattered light emerging from the cell was passed through the analyser prism to allow selection of either the vertically or the horizontally polarized component of the scattered light. Precise measurements of these scattered signals are crucial for the measurement of the depolarization ratio ρ, which is typically of the order of 10^{-2}. A Melles-

Griot Glan-Thompson prism was used in our work, having a square cross-section and dimensions 11 mm by 11 mm by 31 mm. It was mounted in a divided circle with the transmission axis perpendicular to the axis of rotation. The vernier scale permitted angular settings with a precision of 2' of arc.The analyzer prism was linked to the 90° exit window of the scattering cell via a light-tight tube to prevent stray light from interfering with the scattered light signal.

3.1.6 The photomultiplier

The intensity of the 90° scattered light is very small: this is particularly true for the horizontal component, which is typically a hundred times smaller than the vertical component. Clearly, successful measurement of the depolarization ratio ρ relies on precise measurement of the intensity components of the 90° scattered light beam. The need for a highly sensitive light detector can readily be appreciated.

A photomultiplier tube provides the necessary detection capabilities, and can in fact be used to count individual photons if the incident intensity is not too high. A Thorn EMI 9128B photomultiplier was used in this work, operating in the single-photon-counting mode. It has a diameter of 29 mm, and eleven linearly focussed dynodes, resulting in a high gain, excellent single-electron response and good pulse height resolution; all of these properties being essential to the photon counting technique.

The photomultiplier housing was mounted on the 90° optical rail so that the cone of 90° scattered light travelled perpendicularly to the photomultiplier window. The 9128B tube's window is plano-concave, hence focussing photons onto the photocathode. The detector has a maximum angle of acceptance of 4.5° in this configuration, and light stops were used to

reduce the angle of divergence of the cone of scattered light reaching the detector to less than 3°. This should not lead to significant geometrical errors, as shown by Bridge and Buckingham [2].

3.1.7 The neutral density filter

The 9128B photomultiplier was found to have a slightly nonlinear response for count rates in excess of around 100 kHz. Since the vertical component of the scattered light is typically a hundred times that of the horizontal component, its count rate generally falls into the nonlinear region. This problem was overcome by attenuating the vertically polarized scattered light signal by a precisely known factor of about ten. This was achieved by placing a neutral density filter behind the analyzer (so as not to spuriously depolarize the scattered light). A light-tight holder held the filter in place. The attenuation factor of the filter was precisely measured to be 10.27 ± 0.05, this value being used in the measurements of ρ undertaken in this work.

3.1.8 The data acquisition system

An IBM compatible personal computer was used to house the Thorn EMI model C660 counter/timer board, effectively converting the computer into a high performance pulse counting instrument for recording the output of the 9128B photomultiplier when operating in the photon counting mode. Collection and storage of data, as well as the analysis of the depolarization ratio ρ, could be efficiently achieved.

The board is connected to the EMI C604-A amplifier/discriminator module, allowing the pulses coming from the C604-A to be transferred to the board for counting. A wide range of

counting periods can be selected, from a very fast 52 μs up to a maximum of 20 seconds; and the counting period is accurate to within a microsecond. The C660 board is controlled entirely by a set of computer programs written in Microsoft QuickBasic, supplied by Thorn EMI. These programs are menu-driven, readily allowing selection of a range of features. For example, measured count rates can be collectively viewed on the computer screen, and can be printed out or stored in a data file which can be later accessed by other computer programs written for specific requirements. For example, a computer program written by us in BASIC accesses data files of measured count rates of the 90° scattered light , and directly calculates the depolarization ratio ρ and its statistical uncertainty. Other features are the inclusion of a subroutine to statistically correct measured count rates for the dead-time in the photon-counting system's electronic circuitry.

When recording the data in our experiment, a technique of allowing the counter to cycle through a set of counts several times was adopted. The count period was set to 1 second, and sets of 20 counts were measured and stored as elements in an array. Each count in every additional set was added to its corresponding array element, and this was continued until the desired number of cycles had been completed. A total of 100 cycles, for example, would require that each of the 20 elements in the final set of accumulated counts be divided by 100 to yield a set of 20 count rates representing the intensity of the observed light signal. These 20 values could be averaged to yield a mean value $\bar{x}$, and a measure of the uncertainty is the standard deviation s_x given by

$$s_x = \sqrt{\frac{\sum_{i=1}^{N} (x_i - \bar{x})^2}{N-1}} \tag{3.2}$$

where N is the total number of values ($N = 20$ here), with x_i being the i^{th} value.

The counts were stored in data files which were later accessed and analysed using the BASIC program written specifically to calculate the depolarization ratio ρ and its estimated uncertainty.

3.2 Experimental Measurements and Results

The density dependence of the depolarization ratio ρ is best described by the virial expansion, as given by equation (2.30) of chapter 2:

$$\rho = \rho_0 + \frac{B_\rho}{V_m} + \frac{C_\rho}{V_m^2} + \ldots \tag{3.3}$$

where ρ_0 is the ideal-gas depolarization ratio, V_m is the molar volume of the gas, and B_ρ and C_ρ describe the deviation of ρ from ρ_0 due to interacting pairs of molecules and interacting triplets, respectively.

Previous workers, including Couling and Graham [1] of our Physics Department, have measured values of ρ and V_m for a range of gases comprising molecules of linear, and more recently nonlinear, symmetry. These results have been summarized in tables 2.1 and 2.6 of chapter 2. Despite the fact that data were often taken at moderately high pressures of a few MPa, the plots of ρ versus $1/V_m$ generally yielded linear graphs. This indicates that pair interactions predominate, and that the C_ρ and higher-order terms in equation (3.3) are negligible. Deviations from linearity in the plots only occur at higher pressures where the higher order interactions begin to make relatively large contributions to ρ.

Ultimately, the second light-scattering virial coefficient B_ρ is measured as the slope of a ρ

versus $1/V_m$ graph, while ρ_o is extracted from the intercept. The experimental procedure adopted in this work for measuring ρ at a particular pressure and temperature required the measurement of four quantities, namely (i) the intensity I_v of the 90° scattered light reaching the photomultiplier when the transmission axis of the analyzer was set vertical, (ii) the scattered intensity I_h with the analyzer rotated through 90° to set its transmission axis horizontal, (iii) the background intensity $I_v(b)$ after the cell had been evacuated, and finally (iv) the background intensity $I_h(b)$. The depolarization ration ρ was then given by

$$\rho_{true} = \frac{I_h - I_h(b)}{I_v - I_v(b)}. \tag{3.4}$$

It should be mentioned that for the dimethyl ether investigated in this study, ρ_0 is sufficiently large to be adversely affected by the contribution to the polarized light arising from vibrational Raman scattering, so that an isolating filter was not used.

3.2.1 Results for dimethyl ether

Our measurement of the pressure dependence of the depolarization ratio ρ of dimethyl ether was carried out at room temperature with no direct temperature control on the cell. However, our laboratory has no windows to ensure a well insulated environment: bear in mind the significant temperature dependence of B_ρ. Variations in the ambient temperature were less than 1 °C over the entire two months during which measurements were undertaken, the mean being (299.7 ± 0.8) K.

A cylinder of dimethyl ether of 99.99% minimum purity was purchased from Afrox, and was admitted to the scattering cell without further purification, although being passed through the 0.2 μm Millipore filter to remove dust. ρ was measured over the range 90 kPa to 550 kPa in

steps of 50 kPa, the saturation vapour pressure at this temperature being 630 kPa. The molar volume V_m for each vapour pressure P and temperature T was determined first by finding $V_m^{ideal} = RT / P$ as an initial approximation, and then by substituting this value into the virial equation of state

$$V_m = \frac{RT}{P}\left(1 + \frac{B(T)}{V_m}\right). \tag{3.5}$$

The 'corrected' value for V_m thus obtained was further refined by substituting it for V_m in the right hand side of equation (3.5) keeping all other variables fixed, the procedure being reiterated until consecutive values differed by less than one part in a million. The second pressure virial coefficient $B(T)$ in equation (3.5) was estimated by interpolating the measured data of Tripp and Dunlap [3] to the experimental temperatures. The results follow:

Table 3.1. The measured depolarization ratio ρ for dimethyl ether over a range of pressures at $\lambda = 514.5$ nm.

reading	P/kPa	T/°C	V_m^{-1} / mol m^{-3}	$10^3 \times (\rho \pm s_x)$
1	92	27.0	37.50	3.79 ± 0.13
2	102	26.0	41.80	3.77 ± 0.11
3	126	26.5	51.78	3.65 ± 0.14
4	155	26.0	64.19	3.62 ± 0.10
5	157	26.0	65.04	3.69 ± 0.10
6	197	*26.5*	*82.11*	*3.63 ± 0.10*
7	251	26.8	105.67	3.62 ± 0.10
8	251	27.0	105.59	3.63 ± 0.10
9	270	26.8	114.12	3.57 ± 0.09

Table 3.1 (continued)

reading	P/kPa	T/°C	V_m^{-1} / mol m^{-3}	$10^3 \times (\rho \pm s_x)$
10	296	27.0	125.71	3.52 ± 0.08
11	326	26.9	139.41	3.55 ± 0.09
12	353	26.0	152.45	3.47 ± 0.08
13	356	26.5	153.52	3.49 ± 0.09
14	398	26.7	173.14	3.50 ± 0.08
15	404	26.5	176.15	3.46 ± 0.08
16	410	26.5	179.02	3.41 ± 0.09
17	448	27.0	196.93	3.46 ± 0.07
18	451	26.6	198.76	3.42 ± 0.08
19	487	25.7	217.46	3.38 ± 0.07
20	494	27.2	219.40	3.36 ± 0.08
21	514	26.1	230.65	3.31 ± 0.07
22	549	26.4	249.04	3.26 ± 0.07
23	552	27.0	248.23	3.25 ± 0.07

A plot of ρ versus $1/V_m$ is given in figure 3.4. From equation (3.3) it can be seen that B_ρ is obtained as the slope of the linear region of the plot, while the intercept yields a value for ρ_0. The last three data points (i.e. 21 to 23 in table 3.1) show a deviation from linearity, which is not surprising since at these pressures, the dimethyl ether is close to its point of liquefaction, where triplet and higher-order interactions come into play. These points have been omitted from the least squares fit. Data points 10 and 20 have also been omitted from the analysis, since at these low pressures the incident laser beam intensity has to be relatively high in order to obtain a measurable scattered light signal: unfortunately, the resulting stray

reflections from the cell walls lead to an erroneously high depolarized signal, and hence a relatively large ρ value.

Deduced values of ρ_0, B_ρ and S_ρ together with their estimated uncertainties are presented in table 3.2, which also contains the theoretical B_ρ and S_ρ values calculated in chapter 2. Notice how well our $10^3 \times \rho_0$ of 3.77 ± 0.02 agrees with that of 3.71 ± 0.02 measured at λ = 514.5 nm by Bogaard *et al.* [4]. The experimentally deduced S_ρ has quite a large uncertainty of some 9.2%, which is due to the uncertainty of the $B(T)$ value as well as the experimental ρ_0 and B_ρ values, as seen by equations (2.138) and (2.146).

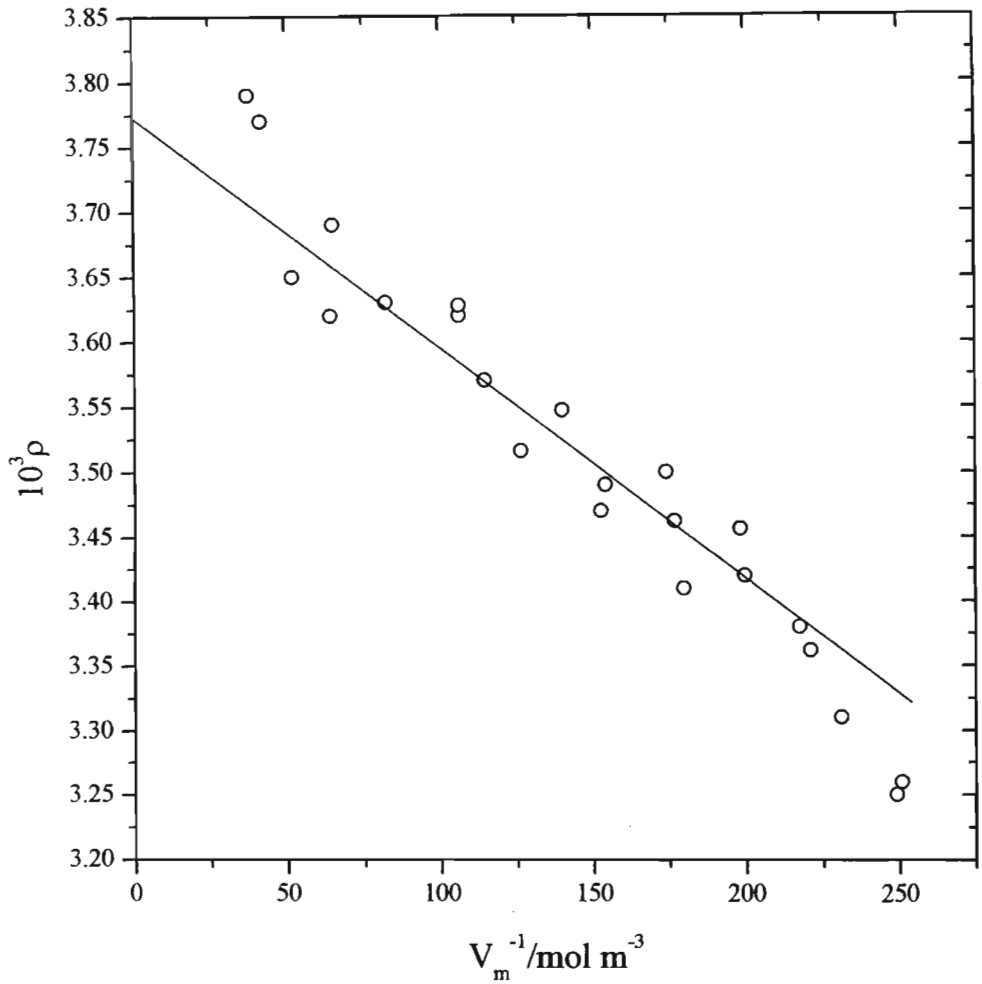

Figure 3.4. Experimental depolarization ratio as a function of gas density for dimethyl ether.

Table 3.2. Our measured B_ρ value for dimethyl ether, together with the deduced S_ρ value. Comparison is made with the theoretical values calculated in chapter 2.

T/K	$10^3 \times \rho_0$	$\frac{10^6 B_\rho^{(exp)}}{m^3 mol^{-1}}$	$\frac{10^6 B_\rho^{(theory)}}{m^3 mol^{-1}}$	$\frac{B_\rho^{(exp)}}{B_\rho^{(theory)}}$	$\frac{10^6 S_\rho^{(exp)}}{m^3 mol^{-1}}$	$\frac{10^6 S_\rho^{(theory)}}{m^3 mol^{-1}}$	$\frac{S_\rho^{(exp)}}{S_\rho^{(theory)}}$
299.68	3.77 ± 0.02	-1.78 ± 0.13	-1.661	1.072	480 ± 44	503.36	0.955

In conclusion, we see that by taking the full molecular symmetry of dimethyl ether into account in our molecular-tensor theory of S_ρ, the calculated value is found to agree with the measured value to within 8.5%. This finding lends credence to earlier claims that comprehensive DID theories of molecular interaction effects, working to higher orders in the molecular tensors, and allowing for the full symmetry of the molecules, explain the observed phenomena adequately [1,5-7].

We now turn to the electro-optic Kerr effect to see whether calculations of the second Kerr-effect virial coefficient B_K of dimethyl ether, using the same molecular parameters as in our theory of B_ρ, are in good agreement with the available measured data.

3.3 References

[1] Couling, V. W., 1995, Ph D thesis, University of Natal (Pietermaritzburg).

[2] Bridge, N. J., and Buckingham, A. D., 1964, J. chem Phys., 40, 2733.

[3] Tripp, T. B., and Dunlap, R. D., 1962, J. phys. Chem., 66, 635.

[4] Bogaard, M. P., Buckingham, A. D., Pierens, R. K., and White, A. H., 1978, J. chem. Soc. Faraday Trans. I, 74, 3008.

[5] Couling, V. W., and Graham, C., 1996, Molec. Phys., 87, 779.

[6] Couling, V. W., and Graham, C., 1998, Molec. Phys., 93, 31.

[7] Couling, V. W., Graham, C., and McKenzie, J. M., 1999, Molec. Phys., 96, 921.

Chapter 4

The Kerr Effect

4.1 Introduction

Recently, a new molecular-tensor theory of the second Kerr-effect virial coefficient B_K, which describes contributions to the molar Kerr constant K_m arising from molecular pair interactions, was used to calculate B_K for the nonlinear polar molecules sulphur dioxide, difluoromethane, dimethyl ether, and hydrogen sulphide [1-3].

We now wish to re-examine the Kerr effect of dimethyl ether in light of our theoretical and experimental investigations reported in chapters 2 and 3 of this thesis. We begin by presenting a brief review of the molecular-tensor theory of B_K.

4.2 Theory

Consider the arrangement in figure 4.1, where the space fixed system of axes (x,y,z) is fixed in a Kerr cell such that z is in the direction of propagation of the light beam, x is the direction of the applied electric field, and y is perpendicular to the field. Once the Kerr cell is filled with a gas, a uniform electric field is applied by means of a pair of parallel-plate electrodes, and a light beam propagating in the z-direction and vibrating in the xz plane will experience a refractive index n_x, which differs from the refractive index n_y experienced by a light beam propagating in the z-direction and vibrating in the yz plane.

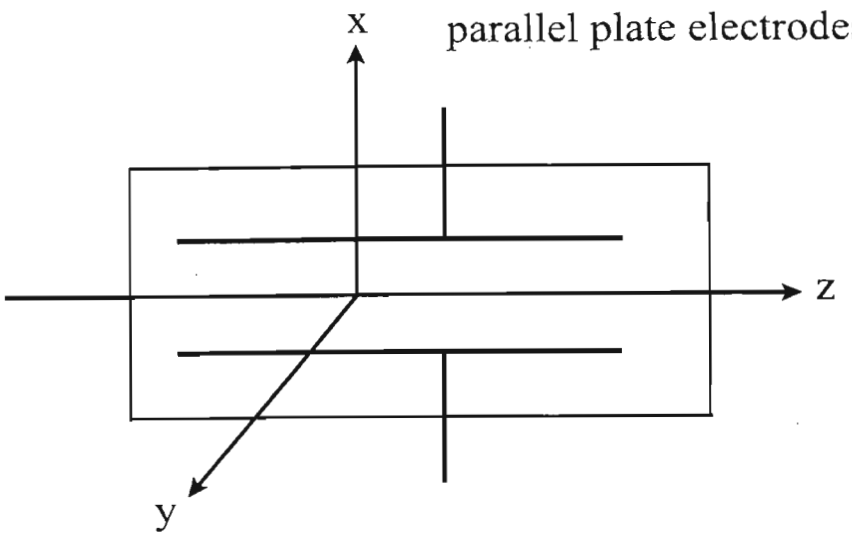

Figure 4.1. The Kerr cell, with space-fixed axes (x,y,z) where z is the direction of propagation of the light beam, x is the direction of the applied electric field, and y is perpendicular to the field.

The observable quantity $(n_x - n_y)$ is the birefringence of the medium, and can be related to the molecular property tensors of the individual molecules in a given gas by a molecular tensor theory, this having been achieved for gases at low pressures by Buckingham and Pople [4]. The molecular Kerr constant K_m is defined as [5]

$$K_m = \frac{18nV_m}{3(n^2+2)^2(\varepsilon_r+2)^2} \lim_{E_x \to 0}\left[\frac{n_x - n_y}{E_x^{\,2}}\right] \tag{4.1}$$

where E_x is the applied electrostatic field, V_m is the molar volume of the gas under study, and n and ε_r are respectively the refractive index and the relative permittivity of the medium in the absence of the field.

In the virial expansion of K_m as a power series in the inverse molar volume [6]

$$K_m = A_K + \frac{B_K}{V_m} + \frac{C_K}{V_m^2} + \ldots, \tag{4.2}$$

the second, third, ... , Kerr effect virial coefficients B_K, C_K, ... , describe deviations from the zero-density molecular Kerr constant A_K due to pair interactions, triplet interactions, ... The expression for A_K in terms of molecular property tensors is [7]

$$A_K = \frac{2\pi N_A}{405(4\pi\varepsilon_0)}\left\{2\gamma_{iijj} + (kT)^{-1}\left[4\beta_{ij}\mu_j^{(0)} + 3(\alpha_{ij}a_{ij} - 3\alpha a)\right] + 3(kT)^{-2}\left[\alpha_{ij}\mu_i^{(0)}\mu_j^{(0)} - \alpha(\mu^{(0)})^2\right]\right\} \tag{4.3}$$

where N_A is Avogadro's number, α_{ij} and a_{ij} are respectively the dynamic and static polarizability tensors, and α and a are the corresponding mean dynamic and static polarizabilities. β_{ij} and γ_{iijj} are the first and the second hyperpolarizability tensors respectively, while $\mu_i^{(0)}$ is the permanent dipole moment of the molecule being studied.

Couling and Graham [1,2] have presented a molecular-tensor theory of B_K in detail. Expressions for the full series of dipole-induced-dipole (DID) contributions to B_K for interacting nonlinear molecules have been given in the appendix of [2], where it was shown that B_K may be written as

$$B_K = \frac{2\pi N_A^2}{27\Omega(4\pi\varepsilon_0)}\int_\tau (\alpha_2 + \alpha_3 + \alpha_4 + \alpha_5 + \cdots + \mu_2\alpha_1 + \mu_2\alpha_2 + \mu_2\alpha_3 + \mu_2\alpha_4 + \cdots + \mu_1\beta_1 + \cdots)\exp(-U_{12}(\tau)/kT)d\tau. \tag{4.4}$$

Here $\Omega = V_m^{-1}\int d\tau$ is the integral over the orientational coordinates of the neighbouring molecule. The series of DID interaction terms is seen to include the collision-induced series

in powers of the dynamic and static polarizability tensors (labelled $\alpha_2, \alpha_3, \alpha_4, \cdots$) which results from the partial orientation of anisotropic pairs; and a series (labelled $\mu_2\alpha_1, \mu_2\alpha_2, \mu_2\alpha_3, \cdots$) which arises since the applied electric field partially orients the permanent dipoles μ_i of two interacting molecules, while these dipoles are also coupled by the dipole-dipole interaction.

The explicit forms of these terms are [1,2]

$$\alpha_2 = (kT)^{-1}\{\alpha^{(1)}_{ab}\alpha^{(2)}_{pq}\}\left\langle a^x_a a^x_b a^x_p a^x_q - a^y_a a^y_b a^x_p a^x_q \right\rangle, \tag{4.5}$$

$$\begin{aligned}\alpha_3 = (kT)^{-1}\{&\alpha^{(1)}_{ad}a^{(1)}_{pq}T_{qr}\alpha^{(2)}_{rs} + \alpha^{(1)}_{ad}a^{(2)}_{pq}T_{qr}\alpha^{(1)}_{rs} \\ &+\alpha^{(1)}_{ab}T_{bc}\alpha^{(2)}_{cd}a^{(1)}_{ps} + \alpha^{(1)}_{ab}T_{bc}\alpha^{(2)}_{cd}a^{(2)}_{ps}\} \\ &\times\left\langle a^x_a a^x_d a^x_p a^x_s - a^y_a a^y_d a^x_p a^x_s \right\rangle,\end{aligned} \tag{4.6}$$

$$\begin{aligned}\alpha_4 = (kT)^{-1}\{&\alpha^{(1)}_{af}a^{(1)}_{pq}T_{qr}\alpha^{(2)}_{rs}T_{ts}\alpha^{(2)}_{tu} + \alpha^{(1)}_{af}a^{(2)}_{pq}T_{qr}\alpha^{(1)}_{rs}T_{ts}\alpha^{(2)}_{tu} \\ &+\alpha^{(1)}_{ab}T_{bc}\alpha^{(2)}_{cf}a^{(1)}_{pq}T_{qr}a^{(2)}_{ru} + \alpha^{(1)}_{ab}T_{bc}\alpha^{(2)}_{cf}a^{(2)}_{pq}T_{qr}a^{(1)}_{ru} \\ &+\alpha^{(1)}_{ab}T_{bc}\alpha^{(2)}_{cd}T_{de}\alpha^{(1)}_{ef}a^{(1)}_{pu} + \alpha^{(1)}_{ab}T_{bc}\alpha^{(2)}_{cd}T_{de}\alpha^{(1)}_{ef}a^{(2)}_{pu}\} \\ &\times\left\langle a^x_a a^x_f a^x_p a^x_u - a^y_a a^y_f a^x_p a^x_u \right\rangle,\end{aligned} \tag{4.7}$$

$$\begin{aligned}\alpha_5 = (kT)^{-1}\{&\alpha^{(1)}_{ah}a^{(1)}_{pq}T_{qr}a^{(2)}_{rs}T_{st}a^{(1)}_{tu}T_{uv}a^{(2)}_{vw} + \alpha^{(1)}_{ah}a^{(2)}_{pq}T_{qr}a^{(1)}_{rs}T_{st}a^{(2)}_{tu}T_{uv}a^{(1)}_{vw}\\ &+\alpha^{(1)}_{ab}T_{bc}\alpha^{(2)}_{ch}a^{(1)}_{pq}T_{qr}a^{(2)}_{rs}T_{st}a^{(1)}_{tw} + \alpha^{(1)}_{ab}T_{bc}\alpha^{(2)}_{ch}a^{(2)}_{pq}T_{qr}a^{(1)}_{rs}T_{st}a^{(2)}_{tw}\\ &+\alpha^{(1)}_{ab}T_{bc}\alpha^{(2)}_{cd}T_{de}\alpha^{(1)}_{eh}a^{(1)}_{pq}T_{qr}a^{(2)}_{rw} + \alpha^{(1)}_{ab}T_{bc}\alpha^{(2)}_{cd}T_{de}\alpha^{(1)}_{eh}a^{(2)}_{pq}T_{qr}a^{(1)}_{rw}\\ &+\alpha^{(1)}_{ab}T_{bc}\alpha^{(2)}_{cd}T_{de}\alpha^{(1)}_{eh}T_{fg}\alpha^{(2)}_{gh}a^{(1)}_{pw} + \alpha^{(1)}_{ab}T_{bc}\alpha^{(2)}_{cd}T_{de}\alpha^{(1)}_{ef}T_{fg}\alpha^{(2)}_{gh}a^{(2)}_{pw}\}\\ &\times\left\langle a^x_a a^x_h a^x_p a^x_w - a^y_a a^y_h a^x_p a^x_w\right\rangle,\end{aligned} \tag{4.8}$$

$$\alpha_1\gamma_1 = \{\gamma^{(1)}_{abcd}T_{be}\alpha^{(2)}_{ef} + \alpha^{(1)}_{ab}T_{be}\gamma^{(2)}_{efcd}\}\left\langle a^x_a a^x_f a^x_c a^x_d - a^y_a a^y_f a^x_c a^x_d\right\rangle, \tag{4.9}$$

$$\mu_2\alpha_1 = (kT)^{-2}\left\{\alpha^{(1)}_{ab}\mu^{(2)}_{oi}\mu^{(2)}_{op} + 2\alpha^{(1)}_{ab}\mu^{(1)}_{oi}\mu^{(2)}_{op}\right\}\left\langle a^x_a a^x_b a^x_i a^x_p + a^y_a a^y_b a^x_i a^x_p\right\rangle, \tag{4.10}$$

$$\begin{aligned}\mu_2\alpha_2 = (kT)^{-2}\{&2\alpha^{(1)}_{ad}\mu^{(1)}_{oi}a^{(1)}_{pq}T_{qr}\mu^{(2)}_{or} + 2\alpha^{(1)}_{ad}\mu^{(2)}_{oi}a^{(2)}_{pq}T_{qr}\mu^{(1)}_{or}\\ &+2\alpha^{(1)}_{ad}\mu^{(1)}_{oi}a^{(2)}_{pq}T_{qr}\mu^{(1)}_{or} + 2\alpha^{(1)}_{ad}\mu^{(2)}_{oi}a^{(1)}_{pq}T_{qr}\mu^{(2)}_{or}\\ &+\alpha^{(1)}_{ab}T_{bc}\alpha^{(2)}_{cd}\mu^{(1)}_{oi}\mu^{(1)}_{op} + \alpha^{(1)}_{ab}T_{bc}\alpha^{(2)}_{cd}\mu^{(2)}_{oi}\mu^{(2)}_{op}\\ &+2\alpha^{(1)}_{ab}T_{bc}\alpha^{(2)}_{cd}\mu^{(1)}_{oi}\mu^{(2)}_{op}\}\left\langle a^x_a a^x_d a^x_i a^x_p + a^y_a a^y_d a^x_i a^x_p\right\rangle,\end{aligned} \tag{4.11}$$

$$\begin{aligned}\mu_2\alpha_3 = (kT)^{-2}\{&\alpha^{(1)}_{af}a^{(1)}_{ij}T_{jk}\mu^{(2)}_{ok}a^{(1)}_{pq}T_{qr}\mu^{(2)}_{or} + \alpha^{(1)}_{af}a^{(2)}_{ij}T_{jk}\mu^{(1)}_{ok}a^{(2)}_{pq}T_{qr}\mu^{(1)}_{or}\\ &+2\alpha^{(1)}_{af}a^{(1)}_{ij}T_{jk}\mu^{(2)}_{ok}a^{(2)}_{pq}T_{qr}\mu^{(1)}_{or} + 2\alpha^{(1)}_{ab}T_{bc}\alpha^{(2)}_{cf}\mu^{(1)}_{oi}a^{(1)}_{pq}T_{qr}\mu^{(2)}_{or}\\ &+2\alpha^{(1)}_{ab}T_{bc}\alpha^{(2)}_{cf}\mu^{(2)}_{oi}a^{(2)}_{pq}T_{qr}\mu^{(1)}_{or} + 2\alpha^{(1)}_{ab}T_{bc}\alpha^{(2)}_{cf}\mu^{(1)}_{oi}a^{(2)}_{pq}T_{qr}\mu^{(1)}_{or}\\ &+2\alpha^{(1)}_{ab}T_{bc}\alpha^{(2)}_{cf}\mu^{(2)}_{oi}a^{(1)}_{pq}T_{qr}\mu^{(2)}_{or} + 2\alpha^{(1)}_{af}\mu^{(1)}_{oi}a^{(1)}_{pq}T_{qr}a^{(2)}_{rs}T_{st}\mu^{(1)}_{ot}\\ &+2\alpha^{(1)}_{af}\mu^{(2)}_{oi}a^{(2)}_{pq}T_{qr}a^{(1)}_{rs}T_{st}\mu^{(2)}_{ot} + 2\alpha^{(1)}_{af}\mu^{(1)}_{oi}a^{(2)}_{pq}T_{qr}a^{(1)}_{rs}T_{st}\mu^{(2)}_{ot}\\ &+2\alpha^{(1)}_{af}\mu^{(2)}_{oi}a^{(1)}_{pq}T_{qr}a^{(2)}_{rs}T_{st}\mu^{(1)}_{ot} + \alpha^{(1)}_{ab}T_{bc}\alpha^{(2)}_{cd}T_{de}\alpha^{(1)}_{ef}\mu^{(1)}_{oi}\mu^{(1)}_{op}\\ &+\alpha^{(1)}_{ab}T_{bc}\alpha^{(2)}_{cd}T_{de}\alpha^{(1)}_{ef}\mu^{(2)}_{oi}\mu^{(2)}_{op} + 2\alpha^{(1)}_{ab}T_{bc}\alpha^{(2)}_{cd}T_{de}\alpha^{(1)}_{ef}\mu^{(1)}_{oi}\mu^{(2)}_{op}\}\\ &\times\left\langle a^x_a a^x_d a^x_i a^x_p - a^y_a a^y_d a^x_i a^x_p\right\rangle,\end{aligned} \tag{4.12}$$

and

$$\mu_1\beta_1 = 2(kT)^{-1}\left\{\beta^{(1)}_{abi}\mu^{(2)}_{op}\right\}\left\langle a^x_a a^x_b a^x_i a^x_p - a^y_a a^y_b a^x_i a^x_p\right\rangle. \tag{4.13}$$

The isotropic averages in equations (4.5) to (4.13) are carried out using the standard results [4,8]

$$\left\langle a^x_i a^x_k a^x_j a^x_l\right\rangle = \tfrac{1}{30}(4\delta_{ik}\delta_{jl} - \delta_{ij}\delta_{kl} - \delta_{il}\delta_{kj})$$

and

$$\left\langle a^x_i a^x_k a^x_j a^x_l\right\rangle = \tfrac{1}{15}(\delta_{ij}\delta_{kl} + \delta_{ik}\delta_{jl} + \delta_{il}\delta_{kj}).$$

The procedure is illustrated by treating the term for α_2 in equation (4.5) above:

$$\begin{aligned}\alpha_2 &= (kT)^{-1}\{\alpha^{(1)}_{ab}a^{(2)}_{pq}\}\left\langle a^x_a a^x_b a^x_p a^x_q - a^y_a a^y_b a^x_p a^x_q\right\rangle \\ &= (kT)^{-1}\{\alpha^{(1)}_{ab}a^{(2)}_{pq}\}\tfrac{1}{30}\left[-2\delta_{ab}\delta_{pq} + 3\delta_{ap}\delta_{bq} + 3\delta_{aq}\delta_{bp}\right] \\ &= \tfrac{6}{30}(kT)^{-1}\left\{\alpha^{(1)}_{ap}a^{(2)}_{ap} - 3\alpha a\right\}\end{aligned} \tag{4.14}$$

where $\alpha^{(1)}_{ap}$ is the dynamic polarizability tensor of molecule 1 expressed in the molecule-fixed axes of molecule 1, (1,2,3), while α is the mean dynamic polarizability. Similarly, $a^{(2)}_{ap}$ is the static polarizability tensor of molecule 2 expressed in (1,2,3), while a is the mean static polarizability.

The exact forms of $\alpha^{(1)}_{ap}$ and α for molecules with D_{2h} and C_{2v} symmetries have already been quoted in chapter 2, but are repeated here for convenience:

$$\alpha^{(1)}_{ij} = \alpha^{(2)}_{i'j'} = \begin{bmatrix}\alpha_{11} & 0 & 0\\ 0 & \alpha_{22} & 0\\ 0 & 0 & \alpha_{33}\end{bmatrix} \qquad \text{and} \qquad \alpha = \tfrac{1}{3}\alpha_{ii} = \tfrac{1}{3}(\alpha_{11} + \alpha_{22} + \alpha_{33}).$$

Similarly,

$$a_{ij}^{(1)} = a_{i'j'}^{(2)} = \begin{bmatrix} a_{11} & 0 & 0 \\ 0 & a_{22} & 0 \\ 0 & 0 & a_{33} \end{bmatrix} \quad \text{and} \quad a = \tfrac{1}{3}a_{ii} = \tfrac{1}{3}(a_{11} + a_{22} + a_{33}).$$

The procedure for expressing $a_{i'j'}^{(2)}$ in the molecule-fixed axes of molecule 1, (1,2,3), is identical to that given in equation (2.122) in chapter 2 such that

$$a_{ap}^{(2)} = \begin{bmatrix} w_{11} & w_{12} & w_{13} \\ w_{12} & w_{22} & w_{23} \\ w_{13} & w_{23} & w_{33} \end{bmatrix} \tag{4.15}$$

where the coefficients $w_{11}, w_{12}, \cdots, w_{33}$ are exactly analogous to the Z_{ij} coefficients for $\alpha_{i'j'}^{(2)}$ given between equation (2.124) and (2.129), the dynamic components $\alpha_{11}, \alpha_{22}, \alpha_{33}$ being replaced by the static components a_{11}, a_{22}, a_{33} respectively.

Now it is matter of replacing all the polarizability components in equation (4.14) with their explicit forms as given above. We obtain

$$\alpha_2 = \frac{6}{30kT}\left(\alpha_{11}w_{11} + \alpha_{22}w_{22} + \alpha_{33}w_{33} - 3\alpha a\right). \tag{4.16}$$

Macsyma's tensor manipulation facilities prove invaluable in handling the higher-order terms, which can lead to sometimes very lengthy expressions.

The evaluation of B_K according to equation (4.4) requires an intermolecular potential $U_{12}(\tau)$.

As in chapter 2, we use the classical potential of general form

$$U_{12}(\tau) = U_{LJ} + U_{\mu,\mu} + U_{\mu,\theta} + U_{\theta,\theta} + U_{\mu,ind\mu} + U_{\theta,ind\mu} + U_{shape} \tag{4.17}$$

where U_{LJ} is the Lennard-Jones 6:12 potential, $U_{\mu,\mu}$, $U_{\mu,\theta}$, and $U_{\theta,\theta}$ are the electrostatic dipole-dipole, dipole-quadrupole and quadrupole-quadrupole interaction energies of the two interacting molecules, and $U_{\mu,ind\mu}$ and $U_{\theta,ind\mu}$ are the dipole-induced dipole and quadrupole-induced dipole interacting energies. U_{shape} accounts for the angular dependence of the short range repulsive forces for non-spherical molecules. Explicit expressions for each of these contributions to $U_{12}(\tau)$ for nonlinear molecules are presented in detail in chapter 2.

Thus the integrals in equation (4.4) were calculated, as previously, by numerical integration using Gaussian quadrature. They were performed for dimethyl ether gas using the molecular data given in table 4.1, yielding a calculated estimate of B_K for this molecule.

4.3 Results of Calculations of B_K for Dimethyl Ether

Table 4.2 gives the relative magnitudes of the various contributions to B_K calculated for dimethyl ether at T = 292.12 K. Here, as found in previous work on sulphur dioxide and difluoromethane [2], we see that the dominant contributor to B_K is the $\mu_2\alpha_2$ term. This predominance of a collision-induced contribution to B_K for polar molecules is in keeping with the findings of Buckingham *et al.* [9]. Although the $\mu_2\alpha_3$ term contributes some 34% to B_K, the $\mu_2\alpha_4$ contribution has dropped to around 7%, which is a clear indication that the series of terms in $\mu\alpha$ has converged. The contributions to B_K from the hyperpolarizability tensors β_{ijk} and γ_{ijkl}, as given by equations (4.13) and (4.9) respectively, could not be evaluated for

dimethyl ether since the hyperpolarizability tensor components are not yet known. However, previous calculations for sulphur dioxide [2] indicated a not unexpectedly negligible contribution of $\mu_1\beta_1$ to B_K of 0.31%, and we feel confident in omitting these terms here.

Table 4.1. Molecular properties used in the calculation of B_K for $(CH_3)_2O$. Dynamic polarizability tensor components are all at the wavelength of 632.8 nm.

Property	Value
R_0(nm)	0.47[a]
ε / k(K)	290.0[a]
D_1	-0.04926[a]
D_2	0.29666[a]
$10^{30}\mu_3$(Cm)	-4.37 ± 0.03 [10]
$10^{40}\theta_{11}$(Cm^2)	11.0 ± 2.0 [11]
$10^{40}\theta_{22}$(Cm^2)	-4.3 ± 2.0 [11]
$10^{40}\theta_{33}$(Cm^2)	-6.7 ± 1.7 [11]
$10^{40}\alpha_{11}$($C^2m^2J^{-1}$)	6.69[b]
$10^{40}\alpha_{22}$($C^2m^2J^{-1}$)	5.46[b]
$10^{40}\alpha_{33}$($C^2m^2J^{-1}$)	5.28[b]
$10^{40}a_{11}$($C^2m^2J^{-1}$)	7.278[c]
$10^{40}a_{22}$($C^2m^2J^{-1}$)	5.744[c]
$10^{40}a_{33}$($C^2m^2J^{-1}$)	5.968[c]
$10^{40}a$($C^2m^2J^{-1}$)	6.33[c]

[a]Obtained by fitting pressure virial coefficients (see chapter 2)

[b]experimental derivation from the Kerr effect, $\lambda = 632.8$ nm [12].

[c]*ab initio* MP2 calculated values [13] scaled according to the experimentally deduced mean static polarizability [14].

Table 4.2. The relative magnitudes of the various contributions to B_K of dimethyl ether calculated at $T = 292.12$ K and $\lambda = 632.8$ nm.

Contributing term	$\frac{10^{30} \times value}{m^3 mol^{-1}}$	% contribution to B_K
α_2	0.0075	0.06
α_3	-0.1736	-1.50
α_4	0.6728	5.82
α_5	0.0531	0.46
$\mu_2\alpha_1$	-3.4294	-29.65
$\mu_2\alpha_2$	9.6910	83.79
$\mu_2\alpha_3$	3.9087	33.79
$\mu_2\alpha_4$	0.8364	7.23
B_K	11.5665	

The temperature dependence of our calculated B_K values for dimethyl ether is compared graphically with the experimental data of Bogaard *et al.* [12] in figure 4.2. The experimental uncertainties of the measured data were quoted to be in the range ±10% to ±20%, and the calculated curve is seen to lie within the error bars of the experimental points over almost the entire temperature range.

During the course of 1999, Dr Couling and Honours student Miss Jean McKenzie have developed an apparatus to measure the density dependence of the molar Kerr constant, as reported in [15]. We have used this Kerr cell to obtain a relatively precise estimate of B_K at

room temperature, and now report briefly on this additional piece of work.

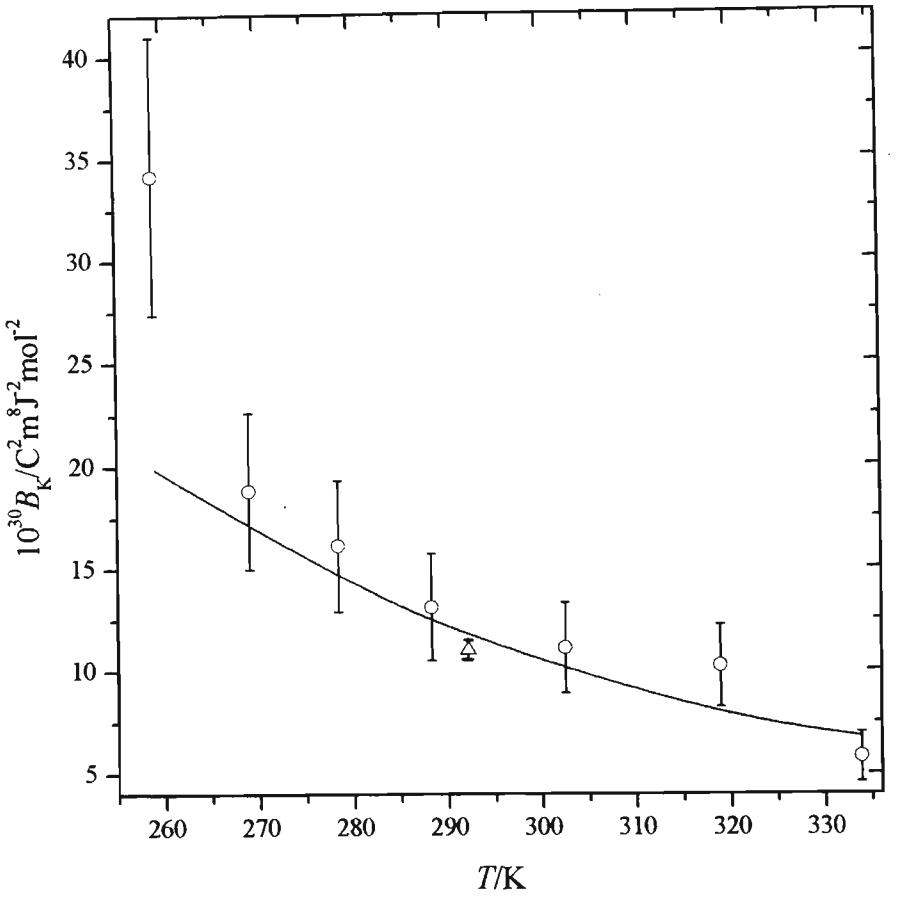

Figure 4.2. The temperature dependence of the measured and calculated B_K values of dimethyl ether. The solid line is our calculated curve, the circles represent the measured values of Bogaard et al. [12], while the triangle is our lone measured value, as described in section 4.4.

4.4 Measurement of B_K for Dimethyl Ether at Room Temperature

The Kerr effect apparatus has been described in detail elsewhere [15], and so will only

briefly be discussed here. A block diagram of the apparatus is given in figure 4.3. The optical cascade comprises various components which are as follows. A 30 mW plane polarized Melles-Griot He-Ne laser, producing a beam of wavelength 632.8 nm. A Glan-Thompson polarizer set at 45° to the vertical. The Kerr cell, which comprises 316-stainless-steel electrodes 1.46809 m in length (at room temperature) and 3.2 cm in width, the electrodes having been machined and then hand polished to be flat and extremely smooth. The electrodes were held in place by fixing 15 polyacetyl rings spaced at regular intervals. The spacing between the electrodes was made as uniform as possible by sandwiching polished Macor blocks between the electrodes, and squeezing the electrodes onto the blocks by placing nickel shim between the polyacetyl rings and the electrodes. The spacing between the electrodes was measured with a travelling microscope at 44 evenly spaced intervals, and found to be 3.148 ± 0.033 mm. The electrodes were placed in a 316-stainless-steel cylinder with a bulkhead for attaching the high voltage lead. One electrode was grounded to the cell wall, the other being connected to hastelloy wire passing to the outside of the cell via a teflon cylinder in the bulkhead. The quarter wave ($\lambda/4$) plate used in the experiment was made of mica sandwiched between Pockels glass, with a retardance of $91.2° \pm 0.3°$ at 632.8 nm. The Faraday cell consisted of a 100 turn coil of heavy-gauge copper wire and a 10 000 turn coil of thinner copper wire, both surrounding a glass tube containing toluene. The tube is 400 mm long and 12 mm in diameter, and is thermally insulated from the coils by a 2 cm layer of polystyrene. Pockels glass windows are situated at either end of the glass tube to contain the liquid and allow unhindered passage of the incident beam. The analyzer is a Glan-Taylor prism housed in a mechanism to allow for very small rotations with the aid of a micometer.

The electronic components are also shown in figure 4.3. Here, a Philips PM 5190 LF synthesizer was used to generate a 363 Hz signal with a peak-to-peak voltage of 1.41 V. This signal was attenuated to 50 mV rms before being fed into the high voltage power supply,

which consisted of a step up transformer immersed in oil, forming a high-voltage amplifier. The output of the secondary coil was linked to the high tension input of the Kerr cell. The cell wall, and hence the second electrode, were grounded to the mains earth. The high voltage output was accurately calibrated. During measurements, the Faraday nulling cell was driven by the same waveform synthesizer as the high voltage circuit. The signal was fed directly into a frequency doubler at 500 mV rms, the 50 mV rms output passing into the current supply combined with a phase shifter so as to provide an ac signal to the 100 turn coil of the Faraday cell which is set to be exactly in antiphase with the Kerr signal. To obtain results from the optical cascade the signal from a photo-diode placed at the end of the cascade was fed into a Princeton Applied Research EG&G model 5210 Lock-In Amplifier (LIA). The reference signal was taken from the waveform synthesizer, and the LIA was used to extract from the photodiode signal that component at twice the reference signal. The LIA output voltage is then proportional to the intensity of the light which is modulated at the desired frequency, and read by a precise HP 3478A digital multimeter connected to an HP 86 microcomputer which recorded and averaged the readings.

4.4.1 Theory

For an electric field E_x applied to a gas sample of path length l, the Kerr effect is exhibited as the gas becomes birefringent, having refractive indices n_x and n_y for light linearly polarized parallel and perpendicular to the electric field respectively. In our experiment, a light beam of wavelength λ, linearly polarized at 45° to the applied electric field, is passed through the gas sample. The emergent light is elliptically polarized due to the phase difference induced by the birefringent gas, and this phase difference δ is given by

$$\delta = \frac{2\pi l}{\lambda}(n_x - n_y). \qquad (4.18)$$

It is useful to introduce the parameter ${}_mK_0$, defined as [12]

$$ {}_mK_0 = \frac{2(n_x - n_y)V_m}{27E_0^2} \tag{4.19} $$

where V_m is the molar volume of the gas, and E_0 is the amplitude of the applied electric field. Combining equations (4.18) and (4.19) yields

$$ {}_mK_0 = \frac{\delta\lambda V_m}{27\pi l E_0^2} \tag{4.20} $$

where λ, l, V_m and E_0^2 are known or can easily be measured. This leaves δ, the phase difference, which is the quntity we wish to measure experimentally so that ${}_mK_0$ can be determined. The first and second Kerr virial coefficients A_K and B_K can be deduced from ${}_mK_0$ using the relation [12]

$$ {}_mK_0 = A_K + \left[B_K + A_K\left(2A_\varepsilon + \tfrac{1}{2}A_R\right)\right]V_m^{-1} + O(V_m^{-2}) \tag{4.21} $$

where A_ε is the low density molar dielectric polarization

$$ A_\varepsilon = \frac{N_A}{3\varepsilon_0}\left\{a_0 + \frac{\mu_0}{3kT}\right\} \tag{4.22} $$

and A_R is the molar refraction

$$ A_R = \frac{N_A\alpha_0}{3\varepsilon_0}, \tag{4.23} $$

both of which can be calculated from tabulated data of the permanent dipole moment μ_0, and the mean static and optical-frequency polarizabilities a_0 and α_0 respectively.

Hence, a plot of ${}_mK_0$ versus $1/V_m$ allows A_K and B_K to be extracted from the slope and the intercept.

4.4.2 Method of measurement

As already mentioned, the quantity we wish to measure is the induced phase difference δ, which will allow for calculation of ${}_mK_0$. The beam of monochromatic light from the He-Ne laser is passed through the polarizer with its transmission axis set at 45° to the electric field. The incident light thus has the components of its oscillating electric field vector parallel and perpendicular to the applied electric field initially equal in magnitude. Once the light beam has passed through the birefringent gas sample, a phase difference δ will have been induced. A precision compensator is required to measure the magnitude of δ, and we have used the toluene-filled Faraday cell in conjunction with the λ/4-plate for this purpose. Because of the induced phase difference, the light that emerges from the Kerr cell is elliptically polarized, but once it is passed through the λ/4-plate it emerges linearly polarized but with its axis of polarization rotated from the initial 45° position. The Faraday cell serves to rotate the plane of polarization by an amount θ_{null} back to the 45° position, and since the Faraday cell can be accurately calibrated, we have a precise measure of this rotation, and hence of δ, since $\theta_{null} = -\delta/2$.

A full Mueller analysis of the optical cascade has been performed [15], and reveals that if the λ/4-plate is offset by a small value ε_1 and the LIA output is plotted as a function of current in the Faraday coil a straight line is obtained. Offsetting the λ/4-plate by a small amount $-\varepsilon_2$ will yield a second line. These lines will intersect at a value θ_{null} where $\theta_{null} = -\delta/2$, hence yielding a precise value for δ. This method is much more sensitive than obtaining a single null value with the Faraday cell [18].

4.4.3 Experimental results of B_K for dimethyl ether

Our measured results of ${}_mK_0$ for dimethyl ether over a range of pressure at a mean $T = 292.12$ K are presented in table 4.2, while a plot of ${}_mK_0$ versus $1/V_m$ is given in figure 4.3. Using equation (4.21), we obtain $A_K = -(12.81 \pm 0.03) \times 10^{-27}$ $C^2m^5J^{-2}mol^{-1}$ and $B_K = (11.0 \pm 0.4) \times 10^{-30}$ $C^2m^8J^{-2}mol^{-1}$. The B_K value interpolated from the experimental results of Bogaard *et al.* [12] at $T = 292.12$ K is $B_K = (12.6 \pm 2.5) \times 10^{-30}$ $C^2m^8J^{-2}mol^{-1}$, which is some 14.5% higher than our experimental value. The calculated B_K value at this temperature and wavelength is (see table 4.2) $B_K = 11.57 \times 10^{-30}$ $C^2m^8J^{-2}mol^{-1}$, which lies in between the two experimental values. We plan to make our Kerr cell temperature dependent during the course of the year 2000, and hope to measure the temperature dependence of B_K for as wide a range of temperature as possible.

Table 4.3. Measured ${}_mK_0$ values for dimethyl ether over a range of pressures at $\lambda = 632.8$ nm.

reading	P/kPa	T/°C	V_m^{-1} / mol m^{-3}	$10^{27}\,{}_mK_0$ / $C^2m^5J^{-2}mol^{-1}$
1	177.9	19.1	75.99	-12.04 ± 0.12
2	119.5	19.1	50.40	-12.33 ± 0.02
3	248.7	18.6	108.18	-11.79 ± 0.02
4	302.6	19.2	132.96	-11.53 ± 0.08
5	351.8	18.5	156.96	-11.28 ± 0.04
6	394.0	19.3	177.05	-11.06 ± 0.03
7	450.0	19.0	205.90	-10.83 ± 0.08

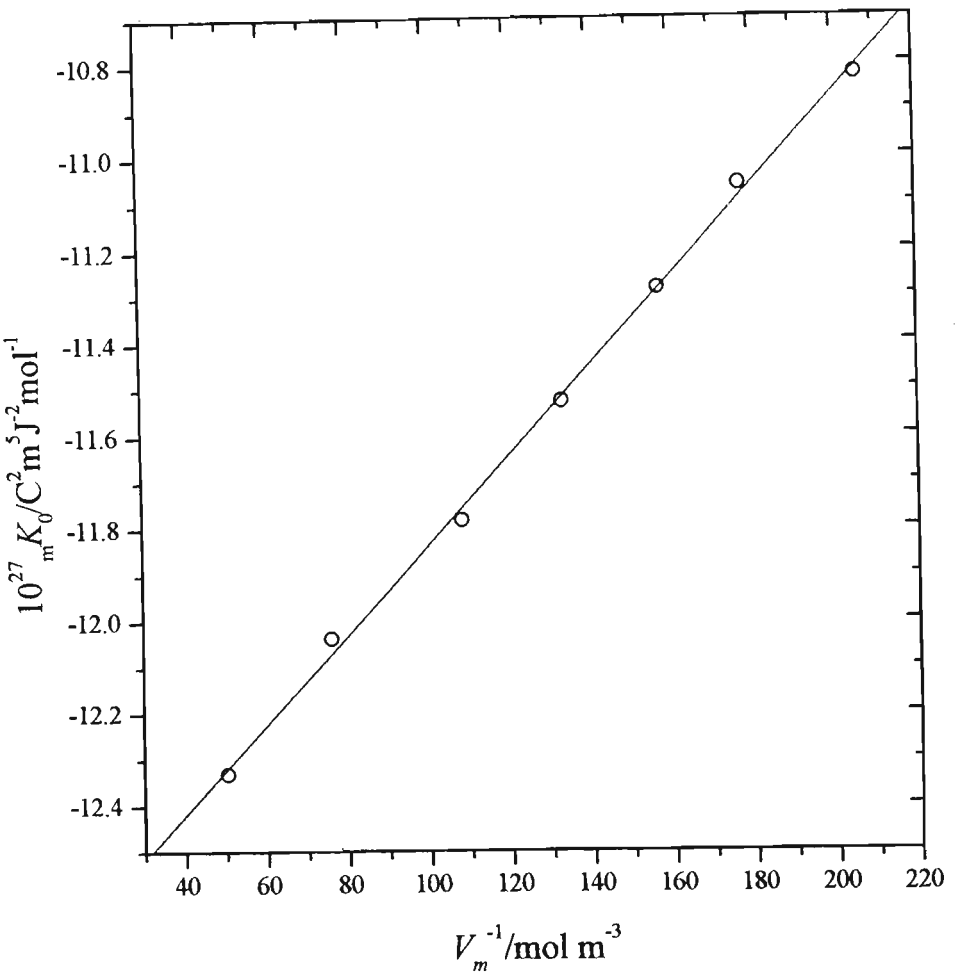

Figure 4.3. A plot of ${}_{m}K_0$ versus $1/V_m$ for dimethyl ether at T = 292.12 K and λ = 632.8 nm.

4.5 Conclusion

This thesis has shown that a unique set of molecular parameters for dimethyl ether, coupled with complete molecular-tensor theories of the pressure, light-scattering and Kerr virial coefficients, generally yields good agreement between experiment and theory for the full range of coefficients. Although beyond the scope of this thesis, we have used the new molecular tensor theory of Graham and Hohls [17] for the second dielectric virial coefficient

B_ε to calculate the temperature dependence of this virial coefficient for dimethyl ether, and agreement with the published measured data (see [17] for a comprehensive list) is within the margins of experimental error.

We can conclude that provided full account is taken of molecular symmetry, the dipole-induced-dipole model accounts reliably for the contribution made by interacting pairs of molecules for a wide range of molecular-optic phenomena.

4.6 References

[1] Couling, V. W., 1995, Ph D thesis, University of Natal (Pietermaritzburg).

[2] Couling, V. W., and Graham, C., 1998, Molec. Phys., 93, 31.

[3] Couling, V. W., and Graham, C., 2000, Molec. Phys., 98, 135.

[4] Buckingham, A. D., and Pople, J. A., 1955, Proc. Phys. Soc. A, 68, 905.

[5] Otterbein, G., 1934, Phys. Z., 35, 249.

[6] Buckingham, A. D., 1955, Proc. Phys. Soc. A, 68, 910.

[7] Buckingham, A. D., 1967, Adv. Chem. Phys., 12, 107.

[8] Andrews, A. L., and Buckingham, A. D., 1960, Molec. Phys., 3, 183.

[9] Buckingham, A. D., Galwas, P. A., and Liu Fan-Chen, 1983, J. molec. Struct., 100, 3.

[10] Blukis, U., Kasai, P. H., and Myers, R. J., 1963, J. chem. Phys., 38, 2753.

[11] Benson, R. C., and Flygare, W. H., 1970, J. chem. Phys., 52, 5291.

[12] Bogaard, M. P., Buckingham, A. D., and Ritchie, G. L. D., 1981, J. chem. Soc. Faraday Trans. II, 77, 1547.

[13] Spackman, M. A., 1999, Private Communication.

[14] Barnes, A. N. M., Turner, D. J., and Sutton, L. E., 1971, Trans. Faraday Soc., 67, 2902.

[15] McKenzie, J. M., 1999, Honours Project Report, University of Natal (Pietermaritzburg).

[16] Williams, J. H., 1993, Adv. Chem. Phys., 85, 361.

[17] Hohls, J., 1997, Ph D thesis, University of Natal (Pietermaritzburg).

[18] Graham, C., Pierrus, J., and Raab, R. E., 1989, Molec. Phys., 67, 939-955.

Appendix A

Electric Multipole Moments

A static distribution of electric charges q_i at positions $\underline{r}_i$ relative to an arbitrarily chosen origin O, positioned within the arrangement of charges, gives rise to an electric potential ϕ at all points in space. For any given point P, with a vector displacement $\underline{R}$ from O with $R >> r_i$, the electric potential is given by the multipole expansion (Buckingahm[1])

$$\phi = \frac{1}{4\pi\varepsilon_0}\left[\frac{1}{R}\sum_i q_i + \frac{R_\alpha}{R^3}\sum_i q_i r_{i\alpha} + \frac{\left(3R_\alpha R_\beta - R^2\delta_{\alpha\beta}\right)}{2R^5}\sum_i q_i r_{i\alpha} r_{i\beta} + \cdots\right] \qquad \text{(A.1)}$$

Here, Greek subscripts denote Cartesian tensor components x, y, or z; with a repeated subscript implying summation over these components. The second-rank tensor $\delta_{\alpha\beta}$ is the Kronecker delta.

The summations in equation (A.1) are the electric multipole moments of the charge distribution:

$$q = \sum_i q_i \qquad \text{(A.2)}$$

is the electric monopole, or the total charge of the distribution;

$$\mu_\alpha = \sum_i q_i r_{i\alpha} \tag{A.3}$$

is the electric dipole moment; and

$$q_{\alpha\beta} = \sum_i q_i r_{i\alpha} r_{i\beta} \tag{A.4}$$

is the primitive electric quadrupole moment; *etc.*

Different definitions have been adopted for electric multipole moments of higher order than the dipole. For instance, an alternative form of the electric quadrupole moment is the *traceless* moment

$$\theta_{\alpha\beta} = \tfrac{1}{2}\sum_i q_i\left(3r_{i\alpha}r_{i\beta} - r_i^2\delta_{\alpha\beta}\right). \tag{A.5}$$

This form of the quadrupole moment is often used by molecular physicists because it vanishes for a spherically-symmetric electric charge distribution, and so is intuitively appealing. Raab [2] has, however, cautioned against the indiscriminate use of the *traceless* multipole moments, pointing out the existence of electrodynamic situations where it is necessary to retain the *primitive* definitions of multipole moments.

References

[1] Buckingham, A. D., 1959, *J. Q. Chem. Rev. Soc.*, **13**, 183.

[2] Raab, R. E., 1975, *Molec. Phys.*, **29**, 1323.

Appendix B

Examples of B_ρ Terms for Linear Molecules

We present here some examples of the explicit expressions for terms contributing to B_ρ for linear molecules:

$$\begin{aligned} a_3 = \frac{\alpha^3}{30(4\pi\varepsilon_0)}\Big\langle R^{-3}(&-27\kappa(\kappa-1)(2\kappa+3)\cos^2\theta_1 \\ &-324\kappa^2(\kappa+1)\cos\theta_{12}\cos\theta_2\cos\theta_1 + 27\kappa(\kappa-1)(2\kappa-1)\cos^2\theta_2 \\ &-108\kappa^2(\kappa+1)\cos^2\theta_{12} + 36\kappa(\kappa-1)\Big\rangle, \end{aligned} \tag{B.1}$$

and

$$\begin{aligned} b_3 = \frac{\alpha^3}{30(4\pi\varepsilon_0)}\Big\langle R^{-3}(&-36\kappa(\kappa-1)(2\kappa+7)\cos^2\theta_1 \\ &-108\kappa^2(2\kappa+7)\cos\theta_{12}\cos\theta_2\cos\theta_1 - 36\kappa^2(2\kappa+7)\cos^2\theta_{12} \\ &+36\kappa(\kappa-1)(2\kappa-5)\cos^2\theta_2 + 144\kappa(\kappa-1))\Big\rangle. \end{aligned} \tag{B.2}$$

The expressions for the higher order terms are too large to reproduce here, but have been quoted explicitly in [1].

References

[1] Couling, V. W., 1993, M Sc thesis, University of Natal (Pietermaritzburg).

Appendix C

Examples of B_ρ Terms for Nonlinear Molecules

Here is an example of an explicit expression for one of the terms contributing to B_ρ for nonlinear molecules:

$$b_3 = \frac{1}{15(4\pi\varepsilon_0)}\Big\langle R^{-3}\{6\alpha(\alpha_{11}(Z_{11}T_{11}+Z_{12}T_{12}+Z_{13}T_{13})+\alpha_{22}(Z_{12}T_{12}+Z_{22}T_{22}+Z_{23}T_{23}) \\ +\alpha_{33}(Z_{13}T_{13}+Z_{23}T_{23}+Z_{33}T_{33})+4(\alpha_{11}^2(Z_{11}T_{11}+Z_{12}T_{12}+Z_{13}T_{13}) \\ +\alpha_{22}^2(Z_{12}T_{12}+Z_{22}T_{22}+Z_{23}T_{23})+\alpha_{33}^2(Z_{13}T_{13}+Z_{23}T_{23}+Z_{33}T_{33}))\}\Big\rangle. \qquad \text{(C.1)}$$

The expressions for the higher order terms are too large to reproduce here, but may be found in [1].

References

[1] Couling, V. W., 1995, Ph D thesis, University of Natal (Pietermaritzburg).

Appendix D

An Example of a Fortran Program to Calculate Contributions to B_ρ

```
PROGRAM SO2_BS
C
C 14 AUGUST 1998
C PROGRAM TO CALCULATE THE BENOIT-STOCKMAYER TERM OF (CH3)2O USING GAUSSIAN
C INTEGRATION WITH 64 INTERVALS FOR THE RANGE, AND 16 INTERVALS FOR ALL
C ANGULAR VARIABLES (I.E. ALPHA1, BETA1, GAMMA1, ALPHA2, BETA2 AND
C GAMMA2).
C DOUBLE PRECISION IS USED THROUGHOUT.
C

C ----------------------
C SYSTEM INITIALIZATION:
C ----------------------

      IMPLICIT DOUBLE PRECISION (A-H,O-Z)
      COMMON COEF1,DCTC
      DIMENSION COEF2(64,2),COEF1(16,2),SEP(64),AL1(16),BE1(16),GA1(16)
     + ,AL2(16),BE2(16),GA2(16),DCTC(9,16,16,16),FI(16,16,16,16,16),D1(6
     + 4),E1(16,16,16,16,16),F1(16,16,16,16,16),SE3(64),SE4(64),SE5(64),
     + SE6(64),SE8(64),SE12(64),G1(16,16,16),DDP(16,16,16,16,16),DQP(16,
     + 16,16,16,16),DIDP(16,16,16,16,16)
      INTEGER X1,X2,X3,X4,X5,X6,X7

C MOLECULAR DATA FOR (CH3)2O: 14 DEC 1999: LATEST DATA (STATIC ALPHA = 6.33)

      SS1=0.0
      SS2=0.0
      SS3=0.0
      SS4=0.0
      SS5=0.0
      SS6=0.0
      SS7=0.0
      DIP=-4.37
      ALSTAT=6.33
      A11=6.37
      A22=5.22
      A33=5.04
```

```
      Q1=11.0
      Q2=-4.3
      AMIN1=0.1
      AMAX1=3.0
      ALPHA=(A11+A22+A33)/3
      DELTA2=(A11**2+A22**2+A33**2-A11*A22-A11*A33-A22*A33)

C
C READ THE GAUSSIAN COEFFICIENTS FROM THE DATAFILE GAUSS64.DAT:
C
      OPEN(UNIT=10,FILE='GAUSS64.DAT')
           DO 10 ICTR1=1,64
            DO 20 ICTR2=1,2
             READ(10,1010,END=11)COEF2(ICTR1,ICTR2)
1010        FORMAT(F18.15)
20        CONTINUE
10       CONTINUE
11      CLOSE(UNIT=10)

C
C CALCULATE THE INTEGRATION POINTS FOR THE RANGE:
C
      SEP1=(AMAX1-AMIN1)/2
      SEP2=(AMAX1+AMIN1)/2
      DO 30 INDX=1,64
           SEP(INDX)=SEP1*COEF2(INDX,1)+SEP2
30    CONTINUE

C
C READ THE GAUSSIAN COEFFICIENTS FROM THE DATAFILE GAUSS16.DAT:
C
      OPEN(UNIT=11,FILE='GAUSS16.DAT')
           DO 100 ICTR1=1,16
            DO 110 ICTR2=1,2
             READ(11,6000,END=12)COEF1(ICTR1,ICTR2)
6000        FORMAT(F18.15)
110      CONTINUE
100     CONTINUE
12      CLOSE(UNIT=11)

C
C CALCULATE THE INTEGRATION POINTS FOR ALPHA1:
C
      AMIN=0.0
      AMAX=2.*3.14159265358979323846

      AL11=(AMAX-AMIN)/2.
      AL12=(AMAX+AMIN)/2.
      DO 120 INDX=1,16
           AL1(INDX)=AL11*COEF1(INDX,1)+AL12
120   CONTINUE

C
C CALCULATE THE INTEGRATION POINTS FOR BETA1:
```

```
C
      AMIN=0.0
      AMAX=3.14159265358979323846

      BE11=(AMAX-AMIN)/2.
      BE12=(AMAX+AMIN)/2.
      DO 121 INDX=1,16
           BE1(INDX)=BE11*COEF1(INDX,1)+BE12
121   CONTINUE

C
C CALCULATE THE INTEGRATION POINTS FOR GAMMA1:
C
      AMIN=0.0
      AMAX=2.*3.14159265358979323846

      GA11=(AMAX-AMIN)/2.
      GA12=(AMAX+AMIN)/2.
      DO 122 INDX=1,16
           GA1(INDX)=GA11*COEF1(INDX,1)+GA12
122   CONTINUE

C
C CALCULATE THE INTEGRATION POINTS FOR ALPHA2:
C
      AMIN=0.0
      AMAX=2.*3.14159265358979323846

      AL21=(AMAX-AMIN)/2.
      AL22=(AMAX+AMIN)/2.
      DO 123 INDX=1,16
           AL2(INDX)=AL21*COEF1(INDX,1)+AL22
123   CONTINUE

C
C CALCULATE THE INTEGRATION POINTS FOR BETA2:
C
      AMIN=0.0
      AMAX=3.14159265358979323846

      BE21=(AMAX-AMIN)/2.
      BE22=(AMAX+AMIN)/2.
      DO 124 INDX=1,16
           BE2(INDX)=BE21*COEF1(INDX,1)+BE22
124   CONTINUE

C
C CALCULATE THE INTEGRATION POINTS FOR GAMMA2:
C
      AMIN=0.0
      AMAX=2.*3.14159265358979323846

      GA21=(AMAX-AMIN)/2.
      GA22=(AMAX+AMIN)/2.
```

```
      DO 125 INDX=1,16
           GA2(INDX)=GA21*COEF1(INDX,1)+GA22
125   CONTINUE

C -------------
C MAIN PROGRAM:
C -------------

      OPEN(UNIT=4,FILE='bs_r31')

C
C INPUT MOLECULAR PARAMETERS FROM THE KEYBOARD:
C

c     WRITE(6,470)
c470  FORMAT(1X,'INPUT THE TEMPERATURE (IN KELVIN)')
c     READ(5,471)TEMP
c471  FORMAT(F10.5)
      temp=303.15
      TEMPK=TEMP*1.380622E-23

c     WRITE(6,472)
c472  FORMAT(1X,'INPUT R(0) (IN nm)')
c     READ(5,473)R
c473  FORMAT(F10.5)
      r=0.47

c     WRITE(6,474)
c474  FORMAT(1X,'E/K (IN K)')
c     READ(5,475)PARAM2
c475  FORMAT(F10.5)
      param2=290.0

c     WRITE(6,476)
c476  FORMAT(1X,'SHAPE1 ')
c     READ(5,477)SHAPE1
c477  FORMAT(F10.5)
      shape1=-0.04926

c     WRITE(6,478)
c478  FORMAT(1X,'SHAPE2 ')
c     READ(5,479)SHAPE2
c479  FORMAT(F10.5)
      shape2=0.29666


C
C CALCULATION OF THE LENNARD-JONES 6:12 POTENTIAL & STORAGE OF THE
C VALUES IN AN ARRAY:
C

      DO 61 X1=1,64

      D1(X1)=4.*PARAM2*1.380622E-23*((R/SEP(X1))**12-(R/SEP(X1))**6)
```

```
      SE12(X1)=SEP(X1)**12
      SE5(X1)=SEP(X1)**5
      SE8(X1)=SEP(X1)**8
      SE3(X1)=SEP(X1)**3
      SE4(X1)=SEP(X1)**4
      SE6(X1)=SEP(X1)**6

61    CONTINUE


C
C THE DIRECTION COSINE TENSOR COMPONENTS ARE STORED IN AN ARRAY:
C

      DO 66 X4=1,16
           DO 77 X3=1,16
            DO 88 X2=1,16

C
C DIRECTION COSINE TENSOR COMPONENTS:
C

      A1=COS(AL1(X2))*COS(BE1(X3))*COS(GA1(X4))-1.*SIN(AL1(X2))*SIN(GA1
     + (X4))
      A2=SIN(AL1(X2))*COS(BE1(X3))*COS(GA1(X4))+COS(AL1(X2))*SIN(GA1(X4
     + ))
      A3=-1.*SIN(BE1(X3))*COS(GA1(X4))
      A4=-1.*COS(AL1(X2))*COS(BE1(X3))*SIN(GA1(X4))-1.*SIN(AL1(X2))*COS
     + (GA1(X4))
      A5=-1.*SIN(AL1(X2))*COS(BE1(X3))*SIN(GA1(X4))+COS(AL1(X2))*COS(GA
     + 1(X4))
      A6=SIN(BE1(X3))*SIN(GA1(X4))
      A7=COS(AL1(X2))*SIN(BE1(X3))
      A8=SIN(AL1(X2))*SIN(BE1(X3))
      A9=COS(BE1(X3))

      DCTC(1,X2,X3,X4)=A1
      DCTC(2,X2,X3,X4)=A2
      DCTC(3,X2,X3,X4)=A3
      DCTC(4,X2,X3,X4)=A4
      DCTC(5,X2,X3,X4)=A5
      DCTC(6,X2,X3,X4)=A6
      DCTC(7,X2,X3,X4)=A7
      DCTC(8,X2,X3,X4)=A8
      DCTC(9,X2,X3,X4)=A9

88      CONTINUE
77     CONTINUE
66    CONTINUE


C
C THE MULTIPOLE INTERACTION ENERGIES ARE CALCULATED AND STORED
C IN ARRAYS:
```

```
C

      DO 939 X7=1,16
      WRITE(4,1000)X7
1000   FORMAT (1X, 'INDEX (IN RANGE 1 TO 16) IS CURRENTLY ',I2 )
           DO 40 X6=1,16
c       WRITE(6,1111)X6
c1111   FORMAT (1X, 'sub-index (in range 1 to 16) is currently ',I2 )
             DO 50 X5=1,16

C
C MOLECULE 2'S DIRECTION COSINE TENSOR COMPONENTS:
C

      B1=DCTC(1,X5,X6,X7)
      B2=DCTC(2,X5,X6,X7)
      B3=DCTC(3,X5,X6,X7)
      B4=DCTC(4,X5,X6,X7)
      B5=DCTC(5,X5,X6,X7)
      B6=DCTC(6,X5,X6,X7)
      B7=DCTC(7,X5,X6,X7)
      B8=DCTC(8,X5,X6,X7)
      B9=DCTC(9,X5,X6,X7)


               DO 60 X4=1,16
                DO 70 X3=1,16
                     DO 80 X2=1,16

C
C MOLECULE 1'S DIRECTION COSINE TENSOR COMPONENTS:
C

      A1=DCTC(1,X2,X3,X4)
      A2=DCTC(2,X2,X3,X4)
      A3=DCTC(3,X2,X3,X4)
      A4=DCTC(4,X2,X3,X4)
      A5=DCTC(5,X2,X3,X4)
      A6=DCTC(6,X2,X3,X4)
      A7=DCTC(7,X2,X3,X4)
      A8=DCTC(8,X2,X3,X4)
      A9=DCTC(9,X2,X3,X4)

C
C CALCULATION OF THE DIPOLE-DIPOLE POTENTIAL:
C
      DDP(X2,X3,X4,X5,X6)=8.98758E-24*DIP**2*(-2*A9*B9+A6*B6+A3*B3)

C
C CALCULATION OF THE DIPOLE-QUADRUPOLE POTENTIAL:
C
      DQP(X2,X3,X4,X5,X6)=8.98758E-25*DIP*(Q2*(-2*A9*B9**2+(2*A6*B6+2*A
     + 3*B3+2*A9**2-2*A8**2-A6**2+A5**2-A3**2+A2**2)*B9+2*A9*B8**2+(-2*A
     + 6*B5-2*A3*B2)*B8+A9*B6**2+(2*A5*A8-2*A6*A9)*B6-A9*B5**2+A9*B3**2+
```

```
     + (2*A2*A8-2*A3*A9)*B3-A9*B2**2)+Q1*(-2*A9*B9**2+(2*A6*B6+2*A3*B3+2
     + *A9**2-2*A7**2-A6**2+A4**2-A3**2+A1**2)*B9+2*A9*B7**2+(-2*A6*B4-2
     + *A3*B1)*B7+A9*B6**2+(2*A4*A7-2*A6*A9)*B6-A9*B4**2+A9*B3**2+(2*A1*
     + A7-2*A3*A9)*B3-A9*B1**2))

C
C CALCULATION OF THE DIPOLE-INDUCED DIPOLE POTENTIAL:
C
      DIDP(X2,X3,X4,X5,X6)=-0.50*ALSTAT*8.07765E-27*DIP**2*(3*B9**2
     + +3*A9**2-2)

C
C CALCULATION OF THE QUADRUPOLE-QUADRUPOLE POTENTIAL:
C
      quad1=-16.*(a6*a9-a5*a8)*(b6*b9-b5*b8)-16.*(a3*a9-a2*a8)*(b3*b9-b
     + 2*b8)+4.*(2.*a9**2-2.*a8**2-a6**2+a5**2-a3**2+a2**2)*(b9-b8)*(b9+
     + b8)+(-4.*a9**2+4.*a8**2+3.*a6**2-3.*a5**2+a3**2-a2**2)*(b6**2-b5*
     + *2)+4.*(a3*a6-a2*a5)*(b3*b6-b2*b5)+(-4.*a9**2+4.*a8**2+a6**2-a5**
     + 2+3.*a3**2-3.*a2**2)*(b3**2-b2**2)

      quad2=-16.*(a6*a9-a4*a7)*(b6*b9-b4*b7)-16.*(a3*a9-a1*a7)*(b3*b9-b
     + 1*b7)+4.*(2.*a9**2-2.*a7**2-a6**2+a4**2-a3**2+a1**2)*(b9-b7)*(b9+
     + b7)+(-4.*a9**2+4.*a7**2+3.*a6**2-3.*a4**2+a3**2-a1**2)*(b6**2-b4*
     + *2)+4.*(a3*a6-a1*a4)*(b3*b6-b1*b4)+(-4.*a9**2+4.*a7**2+a6**2-a4**
     + 2+3.*a3**2-3.*a1**2)*(b3**2-b1**2)

      quad3=4.*(4.*A9**2-2.*(A8**2+A7**2+A6**2+A3**2)+A5**2+A4**2+A2**2
     + +A1**2)*B9**2-16.*(2.*A6*A9-A5*A8-A4*A7)*B6*B9-16*(2.*A3*A9-A2*A8
     + -A1*A7)*B3*B9-4.*(2.*A9**2-2.*A7**2-A6**2+A4**2-A3**2+A1**2)*B8**
     + 2+16.*(A6*A9-A4*A7)*B5*B8+16.*(A3*A9-A1*A7)*B2*B8-4.*(2.*A9**2-2.
     + *A8**2-A6**2+A5**2-A3**2+A2**2)*B7**2+16.*(A6*A9-A5*A8)*B4*B7+16.
     + *(A3*A9-A2*A8)*B1*B7+(-8.*A9**2+4.*(A8**2+A7**2)+6.*A6**2-3.*(A5*
     + *2+A4**2)+2*A3**2-A2**2-A1**2)*B6**2+4.*(2.*A3*A6-A2*A5-A1*A4)*B3
     + *B6+(4.*A9**2-4.*A7**2-3.*A6**2+3.*A4**2-A3**2+A1**2)*B5**2-4.*(A
     + 3*A6-A1*A4)*B2*B5+(4.*A9**2-4.*A8**2-3.*A6**2+3.*A5**2-A3**2+A2**
     + 2)*B4**2-4.*(A3*A6-A2*A5)*B1*B4+(-8.*A9**2+4.*(A8**2+A7**2)+2.*A6
     + **2-A5**2-A4**2+6.*A3**2-3.*(A2**2+A1**2))*B3**2+(4.*A9**2-4.*A7*
     + *2-A6**2+A4**2-3.*A3**2+3.*A1**2)*B2**2+(4.*A9**2-4.*A8**2-A6**2+
     + A5**2-3.*A3**2+3.*A2**2)*B1**2

      E1(X2,X3,X4,X5,X6)=8.98758E-26*(1./3.)*(Q2**2*QUAD1+Q1**2*QUAD
     + 2+Q1*Q2*QUAD3)


C
C CALCULATION OF THE QUADRUPOLE-INDUCED DIPOLE POTENTIAL:
C

      QID1=Q2**2*(4.*A9**4+(-8.*A8**2+4.*A5**2+4.*A2**2)*A9**2+(-8.*A5*
     + A6-8.*A2*A3)*A8*A9+4.*A8**4+(4.*A6**2+4.*A3**2)*A8**2+A6**4+(-2.*
     + A5**2+2.*A3**2-2.*A2**2)*A6**2+A5**4+(2.*A2**2-2.*A3**2)*A5**2+A3
     + **4-2.*A2**2*A3**2+A2**4)+Q1**2*(4.*A9**4+(-8.*A7**2+4.*A4**2+4.*
     + A1**2)*A9**2+(-8.*A4*A6-8.*A1*A3)*A7*A9+4.*A7**4+(4.*A6**2+4.*A3*
     + *2)*A7**2+A6**4+(-2.*A4**2+2.*A3**2-2.*A1**2)*A6**2+A4**4+(2.*A1*
```

```
     + *2-2.*A3**2)*A4**2+A3**4-2.*A1**2*A3**2+A1**4)+Q1*Q2*(8.*A9**4+(-
     + 8.*A8**2-8.*A7**2+4.*A5**2+4.*A4**2+4.*A2**2+4.*A1**2)*A9**2+((-8
     + .*A5*A6-8.*A2*A3)*A8+(-8.*A4*A6-8.*A1*A3)*A7)*A9+(8.*A7**2+4.*A6*
     + *2-4.*A4**2+4.*A3**2-4.*A1**2)*A8**2+(8.*A4*A5+8.*A1*A2)*A7*A8+(4
     + .*A6**2-4.*A5**2+4.*A3**2-4.*A2**2)*A7**2+2.*A6**4+(-2.*A5**2-2.*
     + A4**2+4.*A3**2-2.*A2**2-2.*A1**2)*A6**2+(2.*A4**2-2.*A3**2+2.*A1*
     + *2)*A5**2+(2.*A2**2-2.*A3**2)*A4**2+2.*A3**4+(-2.*A2**2-2.*A1**2)
     + *A3**2+2.*A1**2*A2**2)

      QID2=Q2**2*(4.*B9**4+(-8.*B8**2+4.*B5**2+4.*B2**2)*B9**2+(-8.*B5*
     + B6-8.*B2*B3)*B8*B9+4.*B8**4+(4.*B6**2+4.*B3**2)*B8**2+B6**4+(-2.*
     + B5**2+2.*B3**2-2.*B2**2)*B6**2+B5**4+(2.*B2**2-2.*B3**2)*B5**2+B3
     + **4-2.*B2**2*B3**2+B2**4)+Q1**2*(4.*B9**4+(-8.*B7**2+4.*B4**2+4.*
     + B1**2)*B9**2+(-8.*B4*B6-8.*B1*B3)*B7*B9+4.*B7**4+(4.*B6**2+4.*B3*
     + *2)*B7**2+B6**4+(-2.*B4**2+2.*B3**2-2.*B1**2)*B6**2+B4**4+(2.*B1*
     + *2-2.*B3**2)*B4**2+B3**4-2.*B1**2*B3**2+B1**4)+Q1*Q2*(8.*B9**4+(-
     + 8.*B8**2-8.*B7**2+4.*B5**2+4.*B4**2+4.*B2**2+4.*B1**2)*B9**2+((-8
     + .*B5*B6-8.*B2*B3)*B8+(-8.*B4*B6-8.*B1*B3)*B7)*B9+(8.*B7**2+4.*B6*
     + *2-4.*B4**2+4.*B3**2-4.*B1**2)*B8**2+(8.*B4*B5+8.*B1*B2)*B7*B8+(4
     + .*B6**2-4.*B5**2+4.*B3**2-4.*B2**2)*B7**2+2.*B6**4+(-2.*B5**2-2.*
     + B4**2+4.*B3**2-2.*B2**2-2.*B1**2)*B6**2+(2.*B4**2-2.*B3**2+2.*B1*
     + *2)*B5**2+(2.*B2**2-2.*B3**2)*B4**2+2.*B3**4+(-2.*B2**2-2.*B1**2)
     + *B3**2+2.*B1**2*B2**2)

      F1(X2,X3,X4,X5,X6)=-0.5*8.07765E-29*ALSTAT*(QID1+QID2)

C
C CALCULATION OF THE INTEGRATION ARGUMENT:
C

      BS = 3*(A33**2*A9**2*B9**2+A22*A33*A8**2*B9**2+A11*A33*A7**2*B9**
     1  2+2*A33**2*A6*A9*B6*B9+2*A22*A33*A5*A8*B6*B9+2*A11*A33*A4*A7*B6
     2  *B9+2*A3*A33**2*A9*B3*B9+2*A2*A22*A33*A8*B3*B9+2*A1*A11*A33*A7*
     3  B3*B9+A22*A33*A9**2*B8**2+A22**2*A8**2*B8**2+A11*A22*A7**2*B8**
     4  2+2*A22*A33*A6*A9*B5*B8+2*A22**2*A5*A8*B5*B8+2*A11*A22*A4*A7*B5
     5  *B8+2*A22*A3*A33*A9*B2*B8+2*A2*A22**2*A8*B2*B8+2*A1*A11*A22*A7*
     6  B2*B8+A11*A33*A9**2*B7**2+A11*A22*A8**2*B7**2+A11**2*A7**2*B7**
     7  2+2*A11*A33*A6*A9*B4*B7+2*A11*A22*A5*A8*B4*B7+2*A11**2*A4*A7*B4
     8  *B7+2*A11*A3*A33*A9*B1*B7+2*A11*A2*A22*A8*B1*B7+2*A1*A11**2*A7*
     9  B1*B7+A33**2*A6**2*B6**2+A22*A33*A5**2*B6**2+A11*A33*A4**2*B6**
     :  2+2*A3*A33**2*A6*B3*B6+2*A2*A22*A33*A5*B3*B6+2*A1*A11*A33*A4*B3
     ;  *B6+A22*A33*A6**2*B5**2+A22**2*A5**2*B5**2+A11*A22*A4**2*B5**2+
     <  2*A22*A3*A33*A6*B2*B5+2*A2*A22**2*A5*B2*B5+2*A1*A11*A22*A4*B2*B
     =  5+A11*A33*A6**2*B4**2+A11*A22*A5**2*B4**2+A11**2*A4**2*B4**2+2*
     >  A11*A3*A33*A6*B1*B4+2*A11*A2*A22*A5*B1*B4+2*A1*A11**2*A4*B1*B4+
     ?  A3**2*A33**2*B3**2+A2**2*A22*A33*B3**2+A1**2*A11*A33*B3**2+A22*
     @  A3**2*A33*B2**2+A2**2*A22**2*B2**2+A1**2*A11*A22*B2**2+A11*A3**
     1  2*A33*B1**2+A11*A2**2*A22*B1**2+A1**2*A11**2*B1**2)-9.*ALPHA**2


      FI(X2,X3,X4,X5,X6)=(SIN(BE1(X3))*SIN(BE2(X6)))*BS

C
C CALCULATION OF THE SHAPE POTENTIAL:
```

```
C
      G1(X3,X4,X6)=4.*PARAM2*1.380622E-23*R**12*(SHAPE1*(3.*COS(BE1(X3)
     + )**2+3.*COS(BE2(X6))**2-2.)+SHAPE2*(3.*COS(GA1(X4))**2*SIN(BE1(X3
     + ))**2+3.*COS(GA2(X7))**2*SIN(BE2(X6))**2-2.))


80          CONTINUE
70         CONTINUE
60        CONTINUE
50       CONTINUE
40      CONTINUE

C
C THE INTEGRAL IS CALCULATED:
C

          SS6=0.00
          DO 940 X6=1,16
C      WRITE(6,1911)X6
C1911   FORMAT (1X, 'sub-index (in range 1 to 16) is currently ',I2 )
            SS5=0.00
            DO 950 X5=1,16
              SS4=0.00
              DO 960 X4=1,16
                SS3=0.00
                DO 970 X3=1,16
                      SS2=0.00
                      DO 980 X2=1,16
                        SS1=0.00
                        DO 990 X1=1,64


C
C SUMMATION OF THE ENERGY TERMS WITH SUBSEQUENT DIVISION BY (-kT):
C

      G3=-1.*(D1(X1)+E1(X2,X3,X4,X5,X6)/SE5(X1)+F1(X2,X3,X4,X5,X6)/SE8(
     + X1)+G1(X3,X4,X6)/SE12(X1)+DDP(X2,X3,X4,X5,X6)/SE3(X1)+DIDP(X2,X3,
     + X4,X5,X6)/SE6(X1)+DQP(X2,X3,X4,X5,X6)/SE4(X1))/TEMPK

      IF(G3.LT.-85) GO TO 5000
      G4=2.71828**G3
      GO TO 5010
5000  G4=0
5010  SS1=SS1+FI(X2,X3,X4,X5,X6)*SEP(X1)**2*G4*COEF2(X1,2)
990             CONTINUE
      SS2=SS2+SS1*COEF1(X2,2)
C
C
980           CONTINUE
      SS3=SS3+SS2*COEF1(X3,2)
C
C
```

```
970         CONTINUE
     SS4=SS4+SS3*COEF1(X4,2)
C
C
960         CONTINUE
     SS5=SS5+SS4*COEF1(X5,2)
C
C
950       CONTINUE
     SS6=SS6+SS5*COEF1(X6,2)
C
C
940     CONTINUE
     SS7=SS7+SS6*COEF1(X7,2)

C
C
939   CONTINUE
     ANS=SS7*SEP1*AL11*BE11*GA11*AL21*BE21*GA21*1.E-4*6.022169
    + /(2.*DELTA2*3.14159265358979323846**3*16.)

C
C THE INTEGRAL IS PRINTED TOGETHER WITH MOLECULAR DATA USED
C

     WRITE(4,2266)
2266  FORMAT(1X,'THE BENOIT-STOCKMAYER CONTRIBUTION TO B(Rho) ether:')
     WRITE(4,2267)
2267  FORMAT(1X,'  ')
     WRITE(4,2269)
2269  FORMAT(1X,'  ')
     WRITE(4,1140)ANS
1140  FORMAT(1X,'THE INTEGRAL IS',E15.7)
     WRITE(4,2150)
2150  FORMAT(1X,'INPUT DATA:')
     WRITE(4,2155)TEMP
2155  FORMAT(1X,'TEMPERATURE:          ',F10.5)
     WRITE(4,9259)DIP
9259  FORMAT(1X,'DIPOLE MOMENT:        ',F10.5)
     WRITE(4,9260)ALPHA
9260  FORMAT(1X,'MEAN DYNAMIC ALPHA:    ',F10.5)
     WRITE(4,9261)A11
9261  FORMAT(1X,'DYNAMIC ALPHA11:       ',F10.5)
     WRITE(4,9262)A22
9262  FORMAT(1X,'DYNAMIC ALPHA22:       ',F10.5)
     WRITE(4,9263)A33
9263  FORMAT(1X,'DYNAMIC ALPHA33:       ',F10.5)
     WRITE(4,9265)DELTA2
9265  FORMAT(1X,'(DELTA DYNAMIC ALPHA)**2:',F10.5)
     WRITE(4,9264)ALSTAT
9264  FORMAT(1X,'MEAN STATIC ALPHA:     ',F10.5)
     WRITE(4,2190)Q1
2190  FORMAT(1X,'THETA11:              ',F10.5)
     WRITE(4,2241)Q2
```

```
2241  FORMAT(1X,'THETA22:              ',F10.5)
      WRITE(4,2210)R
2210  FORMAT(1X,'R(0):                 ',F6.5)
      WRITE(4,2220)SHAPE1
2220  FORMAT(1X,'SHAPE FACTOR 1:       ',F10.5)
      WRITE(4,2221)SHAPE2
2221  FORMAT(1X,'SHAPE FACTOR 2:       ',F10.5)
      WRITE(4,2230)PARAM2
2230  FORMAT(1X,'E/K:                  ',F9.5)
      WRITE(4,2235)AMIN1,AMAX1
2235  FORMAT(1X,'MIN AND MAX POINTS OF RANGE (64 INTERVALS):',2(F10.5,3
     + X))
      WRITE(4,2240)
2240  FORMAT(1X,'END B(Rho)')
      WRITE(4,2261)
2261  FORMAT(1X,' ')
      WRITE(4,2262)
2262  FORMAT(1X,' ')
      WRITE(4,2263)
2263  FORMAT(1X,' ')
      WRITE(4,2264)
2264  FORMAT(1X,' ')
      WRITE(4,2265)
2265  FORMAT(1X,' ')

      close(unit=4)
      END
```